

Université Mohamed Khider – Biskra
Faculté des Sciences et de la technologie
Département d'Architecture
Réf :.....



جامعة محمد خيضر بسكرة
كلية العلوم و التكنولوجيا
قسم الهندسة المعمارية
المرجع:.....

Thèse présentée en vue de l'obtention
du diplôme de

Doctorat en Architecture
Spécialité : Projet Urbain

**Toward an oriented choice of building materials for
improving the outdoor thermal comfort in hot dry climates**

Présentée par :

BEN RATMIA Fatima Zahra

Soutenue publiquement le : 24/04/2025

Devant le jury composé de :

Pr. BOUZAHER Soumia	Professeur	Présidente	Université de Biskra
Dr. AHRIZ Atef	MCA	Directeur de thèse	Université de Tebessa
Dr. MADHOU Meriem	MCA	Examinatrice	Université de Biskra
Dr. BADACHE Halima	MCA	Examinatrice	Université de Biskra
Dr. FEZZAI Soufiane	MCA	Examineur	Université de Tebessa

Année Universitaire : 2024 - 2025

بِسْمِ اللَّهِ الرَّحْمَنِ الرَّحِيمِ

Dedication

To the cherished soul of my beloved father,

To my dear mother, the beacon of my strength,

To my loving husband and my precious daughters, my little princesses,

To my wonderful sister and brothers, who have always been my pillars,

To my family and friends, whose unwavering support has enriched my journey,

This work is dedicated with all my love and gratitude.

Acknowledgments

*All praise and thanks are due to **Allah**, the Most Gracious and Most Merciful, for granting me the strength, patience, and guidance to complete this work. Without His blessings, none of this would have been possible.*

*First and foremost, I extend my heartfelt thanks to my esteemed supervisor, **Dr. Atef Ahriz**, for his invaluable guidance, patience, and encouragement throughout this journey.*

*I am deeply grateful to **Professor Soumia Bouzaher** and **Dr. Mostefa Medouki** for their constructive advice and insightful feedback, which greatly enriched this work. To the honorable jury members, thank you for dedicating your time and expertise to evaluating my thesis.*

*With immense love and gratitude, I thank my dear husband, **Dr. Mohamed Elhadi Matallah**, for his unwavering support, encouragement, and constant help throughout this journey. Your belief in me has been a source of strength.*

*I would also like to extend my heartfelt thanks to the University of Pisa, Italy, for the opportunity to conduct a scientific stay in the Department of Energy, Systems, Territory, and Construction Engineering, under the Erasmus+ KA Program. My sincere gratitude goes to **Dr. Giovanni Santi** and the **International Cooperation Programs Unit** of Pisa for their support and collaboration during this enriching experience.*

To all my professors, whose wisdom has inspired me, and to my friends and colleagues, whose companionship and support have lightened the path, I am profoundly thankful.

Finally, to my beloved family and every kind soul who offered encouragement, assistance, or simply a comforting word, I owe my deepest gratitude. You have all contributed to making this journey a meaningful and memorable experience.

Abstract:

This thesis addresses the challenges posed by rapid urbanization and climate change patterns, focusing on outdoor thermal comfort in hot dry environments. Investigating Biskra city, in Algeria, as a case study. It examines how external building materials, and street geometry affect pedestrian-level thermal conditions. The research aims to provide evidence-based guidelines for sustainable urban planning in arid cities. By investigating the localized effects of building materials and street orientation, which have been largely underexplored in previous research, the study bridges critical knowledge gaps. A comprehensive literature review highlights the need for context-specific studies to better understand the interactions between urban geometry and building material properties in regions with extreme weather conditions. Field data collected in Biskra city, including air temperature and relative humidity, validated via ENVI-met simulations modeling with various street orientations (East-West and North-South), height-to-width ratios, and building materials parameterization (brick, concrete, adobe, and limestone). Therefore, deeper street canyons reduce surface temperatures but are less effective in mitigating thermal stress in East-West orientations, emphasizing the dominant role of street alignment. Complementing these findings, limestone as crucial material demonstrates optimal thermal performance, offering high cooling efficiency, particularly in North-South streets, through its reflective properties, which help retain less heat. However, building material choice has strong relationship to street orientation. Thermal comfort indices, such as Physiological Equivalent Temperature (PET), further validate these findings, with North-South streets achieving significantly lower PET index values.

In conclusion, this thesis provides practical urban design guidelines, highlighting building materials selection and North-South street orientation as key components of a comprehensive strategy to enhance outdoor thermal comfort. The findings support sustainable urban planning by mitigating Urban Heat Island (UHI) effects, improving public health, and boosting urban resilience.

Keywords:

Hot dry climate, outdoor thermal comfort, building material, parameterization, numerical modelling, categorization.

Résumé :

La thèse examine les défis majeurs posés par l'urbanisation rapide et les modèles de changement climatique, en se concentrant sur le confort thermique extérieur dans les régions arides. En prenant la ville de Biskra, en Algérie, comme étude de cas, l'étude analyse la corrélation entre matériaux de construction et la géométrie des rues qui affectent les conditions thermiques des piétonniers. La recherche vise une fondation des stratégies pour une meilleure planification urbaine durable des régions arides. En abordant les effets des matériaux de construction et l'orientation des rues, dont sont largement sous-explorés, l'étude comble des lacunes critiques des connaissances actuelles. La recherche bibliographique met en évidence la nécessité d'études contextuelles afin de comprendre les interactions entre la géométrie urbaine et les propriétés des matériaux de construction dans des régions arides. Une collecte de données in-situ dans la ville de Biskra, comprenant la température de l'air et l'humidité relative, qui ont été validées par la suite via ENVI-met en modélisant de différents scénarios de rues (Est-Ouest et Nord-Sud), avec une paramétrisation des matériaux (brique, béton, adobe et calcaire). Les résultats démontrent que les plus profondes rues réduisent les températures de surface, mais s'avèrent moins efficaces pour atténuer le stress thermique dans les orientations Est-Ouest, soulignant le rôle dominant de l'alignement des rues. Autrement, le calcaire se présente comme un matériau crucial, présentant des performances thermiques optimales offrant une efficacité de refroidissement, particulièrement dans l'orientation Nord-Sud. Cependant, le choix des matériaux de construction entretient une forte relation avec l'orientation des rues. L'indice du confort la Température Équivalente Physiologique (PET), valide ces résultats, dont les rues Nord-Sud illustrant des valeurs d'indice PET, significativement plus basses. En conclusion, la recherche fournit des lignes directrices pratiques en matière de planification urbaine, mettant en évidence une catégorisation des matériaux de construction et l'orientation Nord-Sud des rues comme composantes primordiales pour une stratégie effective visant à améliorer le confort thermique extérieur. Les résultats sont pour une planification urbaine durable tout en atténuant les effets d'îlot de chaleur urbain (ICU), améliorant la santé publique et maintenant la résilience urbaine.

Mots-clés :

Climat aride, confort thermique extérieur, matériau de construction, paramétrisation, modélisation numérique, catégorisation.

ملخص:

تتناول هذه الأطروحة التحديات البيومناخية الناجمة عن التوسع الحضري المتسارع وانعكاسات تغير المناخ غير المسبوق، بالتركيز على الراحة الحرارية للإنسان داخل الفضاءات العمرانية في البيئات الحارة والجافة. الأطروحة تخص مدينة بسكرة في الجزائر كحالة دراسة، بحيث تعين كيفية تأثير مواد البناء الخارجية للمباني مع شكل الشوارع على الراحة الحرارية لمستعملي الفضاءات الخارجية. تهدف هاته الدراسة إلى تقديم توجيهات استراتيجية مستندة إلى أدلة بغية التخطيط الحضري المستدام في المدن الصحراوية. لهذا بحثنا هذا يفحص بعمق التأثيرات المنعكسة لمواد البناء و شكل الشوارع، والتي لم يتم دراستها بالشكل الكافي في الدراسات القبلية.

تبرز الدراسة الكنتيية و النظرية امس الحاجة إلى دراسات محددة السياق لفهم أفضل للتفاعلات و الانعكاسات بين الهندسة الحضرية وخصائص مواد البناء في المناطق ذات الظروف المناخية القاسية. تم جمع بيانات ميدانية في مدينة بسكرة، تشمل درجة حرارة الهواء و نسبة الرطوبة السائدة، وكذا النمذجة الرقمية عبر محاكاة ENVI-met استنادا الى اتجاهات شوارع مختلفة (شرق-غرب و شمال-جنوب)، ونسب ارتفاع المباني إلى عرض الشارع، وكذا تغيير خصائص مواد البناء المستعملة (الطوب، والخرسانة، والطين، والحجر الجيري).

أظهرت النتائج أن الشوارع الأعمق تقلل درجات حرارة أسطح المباني المحيطة بها، لكنها أقل فعالية في التخفيف من الإجهاد الحراري للمارة و مستعملي الفضاءات الخارجية في الاتجاهات الشرقية-الغربية، مما يؤكد الدور المهيمن لتوجيه الشوارع. بشكل اضافي، يثبت الحجر الجيري كمادة بناء محورية أداءً حرارياً متفوقاً، مع كفاءة تبريد عالية، خاصة في الشوارع ذات التوجيهات الشمالية-الجنوبية، من خلال خصائصه العاكسة التي تساعد على امتصاص حرارة أقل. بذلك، يرتبط اختيار مواد البناء بعلاقة وثيقة باتجاه الشوارع. وقد أكدت مؤشرات الراحة الحرارية، مثل درجة الحرارة المكافئة الفسيولوجية (PET)، هذه النتائج، حيث حققت الشوارع الشمالية-الجنوبية قيم مؤشر PET أدنى بشكل ملحوظ.

في الختام، تمنح هذه الأطروحة إرشادات عملية و استراتيجية للتصميم الحضري في المناطق الجافة، مع التأكيد على اختيار المواد الإنشائية واتجاه الشوارع الشمالية-الجنوبية كمكونات رئيسية لاستراتيجية شاملة لتعزيز الراحة الحرارية الخارجية. تدعم النتائج التخطيط الحضري المستدام من خلال التخفيف من آثار الجزر الحرارية الحضرية.

الكلمات المفتاحية:

المناخ الجاف، الراحة الحرارية الخارجية، مواد البناء، خاصية التعديل، النمذجة الرقمية، تحديد فئات مواد البناء.

Abbreviations:

ASHRAE	American Society of Heating, Refrigerating, and Air-Conditioning Engineers
CFD	Computational Fluid Dynamics
CNERIB	Algerian Centre for Building Integrated Studies and Research
DTR	Thermal Regulations for Residential Buildings (Algeria)
IPCC	Intergovernmental Panel on Climate Change
ISO	International Organization for Standardization
MBE	Mean Bias Error
PDAU	Urban Development Master Plan
PET	Physiological Equivalent Temperature
PMV	Predicted Mean Vote
POS	Land Occupancy Plan
RMSE	Root Mean Square Error
R-value	Thermal Resistance
SRI	Solar Reflectance Index
SVF	Sky View Factor
T_a	Air Temperature
T_{mrt}	Mean Radiant Temperature
T_s	Surface Temperature
UHI	Urban Heat Island
UTCI	Universal Thermal Climate Index
V_a	Air Velocity
WMO	World Meteorological Organization
ZHUN	New Urban Habitat Zone

TABLE OF CONTENTS

Dedication	I
Acknowledgments	II
Abstract:	I
Résumé :	II
ملخص:	III
Abbreviations:	IV
CHAPTER I: INTRODUCTION, PROBLEMATIC EXPLORATION AND RESEARCH OBJECTIVES	
Introduction	1
1. Background and Context	1
2. Problem Statement and Research Gap:	1
3. Research Questions and Objectives:	2
4. Research Hypotheses:	2
5. Methodology Overview:	3
5.1 Multi-criteria Selection of Building Materials:	3
5.2 Field Measurements and Data Collection:	3
5.3 Numerical Parameterization and Simulation:	4
5.4 Statistical Analysis and Findings Discussion:	4
5.5 Validation and Guideline Development:	4
6. Study Context: Biskra, Algeria:	4
7. Significance and Potential Impact:	5
8. Thesis Structure:	6
Chapter I: Introduction, problematic exploration and research objectives.	6
Chapter II: Urban climate and outdoor thermal comfort: theoretical insights and studies.	6
Chapter III: Building materials and characteristics: an in-depth review of material thermal properties.	6
Chapter IV: Literature review (Part A): a synthesis of urban climate and outdoor thermal comfort.	7
Chapter V: Literature review (Part B): a review of modelling techniques, contextual applications and building materials.	7
Chapter VI: Method and materials: methodology, data collection, and analytical techniques.	7
Chapter VII: Results and analysis: presentation and interpretation of field measurements and simulation results.	8
Conclusion: Conclusion and recommendations.	8

CHAPTER II: URBAN CLIMATE AND OUTDOOR THERMAL COMFORT: THEORITICAL INSIGHTS AND STUDIES	10
Introduction:	10
1. Overview on Climate:	11
1.1. Definition of climatology and climate:	11
1.2. Climate classification:	11
2. Urban climate:	14
2.1. Definition of urban climate:	14
2.2. Scales of urban climate:	14
2.2.1. Horizontal scales of urban climate:	15
2.2.2. Vertical scales of urban climate:	16
2.3. The elements of urban climate:	18
2.3.1. Temperature:	18
2.3.2. Humidity:	18
2.3.3. Wind:	20
2.3.4. Precipitation:	21
2.3.5. Solar Radiation:	21
2.4. The urban energy balance:	22
2.5. Factors Affecting Urban Climate:	24
2.5.1. Natural Factors:	24
2.5.2. Anthropogenic Factors:	25
3. Thermal Comfort:	29
3.1. Definitions of thermal comfort:	29
3.2. Definitions of outdoor thermal comfort:	30
3.3. Factors of outdoor thermal comfort:	30
3.3.1. Environmental Factors:	31
3.3.2. Personal Factors:	32
3.4. The outdoor thermal comfort indices:	33
3.4.1. Predicted Mean Vote (PMV):	34
3.4.2. Universal Thermal Climate Index (UTCI):	34
3.4.3. Physiological Equivalent Temperature Index (PET):	35
Conclusion:	36
CHAPTER III: BUILDING MATERIALS AND CHARACTERISTICS: AN IN-DEPTH REVIEW OF MATERIAL THERMAL PROPRIETIES	37
Introduction:	37

1. Building Materials:	38
1.1. Definitions and History:	38
1.2. Classification of Building Materials:	40
1.3. Building Materials Properties:	41
1.4. Thermal properties of materials:	43
2. Glossary of Thermal Properties of Materials:	46
2.1. The Albedo:	46
2.2. Absorptivity (α):	47
2.3. Density (ρ):	47
2.4. Dry Density:	48
2.5. Emissivity (ϵ):	48
2.6. Reflectivity (ρ):	49
2.7. Roughness:	49
2.8. Specific Heat Capacity (c):	49
2.9. Thermal Bridging:	50
2.10. Thermal Capacity:	50
2.11. Thermal Conductance:	50
2.12. Thermal Conductivity (k or λ):	51
2.13. Thermal Diffusivity (α):	51
2.14. Thermal Effusivity (e):	51
2.15. Thermal Inertia (I):	52
2.16. Thermal Lag (Time Lag):	52
2.17. Thermal Mass:	53
2.18. Thermal Radiation:	54
2.19. Thermal Resistivity (R-value):	55
2.20. Transmissivity (τ):	55
3. Thermal Properties According to Algeria's Thermal Regulations for Residential Buildings (CNERIB):	55
Conclusion:	58
CHAPTER IV: LITERATURE REVIEW (PART A): A SYNTHESIS OF URBAN CLIMATE AND OUTDOOR THERMAL COMFORT	60
Introduction	60
1. Cluster identification and topic analysis:	62
2. Cluster identification and topic analysis:	63
2.1. Central concepts and bridging terms:	63

2.2. Quantitative Observations:	64
3. Cluster identification and topic analysis:	67
3.1. Emerging Topics:	67
3.2. Geographical Focus:	67
3.3. Quantitative Analysis:	67
3.4. Research Focus:	68
3.5. Methodological Approaches:	68
3.6. Emerging Concerns:	68
3.7. Temporal Dynamics:	69
Conclusion	81
CHAPTER V: LITERATURE REVIEW (PART B): A REVIEW OF MODELLING TECHNIQUES, CONTEXTUAL APPLICATIONS AND BUILDING MATERIALS.....	82
Introduction.....	82
Conclusion	94
CHAPTER VI: METHOD AND MATERIAL: METHODOLOGY, DATA COLLECTION, AND ANALYTICAL TECHNIQUES	96
Introduction.....	96
1. Research method	97
2. Case study	98
2.1. General climate conditions of the study context.....	98
2.2. Characterization of Biskra city housing sector	99
2.3. Building materials envelops' use within Biskra city over the history	101
2.3.1. Precolonial era (before 1848):	101
2.3.2. The colonial era (1848 - 1962):	102
2.3.3. After independence (after 1962):	103
2.3.4. The contemporary period (nowadays):	103
3. Continuous field measurement and model validation:	107
3.1. Field measurement protocol:	107
3.2. Sample selection:	108
3.3. Field measurement:	109
3.4. Validation and calibration of ENVI-met model:	111
4. Development of the Analysis Model:	112
4.1. Developing based-criteria:	112
4.1.1. Height-to-width (H/W) ratio variable:	112
4.1.2. Street orientation variable:	112

4.1.3. Building materials variable:.....	113
5. Numerical modelling Inputs and simulation via ENVI-met:	114
Conclusion:	119
CHAPTER VII: RESULTS AND ANALYSIS: PRESENTATION AND INTERPRETATION OF FIELD MEASUREMENTS AND SIMULATION RESULTS	120
Introduction.....	120
1. Assessment of the Mean Radiant Temperature (T _{mrt}):	120
2. Assessment of the Surface Temperature (T _s):.....	122
2.1. Thermal mapping of the surface temperature (T _s) by Leonardo interface:	124
3. Evaluation of the Physiological Equivalent Temperature Index (PET):	130
3.1. Evaluation of the thermal stress levels.....	132
Conclusion	140
CONCLUSION: CONCLUSION AND RECOMMENDATIONS.....	142
Conclusion and recommendations.....	142
1. Main Findings:	142
1.1. Thermal behavior of building materials:	142
1.1.1. Limestone emerged as the most effective material for mitigating heat stress:	142
1.1.2. Brick and Concrete showed pronounced thermal retention:.....	143
1.1.3. Adobe displayed intermediate performance:	143
1.2. Integration of building materials with urban canyon (street):	143
1.2.1. Height-to-Width ratio (H/W):.....	143
1.2.2. Impact of the street orientation:	144
1.3. Surface Temperature (T _s) Dynamics:.....	144
1.4. Mean Radiant Temperature (T _{mrt}) and radiative heat exchange:.....	144
1.5. Physiological Equivalent Temperature (PET):	145
1.6. Temporal patterns and diurnal cooling cycles:.....	145
2. Strengths of the research:.....	146
2.1. Innovative research focus:.....	146
2.1.1. Comprehensive and systematic scenario design:	146
2.1.2. Advanced methodological numerical tools:	146
2.2. Localized relevance with broader implications:.....	147
2.3. Granular analysis of building materials:	147
2.4. Interdisciplinary approach:	147
2.5. Practical urban design applications:	148
2.6. Climate-Responsive and sustainable focus:	148

3. Limitations of the research:	148
3.1. Limited temporal scope:	149
3.2. Assumptions in simulation models:	149
3.3. Limited exploration of energy implications:	149
3.4. Social and Behavioral Dimensions:	149
4. Recommendations for further research:	150
4.1. Seasonal and longitudinal analysis:	150
4.2. Dynamic vegetation modeling:	150
4.3. Innovative and emerging building materials:	150
4.4. Human-centric approaches:	151
REFERENCES	152

LIST OF FIGURES

Figure 1.1. Thesis outline of main steps and chapters	9
Figure 2.1. World Map of Köppen-Geiger climate classification updated with mean monthly CRU TS 2.1 temperature and VASCLimO v1.1 precipitation data for the period 1951 to 2000 on a regular 0.5-degree latitude/longitude grid	12
Figure 2.2. Key to calculate the climate formula of Köppen and Geiger for the main climates and subsequent precipitation conditions, the first two letters of the classification	13
Figure 2.4. Hierarchical diagrams of the different scales of urban climatology	15
Figure 2.5. Schematic topics concerned in urban climatology to the relevant spatial scales	16
Figure 2.6. Structure of the urban boundary layer. (Z_i) is the height of the urban boundary layer, (h_e) is the height of the urban canopy layer	17
Figure 2.7. The interplay of air temperature, relative humidity, and dew point over time.	19
Figure 2.8. Wind velocity in urban areas	20
Figure 2.9. Global solar radiation components: direct, diffuse, and reflected radiations	22
Figure 2.10. Schematic of the volumetric averaging approach to urban energy balance	23
Figure 2.11. (a) Schematic representation of an urban canyons and multiple reflections and absorption that occurs within it (processing of Nunez and Oke, 1977); (b) Schematic representation of the SVF (Unger, 2009); (c) Schematic representation of urban morphology capable of exploiting the contribution made by natural ventilation in UHI mitigation (processing of Santamouris et. Al, 1999)	26
Figure 2.12. Pavement surface energy balance	28
Figure 2.13. Distribution of UHI effect across different land use types	29
Figure 2.14. The Factors of outdoor thermal comfort	31
Figure 2.15. Relevant radiation fluxes and urban entities on the determination of outdoor MRT	32
Figure 2.16. The PMV Thermal Comfort Scale	34
Figure 3.1. The development of materials over time	39
Figure 3.2. The difference between high albedo surface and low albedo surface	47
Figure 3.4. Thermal mass introduces a time lag	52
Figure 3.5. The schematic representation of time lag and decrement factor	53
Figure 3.6. Behaviour of a semi-transparent material when receiving incident radiation	54
Figure 4.1. Literature review flowchart on the field of outdoor thermal comfort between 2012 – 2023	61
Figure 4.2. Literature review flowchart on the field of outdoor thermal comfort and building materials between 2008 – 2023	65
Figure 4.3. Literature review flowchart on the field of urban heat island (UHI) mitigation strategies between 2008 – 2023	66
Figure 4.4. Urban environment conditions' impact on human health and behavior: (a) Health outcomes and the urban environment: connections; (b) Connections of the urban heat island and health	76

Figure 6.1. Research Study Conceptual Framework from the data collection, modeling, simulations, and data analysis	97
Figure 6.2. Climatic conditions of the study context: (a) air temperature; (b) relative humidity	98
Figure 6.3. Different urban fabrics distribution within Biskra city, from precolonial tissue to contemporary period	99
Figure 6.4. Housing typology in the city of Biskra 2018 (Algerian National Statistics Office, 2018)	100
Figure 6.5. Adobe blocks implemented for walls in old houses throughout ancient urban fabrics in Biskra city	101
Figure 6.6. Stone blocks in the French buildings' typologies covering the external envelops	102
Figure 6.7. Testo Comfort Software Basic Interface: data logger configuration and data import	108
Figure 6.8. The location of the site in Biskra City	109
Figure 6.9. The field measurements of air temperature (T _{air}) and relative humidity (RH)	110
Figure 6.10. The developed scenarios based on: geometry, orientation and building materials	113
Figure 7.1. Hourly mean radiant temperature (MRT) values for the 24 scenarios, E-W (left) for the (A, B, C) ratio. N-S (right) for the (A, B, C) ratio	121
Figure 7.2. Box plots of surface temperatures (T _s) values: E-W orientation for the (A, B, C) ratios, (1) north side, (2) south side.	123
Figure 7.3. Box plots of surface temperatures (T _s) values: N-S orientation for the (A, B, C) ratios (1) east side, (2) West side	124
Figure 7.4. Surface temperature (T _s) values within E-W orientation, by Leonardo interface	125
Figure 7.5. Surface temperature (T _s) values within N-S orientation, by Leonardo interface	128
Figure 7.6. Hourly PET values for the 24 scenarios, E-W (left) for the (A, B, C) ratio. N-S (right) for the (A, B, C) ratio	132
Figure 7.7. Variation of human thermal stress levels within the 24 scenarios	134
Figure 7.8. Thermal behavior of the externally modelled walls	136
Figure 7.9. Virtual model of the thermal behavior of building materials within urban fabrics based on the research findings	141

LIST OF TABLES

Table 2.1. Overview of Common Thermal Comfort Indices and Their Descriptions.	33
Table 2.2. Universal Thermal Climate Index (UTCI) equivalent temperatures categorized in terms of thermal stress and thermal perception.	35
Table 2.3. Thermal perception classification according to PET values.	36
Table 3.1. Classification of building Materials.	40
Table 3.2. Classification of building Material Properties.	42
Table 3.3. Studies and Thermal Properties of Materials.	44
Table 3.4. Thermal Properties from ASHRAE, ISO, and DTR C 3-2.	45
Table 3.5. Thermal Properties of Buildings Materials as Defined by Algeria's DTR C 3-2.	56
Table 3.6. Thermal Properties of common Buildings Materials as Defined by Algeria's DTR C 3-2.	57
Table 4.1. Sample summary used of main recent literature about thermal comfort assessment and outdoor heat mitigation.	70
Table 4.2. Summary of various studies about the relationships among the spatial characteristics within cities and the thermal fluctuations under different weather conditions.	78
Table 4.3. Summary of characteristics of the studies on the thermal impact of a possible increase of urban albedo.	80
Table 5.1. Analysis of numerical tools for environmental and architectural simulation: a comparative overview.	83
Table 5.2. Summary of some relevant studies regarding relationships between buildings external envelopes and outdoor thermal fluctuations based on field measurements.	89
Table 6.1. Overview of distinct neighbourhoods containing various building materials characteristics in Biskra city: from the oldest to the recent.	105
Table 6.2. The details of the monitoring device used for this study.	107
Table 6.3. Statistical metrics for the validation of the numerical models.	111
Table 6.4. Thermal properties of building materials used within the studies scenarios.	114
Table 6.5. ENVI-met modelling inputs parameters: space geometry, model geometry, construction material, and simulation.	117
Table 7.1. Building materials' external thermal efficiency related to H/W ratio and street orientation.	138

CHAPTER I: INTRODUCTION, PROBLEMATIC EXPLORATION AND RESEARCH OBJECTIVES

Introduction

1. Background and Context

The 21st century has been marked by unprecedented urban growth, with the United Nations projecting that 68% of the world's population will reside in urban areas by 2050 (UN DESA, 2018). This rapid urbanization presents numerous challenges, among which the management of urban microclimates stands out as a critical issue, particularly in regions characterized by hot arid climates. The transformation of natural landscapes into built environments significantly alters local climate patterns, often resulting in phenomena such as the Urban Heat Island (UHI) effect, which can exacerbate thermal stress for city dwellers (Oke et al., 2017).

In the context of global climate change, where extreme heat events are predicted to increase in frequency and intensity (IPCC, 2021), the need to create thermally comfortable urban spaces has become more pressing than ever. This is especially true for hot arid regions, where cities must contend with naturally challenging climatic conditions that are further aggravated by urbanization processes.

The built environment, comprising buildings, streets, and other urban infrastructure, plays a pivotal role in shaping the thermal conditions experienced at the pedestrian level. Urban geometry, material properties, anthropogenic heat emissions, and the presence or absence of vegetation all contribute to the complex thermal dynamics of city spaces (Santamouris, 2015). Among these factors, the thermal properties of building materials have emerged as a crucial yet often underexplored component in the quest for improved outdoor thermal comfort.

2. Problem Statement and Research Gap:

While extensive research has been conducted on various aspects of urban design and its impact on thermal comfort including studies on urban canyon effects (Oke, 1988), the cooling potential of urban greenery (Bowler et al., 2010), and the influence of urban morphology on pedestrian comfort (Sharmin et al., 2017) there remains a significant knowledge gap regarding the specific influence of building materials on outdoor thermal conditions in hot arid climates. Previous studies have

predominantly focused on the energy efficiency of buildings (Akbari et al., 2016) or the mitigation of the UHI effect at a macro scale (Santamouris, 2014). However, the direct impact of building material choices on pedestrian-level thermal comfort in arid urban contexts has not been comprehensively examined. This gap is particularly notable given the unique challenges posed by hot arid climates, where intense solar radiation and high ambient temperatures create an urgent need for effective heat mitigation strategies. Furthermore, while the concept of ‘cool materials’ has gained traction in urban heat mitigation efforts (Santamouris et al., 2011), the application and effectiveness of these materials in the specific context of hot arid urban environments remain understudied. There is a need for a nuanced understanding of how different building materials interact with the extreme climatic conditions of arid regions to influence outdoor thermal comfort at the micro-urban scale.

3. Research Questions and Objectives:

In light of these identified gaps, this research aims to address the following key questions:

- a. What is the impact of building materials’ envelopes on outdoor thermal comfort in hot dry climate, with a particular focus on the critical summer season under extreme weather conditions?
- b. What are the key parameters of building materials that contribute to improving outdoor thermal comfort in hot dry cities?

The main objectives of this research are:

- c. Quantify the thermal performance of various building materials commonly used in hot dry climates within different urban geometries and streets orientations.
- d. Develop a comprehensive understanding of the relationships between building material properties, built environment, and outdoor thermal comfort metrics in hot dry climates.
- e. Formulate evidence-based guidelines for the selection and application of optimal or nearly optimal building materials to improve outdoor thermal comfort in hot dry cities.

4. Research Hypotheses:

Based on preliminary literature review and initial observations, we propose the following hypotheses:

- a. The thermal properties of building envelope materials in hot dry climates significantly influence outdoor thermal comfort levels, particularly during summer peak hours, through their impact on surface temperatures and radiation heat exchange. Therefore, higher albedo materials and those with lower thermal storage capacity are expected to reduce the urban heat stress experienced by pedestrians, specifically in hot dry climate within extreme weather conditions.
- b. The optimization of specific building material parameters (such as albedo, conductivity, emissivity, and thermal mass) can lead to remarkable improvements in outdoor thermal comfort levels in hot dry cities, with their effectiveness varying based on the material's application location within the building envelope.

5. Methodology Overview:

To address these research questions and test our hypotheses, we employ a multi-faceted methodological approach that combines empirical measurements, advanced numerical modeling, and statistical analysis. Our methodology encompasses the following key components:

5.1 Multi-criteria Selection of Building Materials:

We start with a comprehensive review and selection of building materials based on their thermal properties, including but not limited to solar reflectance, infrared emittance, and solar reflectance. This selection process is informed by an extensive review of both local and international literature, with a focus on materials relevant to our study context. We pay particular attention to both traditional materials used in vernacular architecture of arid regions and modern materials with potential heat-mitigating properties.

5.2 Field Measurements and Data Collection:

Comprehensive microclimatic measurements are conducted within selected urban zones of Biskra, Algeria, during peak thermal stress periods. These measurements, carried out over long-term field measurements during the hottest days of the year, serve to:

- a. Calibrate our numerical models,
- b. Provide ground-truth data for subsequent analyses,
- c. Capture the diurnal and nocturnal variations in thermal conditions,

- d. Parameters measured include air temperature, and relative humidity.

5.3 Numerical Parameterization and Simulation:

We utilize advanced computational tools, specifically ENVI-met (CFD) software integrated with environmental analysis plugins, to develop numerical models of urban environments. These models allow us to:

- a. Simulate a wide range of urban configurations and material combinations
- b. Analyze the impact of various factors on outdoor thermal comfort
- c. Generate a comprehensive dataset for statistical analysis

5.4 Statistical Analysis and Findings Discussion:

Employing statistical techniques, including multiple regression analysis, we aim to:

- a. Identify significant relationships between building material properties, urban geometry, and thermal comfort levels.
- b. Elaborate guidelines for building material selection and evaluate their impact on outdoor thermal environment, with specific focus on residential building typologies.
- c. Quantify the relative importance of different factors in determining thermal comfort sensitivity.

5.5 Validation and Guideline Development:

The final phase of our methodology involves:

- a. Synthesizing our findings into practical guidelines for material selection and application.
- b. Developing recommendations for urban planning and design practices in hot dry regions.

6. Study Context: Biskra, Algeria:

Our research is contextualized within Biskra, a populous Saharan city in Algeria, classified as BWh under the Köppen-Geiger climate classification system. This location provides an ideal setting for our research due to several factors:

- a. Representative hot dry climate: Biskra experiences a hot desert climate, characterized by extremely hot summers, mild winters, and very low annual precipitation. This climate is representative of many rapidly growing urban areas in arid regions globally.

- b. Diverse urban morphology: the city encompasses a range of urban fabrics, from traditional compact layouts to modern, more open urban configurations. This diversity allows for the examination of material performance across various urban geometries.
- c. Rapid urban growth: like many cities in developing countries, Biskra is experiencing rapid urbanization, making it an important case study for developing sustainable urban design strategies.
- d. Cultural and historical significance: as part of the Ziban region, Biskra has a rich cultural heritage, including traditional building practices adapted to the local climate. This allows for the study of both vernacular and contemporary building materials and techniques.

7. Significance and Potential Impact:

This research aims to bridge a critical gap in our understanding of urban thermal dynamics in hot arid climates. By focusing on the role of building materials in shaping outdoor thermal comfort, we address an often overlooked but crucial aspect of urban design in these challenging environments. The potential impacts of this research include:

- a. Informing evidence-based urban design: our findings can guide urban planners, architects, and policymakers in making informed decisions about material selection and application in hot arid urban contexts.
- b. Enhancing urban livability: by contributing to improved outdoor thermal comfort, this research has the potential to enhance the overall livability and usability of urban spaces in hot arid regions.
- c. Climate change adaptation: the insights gained from this study can inform climate adaptation strategies for cities in arid regions, helping to build resilience against increasing heat stress due to global climate change.
- d. Advancing urban climatology: our methodology and findings will contribute to the broader field of urban climatology, particularly in the context of arid regions which have been relatively understudied compared to temperate climates.
- e. Energy conservation: by optimizing outdoor thermal comfort through passive means, this research may indirectly contribute to reduced energy consumption for cooling in buildings.

8. Thesis Structure:

This thesis is mainly structured as follows:

- **Chapter I:** *Introduction, problematic exploration and research objectives.*

The introduction sets the foundation for this research by addressing the critical challenges of urban thermal comfort in the context of rapidly evolving cities. This chapter establishes the research gap regarding how building materials within built environment influence outdoor thermal comfort, specifically in the context of Biskra, arid climate. Clear research objectives are outlined, focusing on quantifying the relationship between building material properties, built environment configuration, and microclimate conditions. The chapter presents specific hypotheses about how different building materials and urban layouts affect thermal comfort parameters. Research boundaries are clearly defined, acknowledging both the scope and limitations of the study.

- **Chapter II:** *Urban climate and outdoor thermal comfort: theoretical insights and studies.*

The theoretical framework of urban climatology is extensively explored in this chapter, beginning with fundamental concepts and extending to complex urban atmospheric phenomena. It provides an analysis of urban heat island formation, examining the various factors that contribute to its intensity and distribution. The chapter explores the intricate relationships between urban morphology and local climate modifications, including the effects of building density, street configuration, and anthropogenic heat sources. Global research on urban climate is reviewed, presenting significant findings from different geographical and climatic contexts.

- **Chapter III:** *Building materials and characteristics: an in-depth review of material thermal properties.*

This chapter presents a comprehensive analysis of building materials commonly used, examining their thermal behavior and impact on urban microclimates. It delves into the fundamental properties of materials, including their thermal conductivity, heat capacity, and surface characteristics such as albedo and emissivity. The review encompasses both traditional and contemporary building materials. The chapter includes detailed case studies demonstrating how material selection influences building energy performance and outdoor thermal conditions. The

evolution of building material technologies and their role in sustainable urban development is thoroughly examined.

- **Chapter IV:** *Literature review (Part A): a synthesis of urban climate and outdoor thermal comfort.*

This chapter synthesizes current knowledge on outdoor thermal comfort, examining the complex interplay between human physiology/biometeorology, urban design, and building envelopes through numerous field studies. It provides a detailed analysis of various thermal comfort indices and their applicability in different contexts.

- **Chapter V:** *Literature review (Part B): a review of modelling techniques, contextual applications and building materials.*

This chapter explores the use of numerical modelling tools for building materials parameterization, and reviews the most relevant studies from different climatic regions, analyzing how building materials and urban form influence thermal comfort perceptions.

- **Chapter VI:** *Method and materials: methodology, data collection, and analytical techniques.*

This chapter outlines the comprehensive research methodology employed in the study. It details the systematic approach to field measurements, including the selection of climatic measurement parameters monitored, and equipment specifications in Biskra city as study area. The protocol for data collection and quality control is thoroughly explained. As well, the chapter then describes the ENVI-met simulation steps, including model parameterization, calibration procedures, and validation methods. The integration of field measurements with computational simulations is explained, demonstrating how both approaches complement each other to provide a robust analysis. Data analysis methods are detailed, including statistical metrics and comfort index calculations such as Physiological Equivalent Temperature (PET). The methodology is designed to ensure reliable and reproducible results while addressing the research objectives.

- **Chapter VII:** *Results and analysis: presentation and interpretation of field measurements and simulation results.*

The findings from both field measurements and numerical simulations are presented in this chapter, providing a comprehensive approach of the thermal environment in Biskra's urban areas. Results include detailed temporal and spatial analyses of thermal parameters, building material temperature profiles, and microclimate characteristics. The ENVI-met simulation results are presented through temperature distribution maps, wind flow patterns, and thermal comfort index distributions. Comparative analyses of different 24 designed urban scenarios demonstrate the impact of various design choices on thermal comfort. Statistical analyses reveal significant relationships between urban design parameters and thermal comfort indicators. The chapter presents these findings through clear visualizations and detailed explanations. Although, this chapter provides a critical synthesis of the research findings, integrating results from field measurements and numerical simulations to address the initial research questions and hypotheses.

- **Conclusion:** *Conclusion and recommendations.*

The conclusion chapter synthesizes the key findings of the research and demonstrates how the study objectives were achieved. It provides practical recommendations for urban planners and designers, including specific guidelines for material selection and urban geometry optimization to enhance thermal comfort. The limitations of the study are acknowledged, and future research directions are proposed to address remaining questions and challenges. The chapter concludes by highlighting the significant contributions of this research to both theoretical understanding and practical applications in urban design and planning. Policy implications are discussed, emphasizing how findings can inform better urban development practices in similar climatic contexts.

Through this structured approach, we aim to provide a comprehensive examination of the role of building materials in shaping outdoor thermal comfort in hot arid urban environments, contributing valuable insights to the fields of urban climatology, sustainable urban design, and architectural engineering. Figure 1.1 presents the general research framework and outlines with the main steps and methods.

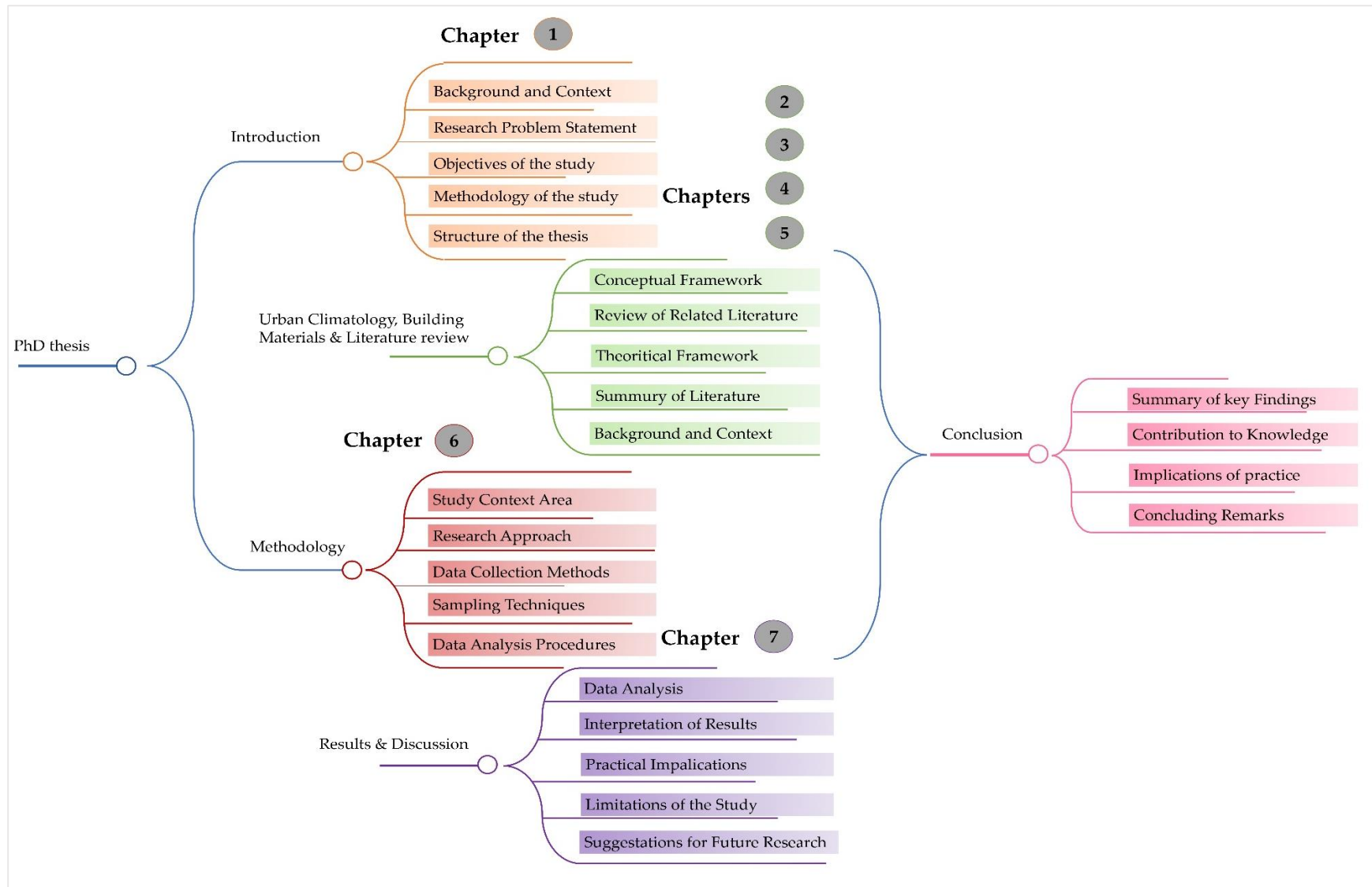


Figure 1.1. Thesis outline of main steps and chapters.

Source: Author, 2020.

CHAPTER II: URBAN CLIMATE AND OUTDOOR THERMAL COMFORT: THEORITICAL INSIGHTS AND STUDIES

Introduction:

Urban climatology is an essential discipline that examines the intricate relationships between urban environments and the atmospheric processes that influence them. Understanding these dynamics is essential for reducing the adverse effects of extreme weather and enhancing outdoor thermal comfort in hot, dry regions like Biskra's. The purpose of this chapter is to first define urban climatology and discuss how it relates to sustainable urban development. Urban heat islands (UHIs), which are defined by greater temperatures in cities relative to nearby rural regions because of changes in land cover, human activity, and the density of built buildings, are among the major climate phenomena seen in urban areas that are covered first (Oke, 1987). This section also emphasizes how wind patterns, radiation balance, and heat retention influence urban climates, and gives a basis for comprehending the ensuing urban climate challenges. The chapter looks at the main determinants of urban climate, with particular attention on land surface features, urban morphology, and human-caused heat emissions. How heat is absorbed, stored, and released in cities is greatly influenced by urban morphology, which includes the urban canyons, buildings, and open areas (Grimmond & Oke, 2002). Furthermore, the selection of building materials and their thermal characteristics have a direct impact on how urban spaces regulate their temperature (Santamouris, 2015). High thermal mass materials, for example, are better at absorbing and releasing heat, which lessens daytime and nighttime temperature variations. The chapter also looks into how human activities like industrial processes and transportation contribute to the emission of pollutants and heat, which exacerbates the urban heat island effect (Landsberg, 1981).

Additionally, the chapter's second section explores outdoor thermal comfort, defining it and outlining the different indices and factors that impact people's thermal experience in outdoor urban settings. This section guarantees a thorough comprehension of both the environmental factors influencing urban climates and the human centered aspects of thermal comfort, which is essential for enhancing urban quality of life. The second part presents a variety of indices for evaluating outdoor thermal comfort, including the Predicted Mean Vote (PMV), the Physiologically Equivalent Temperature (PET), and the Universal Thermal Climate Index (UTCI) (Fanger, 1970).

These indices aid in measuring the temperature in outdoor areas and offer a framework for comprehending the ways in which various urban components.

1. Overview on Climate:

1.1. Definition of climatology and climate:

Climatology is the scientific study of climate, scientifically defined as weather conditions averaged over a period of time. It encompasses the study of average weather conditions for an area over long periods, typically spanning at least 30 years, as well as the investigation of climate patterns, variations, and changes over space and time (Oliver, 2005).

According to the American Meteorological Society (AMS, 2019), climatology is "the description and scientific study of climate," where climate refers to the "slowly varying aspects of the atmosphere–hydrosphere–land surface system."

Climate represents the composite or generally prevailing weather conditions of a region, including temperature, air pressure, humidity, precipitation, sunshine, cloudiness, and winds, throughout the year, averaged over a series of years (World Meteorological Organization [WMO], 2017). The World Meteorological Organization defines climate as the statistical description of weather conditions over a period of time, typically 30 years (WMO, 2017).

According to (GIVONO, 1978), the climate of a given region is determined by regimes of variations of several elements and by their combinations. The main climatic elements to be considered when designing buildings are solar radiation, long-wavelength radiation from the sky, air temperature, humidity, wind and precipitation.

1.2. Climate classification:

Climate classification involves categorizing the world's regions based on their prevailing weather patterns, temperature, precipitation, and vegetation types. The most widely used climate classification system is the Köppen-Geiger classification (Figure 2.1), first developed by Wladimir Köppen in 1884 and later modified by Rudolf Geiger. This system divides the world's climates into five main groups (Kottek & al., 2006).

Major Climate Types:

A - Tropical Climates: High temperatures year-round and significant precipitation.

B - Dry Climates: Low precipitation, subdivided into arid (desert) and semi-arid (steppe) regions.

C - Temperate Climates: Moderate temperatures with seasonal variation.

D - Continental Climates: Large seasonal temperature variations with cold winters.

E - Polar Climates: Extremely cold temperatures with minimal vegetation.

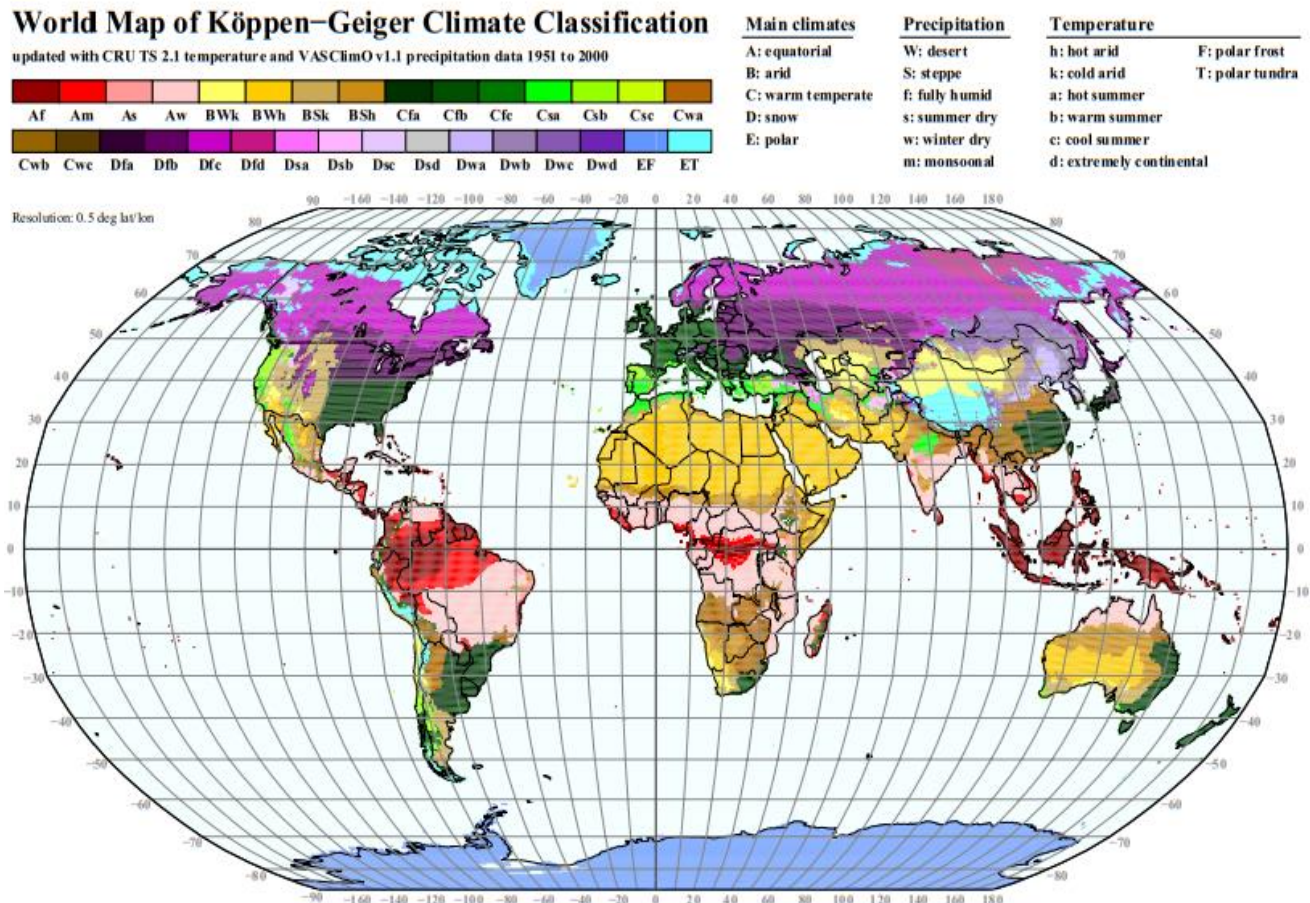


Figure 2.1. World Map of Köppen-Geiger climate classification updated with mean monthly CRU TS 2.1 temperature and VASCLimO v1.1 precipitation data for the period 1951 to 2000 on a regular 0.5-degree latitude/longitude grid.

Source: Kottek et al, 2006.

The first two letters of the classification (Figure 2.2): for the polar climates (E) no precipitation differentiations are given, only temperature conditions are defined. This key implies that the polar climates (E) have to be determined first, followed by the arid climates (B) and subsequent

differentiations into the equatorial climates (A) and the warm temperate and snow climates (C) and (D), respectively (Kottek & al, 2006).

Type	Description	Criterion
A	Equatorial climates	$T_{\min} \geq +18^{\circ}\text{C}$
Af	Equatorial rainforest, fully humid	$P_{\min} \geq 60 \text{ mm}$
Am	Equatorial monsoon	$P_{\text{ann}} \geq 25 (100 - P_{\min})$
As	Equatorial savannah with dry summer	$P_{\min} < 60 \text{ mm in summer}$
Aw	Equatorial savannah with dry winter	$P_{\min} < 60 \text{ mm in winter}$
B	Arid climates	$P_{\text{ann}} < 10 P_{\text{th}}$
BS	Steppe climate	$P_{\text{ann}} > 5 P_{\text{th}}$
BW	Desert climate	$P_{\text{ann}} \leq 5 P_{\text{th}}$
C	Warm temperate climates	$-3^{\circ}\text{C} < T_{\min} < +18^{\circ}\text{C}$
Cs	Warm temperate climate with dry summer	$P_{\text{smin}} < P_{\text{wmin}}, P_{\text{wmax}} > 3 P_{\text{smin}}$ and $P_{\text{smin}} < 40 \text{ mm}$
Cw	Warm temperate climate with dry winter	$P_{\text{wmin}} < P_{\text{smin}}$ and $P_{\text{smax}} > 10 P_{\text{wmin}}$
Cf	Warm temperate climate, fully humid	neither Cs nor Cw
D	Snow climates	$T_{\min} \leq -3^{\circ}\text{C}$
Ds	Snow climate with dry summer	$P_{\text{smin}} < P_{\text{wmin}}, P_{\text{wmax}} > 3 P_{\text{smin}}$ and $P_{\text{smin}} < 40 \text{ mm}$
Dw	Snow climate with dry winter	$P_{\text{wmin}} < P_{\text{smin}}$ and $P_{\text{smax}} > 10 P_{\text{wmin}}$
Df	Snow climate, fully humid	neither Ds nor Dw
E	Polar climates	$T_{\text{max}} < +10^{\circ}\text{C}$
ET	Tundra climate	$0^{\circ}\text{C} \leq T_{\text{max}} < +10^{\circ}\text{C}$
EF	Frost climate	$T_{\text{max}} < 0^{\circ}\text{C}$

Figure 2.2. Key to calculate the climate formula of Köppen and Geiger for the main climates and subsequent precipitation conditions, the first two letters of the classification.

Source: Kottek et al, 2006.

The third letter temperature classification (Figure 2.3): (h) and (k) for the arid climates (B) and (a) to (d) for the warm temperate and snow climates (C) and (D). Note that for type (b), warm summer, a threshold temperature value of $+10^{\circ}\text{C}$ has to occur for at least four months (Kottek & al, 2006).

Type	Description	Criterion
h	Hot steppe / desert	$T_{\text{ann}} \geq +18^{\circ}\text{C}$
k	Cold steppe / desert	$T_{\text{ann}} < +18^{\circ}\text{C}$
a	Hot summer	$T_{\text{max}} \geq +22^{\circ}\text{C}$
b	Warm summer	not (a) and at least 4 $T_{\text{mon}} \geq +10^{\circ}\text{C}$
c	Cool summer and cold winter	not (b) and $T_{\min} > -38^{\circ}\text{C}$
d	extremely continental	like (c) but $T_{\min} \leq -38^{\circ}\text{C}$

Figure 2.3. Key to calculate the third letter temperature classification.

Source: Kottek et al, 2006.

2. Urban climate:

2.1. Definition of urban climate:

Urban climate refers to the modified atmospheric conditions in urban areas resulting from the interaction between the built environment and atmospheric processes. It encompasses all atmospheric and surface conditions that differ from those of the surrounding rural areas due to urban development and human activities (Oke et al., 2017).

According to Landsberg (1981), urban climate is "the modification of the local climate by the works of man, with the city being the most dramatic example of such modification."

Urban areas alter local climate patterns through changes in surface properties, reduced vegetation, and increased energy consumption, leading to phenomena like the Urban Heat Island (UHI), where urban temperatures are higher than surrounding rural areas (Oke, 1987). Urban climate is influenced by factors such as building density, surface materials, anthropogenic heat emissions, and air pollution.

2.2. Scales of urban climate:

Urban climate represents a complex system of atmospheric modifications created by the interaction between cities and their environment. The study of urban climate requires understanding different spatial scales (Figure 2.4), as atmospheric processes in urban areas operate across multiple dimensions and interact in complex ways (Oke et al., 2017).

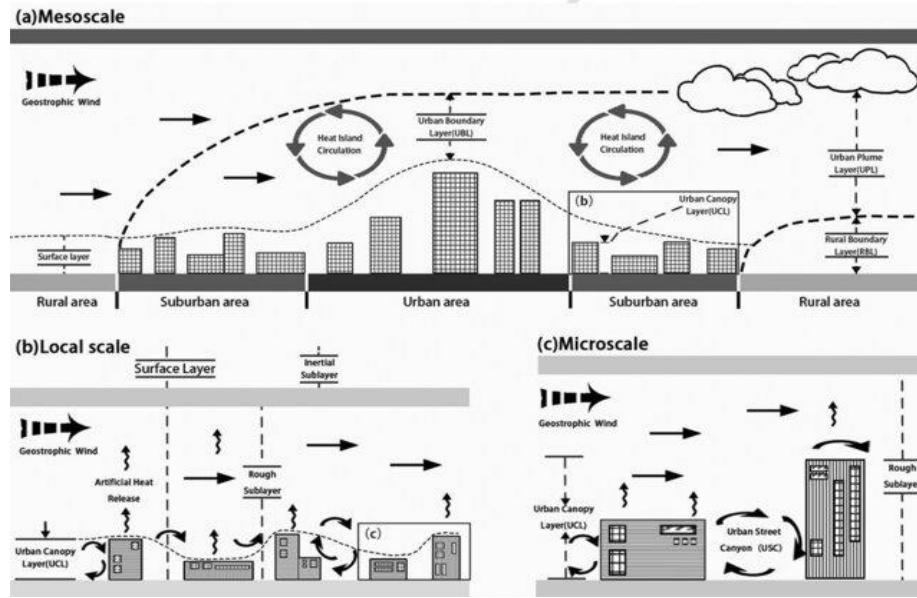


Figure 2.4. Hierarchical diagrams of the different scales of urban climatology.

Source: Urban Environments by Timothy R. Oke.

2.2.1. Horizontal scales of urban climate:

Urban climate can be studied at varying horizontal spatial extents, from small localized areas to entire metropolitan regions and beyond, traditionally recognize three main spatial scales for analyzing urban atmospheric phenomena (Figure 2.5), micro-, local- and, meso-scales (Arnfield, 2003):

- **Microscale (10^{-2} - 10^3 m):** Encompasses individual buildings, streets, and urban canyons. At this scale, atmospheric conditions are primarily influenced by the immediate surroundings, such as building materials, geometry, and local heat sources.
- **Local scale (10^2 - 5×10^4 m):** Represents neighborhoods or city districts with similar urban characteristics. This scale captures phenomena like local heat islands and wind patterns influenced by the urban fabric.
- **Mesoscale (10^4 - 2×10^5 m):** Covers entire cities and their surrounding areas, showing the broad impact of urbanization on regional climate patterns.

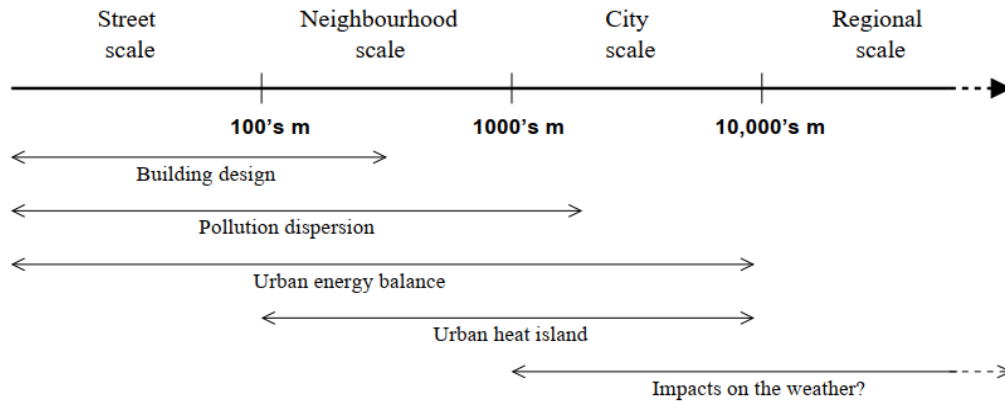


Figure 2.5. Schematic topics concerned in urban climatology to the relevant spatial scales.

Source: Britter and Hanna, 2003.

This (Figure 2.5) illustrates the spatial scales at which different urban environmental phenomena occur and interact, from street level to regional dimensions. At the smallest scale (~100 to 200 m), building design primarily influences local conditions. Moving up in scale, pollution dispersion extends from street to neighborhood levels (~1 to 2 km), while urban energy balance operates across neighborhood to city scales (~10 to 20 km). The urban heat island effect manifests most prominently at the city to regional scale (~100 to 200 km), ultimately contributing to broader weather impacts at the regional scale and beyond.

2.2.2. Vertical scales of urban climate:

The urban atmosphere is divided into layers, from the urban canopy layer (UCL), where buildings and vegetation dominate, to the urban boundary layer (UBL), which extends above cities and interacts with larger atmospheric systems (Figure 2.6). These vertical structures help explain how urban modifications affect heat, wind, and pollution dispersion.

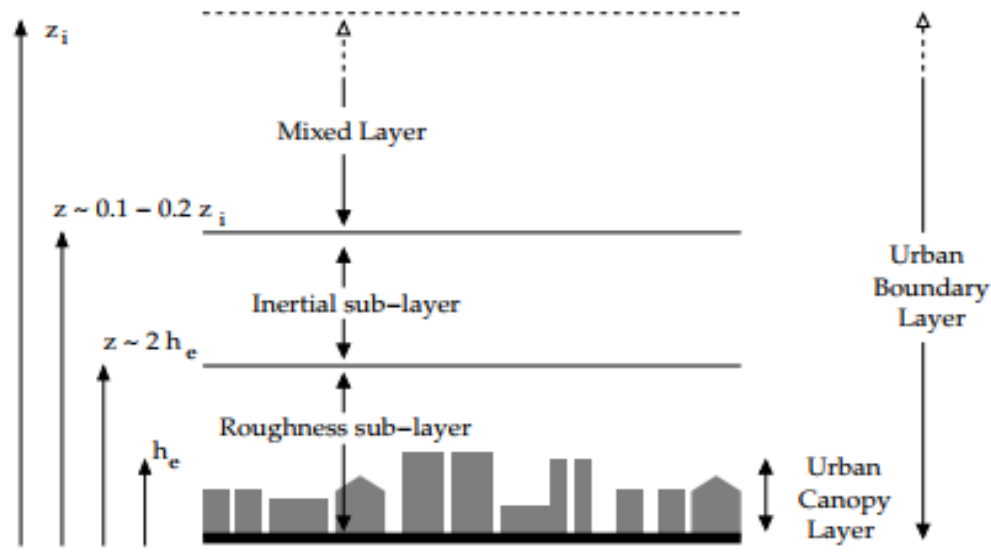


Figure 2.6. Structure of the urban boundary layer. (z_i) is the height of the urban boundary layer, (h_e) is the height of the urban canopy layer.

Source: Roth, 2000.

- Urban Canopy Layer (UCL):

The **Urban Canopy Layer (UCL)** is the lowest layer of the atmosphere within an urban environment, extending from the ground to the average height of buildings and other structures. It is directly influenced by the built environment, vegetation, and human activities. Within this layer, the effects of urban surfaces and human activities dominate, creating microclimates characterized by spatial variability in temperature, humidity, and airflow.

- Strongly influenced by urban geometry and surfaces (Oke 1976, 1988)
- Characterized by modified heat, moisture, and momentum fluxes (Roth 2000)
- Important for understanding urban microclimate, pollutant dispersion, and building design (Grimmond et al. 2010, Harman & Belcher 2006)

- Urban Boundary Layer (UBL):

The **Urban Boundary Layer (UBL)** is the atmospheric layer above the urban environment that is directly influenced by urbanization. It extends from the top of the **Urban Canopy Layer** to the height where urban effects dissipate into the surrounding atmosphere. The UBL can reach heights

ranging from a few hundred meters during the night to several kilometers during the day, depending on atmospheric stability, wind speed, and heat emissions from the urban surface.

- Influenced by the integrated effects of the urban surface (Oke 1976, 1982)
- Exhibits enhanced turbulence, modified heat and moisture fluxes (Rotach 1993)
- Crucial for urban weather forecasting and regional climate modeling (Barlow 2014)

2.3. The elements of urban climate:

The “climate” of a given region is determined by the pattern of variations of several elements and their combinations. The principal climatic elements, when human comfort and building design are being considered, are solar radiation, longwave radiation to the sky, air temperature, humidity, wind and precipitation such as rain, snow, etc. (Givoni, 1976).

The urban climate is a localized climate specific to cities and towns, distinct from the surrounding rural climate. This phenomenon arises due to the unique combination of natural and anthropogenic factors present in urban areas. Understanding the elements of urban climate is essential for addressing challenges such as thermal comfort, air quality, energy consumption, and urban heat islands, especially in the context of climate-sensitive urban planning and design.

2.3.1. Temperature:

Temperature is a fundamental element of urban climate that plays a crucial role in characterizing the thermal environment of cities. Urban areas typically experience higher temperatures compared to their rural surroundings due to the urban heat island (UHI) effect. This is caused by factors such as reduced vegetation, heat-retaining materials (e.g., asphalt, concrete), and waste heat from buildings and vehicles.

Givoni (1976), reports that the rate of heating and cooling of the surface of the earth is the main factor determining the temperature of the air above it. As the air is transparent to almost all solar radiation, it has only an indirect effect on air temperature.

2.3.2. Humidity:

Humidity is a fundamental concept in microclimatology and is considered an essential element for thermal comfort as well. Humidity refers to the amount of water vapor present in the air (Oliver,

2008). It is a key element of urban climate, as it is influenced by various factors within the urban environment.

Givoni (1976) reports that the moisture content of the atmosphere can be expressed in several terms, such as the absolute humidity, specific humidity, vapour pressure and relative humidity. Absolute humidity is defined as the weight of water vapour per unit volume of air (g/m^3) and the specific humidity as the weight of water vapour per unit weight of air (g/kg). The vapour pressure of the air is the part of the whole atmospheric pressure that is due to the water vapour and is measured in mm Hg. The relative humidity at any temperature is the ratio of the actual absolute humidity to the maximum moisture capacity of the air at that temperature which can be defined as the percentage of the absolute saturation humidity.

- **Relation between temperature and relative humidity:**

There is an inverse relationship between relative humidity and air temperature for a given location. Relative humidity reaches its highest values when air temperature is at its lowest (typically at night) and decreases as air temperature rises during the day" (Ackerman, 1987; Comet, 2016).

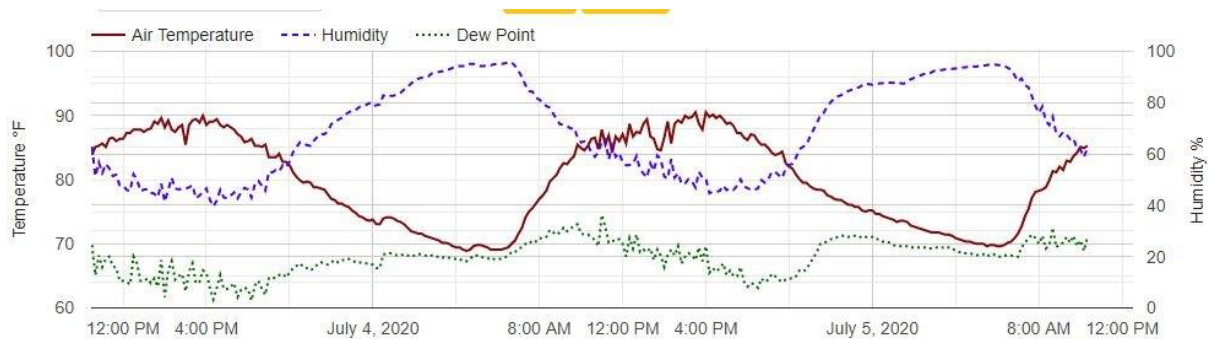


Figure 2.7. The interplay of air temperature, relative humidity, and dew point over time.

Source: Weather Briefing, L.C, July 2020.

The meteograph (Figure 2.7) above is from the Weather Briefing, LC weather station. It graphs temperature, dew point, relative humidity and time during a 48-hour period. Graphs are very useful for visualizing relationships between weather elements.

The solid red line is temperature, the dotted green line is dew point where air becomes saturated and condensation begins. It provides a direct measure of moisture in the air and its interplay with temperature., and the dashed magenta/blue line is relative humidity. Time is plotted on the

horizontal axis. Temperature is plotted on the left vertical axis and relative humidity is plotted on the right vertical axis.

This interplay highlights the diurnal cycle typical of urban and natural climates, where relative humidity depends strongly on temperature variations. When the air temperature approaches the dew point at night, saturation occurs, leading to conditions favorable for dew formation or fog, especially in humid climates. During the day, reduced relative humidity may contribute to perceived dryness, while elevated temperatures paired with a high dew point may lead to discomfort due to reduced evaporative cooling efficiency. This dynamic is particularly relevant in urban climates, where increased surface temperatures exacerbate such variations through the urban heat island effect (Givoni, 1998; Oke, 1987).

2.3.3. Wind:

According to Givoni (1976), the distribution and characteristics of the winds over a region are determined by several global and local factors. The main determinants are the seasonal global distribution of air pressure, the rotation of the earth, the daily variations in heating and cooling of land and sea and topography of the given region and its surroundings.

Several factors influence wind flow through urban areas (Figure 2.8), leading to a gradual reduction in wind speed. Some of these factors are related to the Earth's surface, while others are associated with the shape of buildings and the overall urban configuration (Houda & al., 2011).

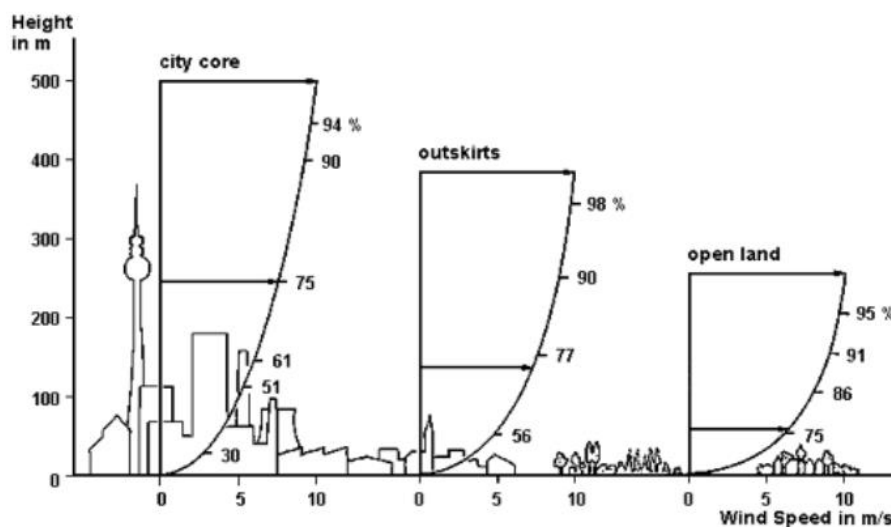


Figure 2.8. Wind velocity in urban areas.

Source: Hudişteanu, et al , 2018.

2.3.4. Precipitation:

Precipitation is any form of water (liquid or solid) that condenses in the atmosphere and falls to the ground. It includes rain, snow, sleet, hail, and drizzle, and it results from atmospheric processes that transport and cool moist air, leading to condensation and the formation of water droplets or ice crystals in clouds. Once these droplets or crystals grow large enough to overcome atmospheric resistance, they fall as precipitation.

2.3.5. Solar Radiation:

Solar radiation refers to the energy emitted by the Sun, which reaches the Earth in the form of electromagnetic waves. This radiation includes a spectrum of wavelengths from short ultraviolet (UV) rays to long infrared (IR) radiation. It is the primary source of energy for the Earth's climate system, driving atmospheric processes, ocean currents, and plant growth (Tiwari & Ghosal, 2011).

In urban areas, the radiative balance is influenced by both solar radiation and radiation emitted from the Earth's surface. These two types of radiation contribute to the energy exchanges that determine local temperature, the urban heat island effect, and overall climatic conditions.

A. Short-Wavelength Radiation:

This type of radiation includes (Figure 2.9):

- Direct Solar Radiation: The sunlight that reaches the Earth without being scattered or diffused. It is the most intense form of solar radiation.
- Diffuse Solar Radiation: This is the portion of solar radiation that has been scattered by particles in the atmosphere. While it is less intense than direct solar radiation, it still significantly contributes to the overall energy received by the Earth.
- Reflected Solar Radiation: This is radiation that is reflected off surfaces (like buildings, roads, and natural terrain) after being incident on them. The amount of reflection depends on the albedo of the surface.

Short-wavelength radiation is crucial in determining the energy received at the surface, especially during daylight hours. It affects urban temperatures, as cities tend to absorb and retain more heat compared to rural areas, partly due to the urban "heat island" effect. (Santamouris & Kolokotsa, 2013)

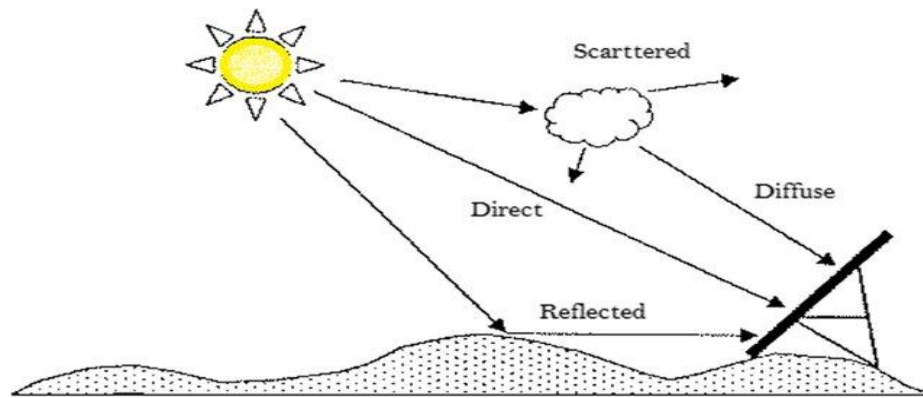


Figure 2.9. Global solar radiation components: direct, diffuse, and reflected radiations.

Source: El Mghouchi, 2022.

B. Long-Wavelength Radiation:

Long-wavelength radiation consists of:

- Radiation from the Atmosphere and Sky: The atmosphere, particularly clouds and water vapor, can absorb and emit radiation, especially in the infrared range. This radiation is typically reradiated back toward the surface.
- Radiation from the Earth's Surface: The Earth emits long-wavelength infrared radiation after absorbing solar energy. Surfaces like buildings, roads, and other urban features absorb solar radiation and then emit it back in the form of thermal radiation.

2.4. The urban energy balance:

The urban energy balance refers to the complex set of energy exchanges occurring in urban environments, primarily driven by human activity, urban infrastructure, and atmospheric conditions. It quantifies how energy from various sources (solar radiation, anthropogenic heat, etc.) is absorbed, reflected, and redistributed within urban areas (Oke, 1987). The urban energy balance plays a vital role in understanding urban microclimates, including phenomena such as the Urban Heat Island (UHI) effect.

The urban energy balance is the accounting of all energy fluxes at the urban surface (Figure 2.10). It includes contributions from natural sources (e.g., solar radiation) and human-induced sources (e.g., industrial heat) (Grimmond & Oke 1999). It is often expressed as:

$$Q_* = Q_H + Q_E + Q_G + Q_F \quad (2.1)$$

Where:

- Q_* : Net all-wave radiation.
- Q_H : Sensible heat flux.
- Q_E : Latent heat flux.
- Q_G : Ground heat flux.
- Q_F : Anthropogenic heat flux.

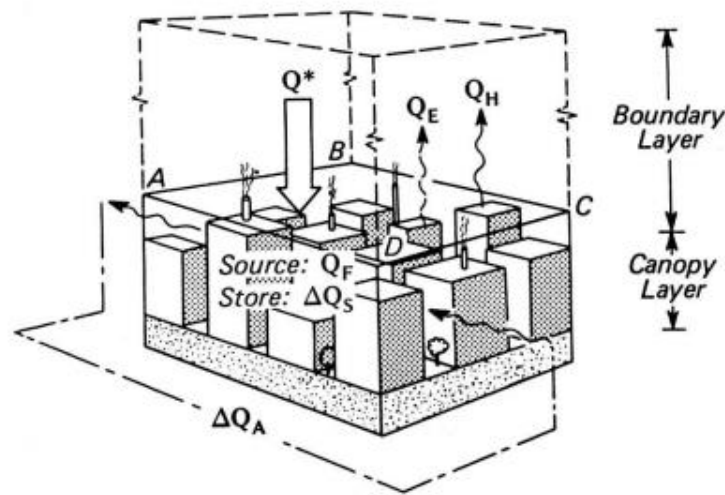


Figure 2.10. Schematic of the volumetric averaging approach to urban energy balance.

Source: Oke, 1987.

2.4. Components of the Urban Energy Balance:

- **Net Radiation (Q_*):** Includes incoming shortwave radiation from the sun and outgoing longwave radiation from the Earth's surface.

$$Q_* = (K \downarrow - K \uparrow) + (L \downarrow - L \uparrow) \quad (2.2)$$

Where:

- $K \downarrow$: Incoming shortwave radiation.
- $K \uparrow$: Reflected shortwave radiation.
- $L \downarrow$: Incoming longwave radiation.
- $L \uparrow$: Outgoing longwave radiation.

- **Sensible Heat Flux (Q_H):** The heat transferred from the surface to the atmosphere through conduction and convection.
- **Latent Heat Flux (Q_E):** Energy associated with the phase change of water (e.g., evaporation and condensation).
- **Ground Heat Flux (Q_G):** Energy conducted into or out of the ground.
- **Anthropogenic Heat Flux (Q_F):** Heat generated by human activities, including vehicular emissions, industrial processes, and building heating/cooling systems.

2.5. Factors Affecting Urban Climate:

Urban climate is a complex and dynamic system significantly influenced by the built environment and human activities, creating distinct microclimatic conditions that differ dramatically from surrounding rural landscapes. The transformation of natural landscapes into urban areas fundamentally alters energy balance, radiation absorption, heat retention, and atmospheric processes through multiple interconnected factors. Key factors include natural and human-induced factors that alter the atmospheric conditions in urban areas, creating distinct microclimates., exacerbates these effects through changes in factors urban morphology, surface materials, anthropogenic heat emissions, and the notorious urban heat island (UHI) effect (Oke, 1982; Arnfield, 2003).

2.5.1. Natural Factors:

According to Dorer et al. (2013), "the urban microclimate is determined by local air velocity, temperature and humidity; solar irradiation and specular and diffuse reflections, surface temperatures of building and ground, and the respective long-wave radiation exchange, also with the sky".

Natural elements play a foundational role in shaping the urban climate by influencing the baseline atmospheric conditions before urbanization:

- A. Geographical Location: Latitude, altitude, and proximity to water bodies determine **solar radiation, temperature, and humidity patterns**.
- B. Topography: Hills, valleys, and flat terrains modify wind flow, air drainage, and the formation of localized microclimates.

c. Vegetation and Water Bodies:

- Vegetation: Enhances cooling through evapotranspiration, increases humidity, and influences wind flow.
- Water Bodies: Act as thermal moderators, reducing temperature fluctuations and contributing to cooling through evaporation.

d. Climatic and Seasonal Variability: Prevailing climate types (e.g., hot-dry, humid, or cold) and seasonal shifts affect overall **temperature, precipitation, and wind patterns.**

2.5.2. Anthropogenic Factors:

Givoni (1998) wrote "the urban geometry and profile (shape, height, size of the buildings, orientation of streets and of buildings, and nature of the surfaces of the urban open areas) have an impact on the urban climate", therefore, each urban element (buildings, roads, parking area, factories, etc.) creates around and above it a modified climate with which it interacts"

A. Urban Geometry:

Urban geometry refers to the structural layout of a city, encompassing the height, spacing, and arrangement of buildings and streets. It plays a crucial role in shaping the formation and attributes of urban canyons. By influencing the interaction between urban surfaces and atmospheric processes, and affects the key factors such as solar exposure, wind circulation, and heat transfer.

Urban canyons, as integral elements of urban geometry, play a pivotal role in shaping urban climates, a subject explored extensively in various studies. Oke (1987) laid the foundation by defining urban canyons and analyzing their impact on heat retention, radiative cooling, and the Urban Heat Island (UHI) effect through geometric parameters like aspect ratio (H/W). Santamouris et al. (2001) highlighted the role of deep urban canyons in exacerbating the UHI due to reduced ventilation and prolonged heat storage. Hang et al. (2012), using computational fluid dynamics (CFD), examined airflow and pollutant dispersion within canyons, linking their geometry to reduced ventilation and heat buildup. Taleghani et al. (2015) investigated outdoor thermal comfort in urban canyons, showing how their depth and shading influence daytime cooling and nighttime heat retention. Collectively, these studies and others demonstrate the critical impact of urban canyon geometry on thermal comfort, airflow, and microclimatic conditions in cities.

- **Urban Canyons:**

Urban canyons are one of the most studied components of urban geometry because of their significant role in shaping urban microclimates. An urban canyon refers to the space created between two rows of buildings on opposite sides of a street. This space is defined by its aspect ratio (H/W), which is the ratio of building height (H) to street width (W). Urban canyons influence solar radiation, heat retention, airflow, and pollutant dispersion, making them a critical factor in understanding urban climate.

According to Oke (1987), urban canyons are classified based on their aspect ratio:

- Deep Canyons: High H/W ratio, where buildings are tall relative to the street width.
- Shallow Canyons: Low H/W ratio, where streets are wide compared to building heights.
- Regular vs. Irregular Canyons: Determined by the uniformity of building heights and street layouts.

Urban canyons significantly influence various climatic factors such as temperature, air circulation, solar radiation, and pollutant dispersion (figure 2.11):

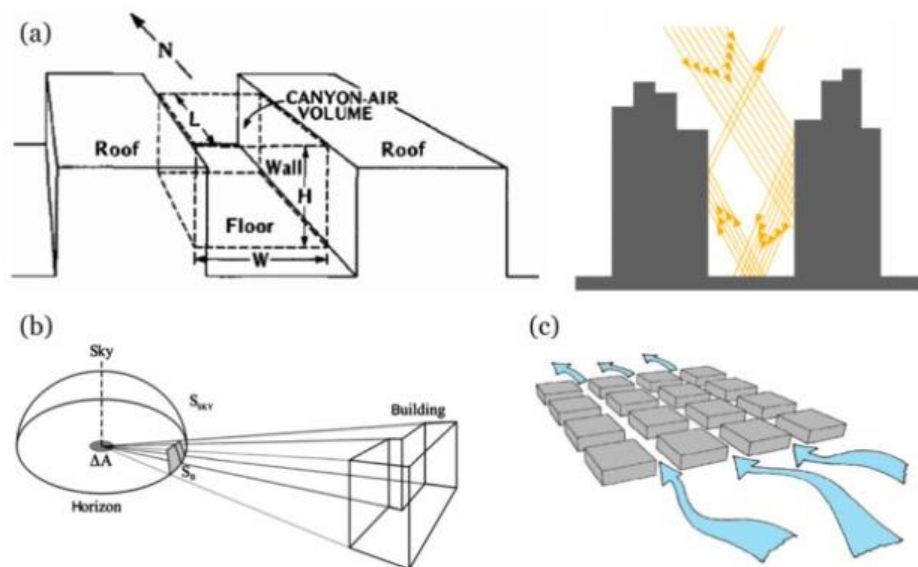


Figure 2.11. (a) Schematic representation of an urban canyons and multiple reflections and absorption that occurs within it (processing of Nunez and Oke, 1977); (b) Schematic representation of the SVF (Unger, 2009); (c)

Schematic representation of urban morphology capable of exploiting the contribution made by natural ventilation in UHI mitigation (processing of Santamouris et. Al, 1999).

Source: Gerundo, 2016.

- Heat Retention and UHI Intensification: Urban canyons trap heat through multiple reflections of solar radiation and reduced the reduced **Sky View Factor (SVF)**. This leads to higher temperatures in densely built areas.
- Modification of Wind Patterns: Buildings obstruct natural wind flow, creating wind shadows, turbulence, and localized wind channels. This reduces urban ventilation and pollutant dispersion.
- Shading and Solar Radiation Distribution: Tall buildings shade surrounding areas, reducing solar exposure and cooling some spaces while increasing heating in others due to reflected and absorbed radiation.
- Thermal Comfort and Outdoor Spaces: Urban geometry affects outdoor thermal comfort by influencing wind speed, shading, and surface temperatures.

B. Building materials Properties:

Surface properties of building materials in urban areas such as **albedo**, **thermal conductivity**, **emissivity**, and **surface roughness** have a significant impact on the urban climate and influence the Urban Heat Island development: they determine how the sun energy is reflected, emitted, and absorbed (Figure2.12). Furthermore, most materials used in the construction buildings and paving roads and walkways are impermeable to moisture. Consequently, more energy is available for long-wave emission, sensible heat flux and conduction to the surface.

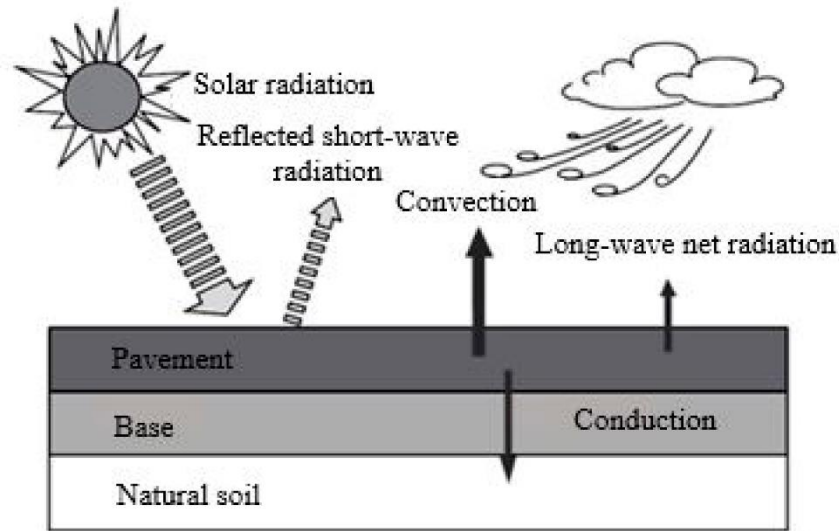


Figure 2.12. Pavement surface energy balance.

Source: Hu et al, 2021.

C. Urban Heat Island (UHI):

The urban Heat Island (UHI) may be defined as a phenomenon where surface and atmospheric modifications due to urbanization, described in the early 19th century by Luke Howard, who observed that urban areas retained heat more effectively than rural areas (Figure 2.13). generally, lead to modifying the urban climate that becomes warmer than the surrounding areas (Voogt, 2003, Coseo et al., 2014). Urban Heat Island describes a characteristic of the urban area in which the nocturnal temperatures are warmer than the surroundings landscape. Warmer urban air temperatures are a result of some interrelated causes associated with the urban modification to the natural surface, such the heat and the pollution released from the anthropogenic activities in the urban environment (Morris and Simmonds, 2000).

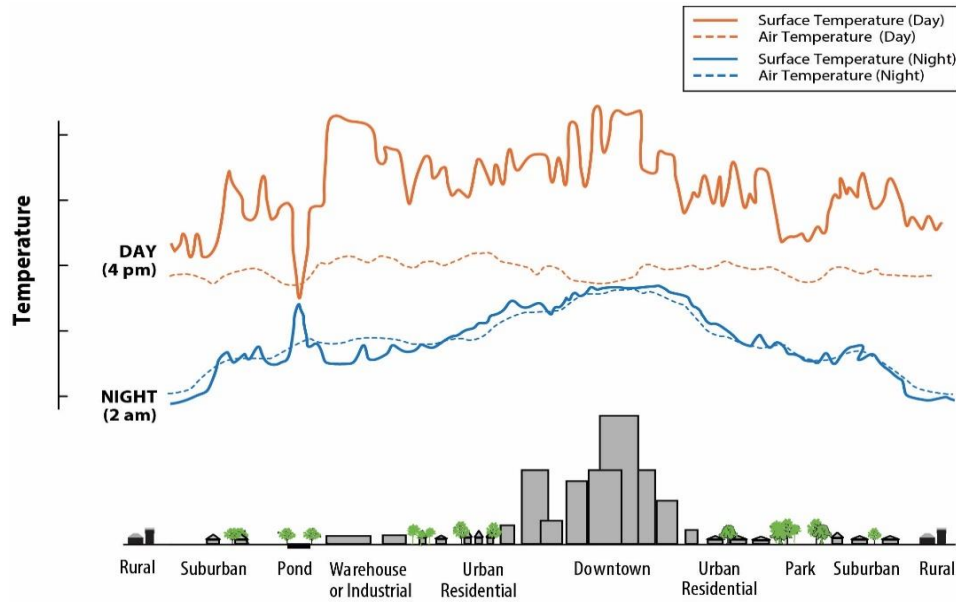


Figure 2.13. Distribution of UHI effect across different land use types.

Source: U.S. Environmental Protection Agency.

The Urban Heat Island (UHI) effect significantly impacts **outdoor thermal comfort** by increasing air and surface temperatures in urban areas compared to their rural surroundings. This phenomenon amplifies thermal stress, particularly in hot climates, by elevating the temperature and reducing the cooling effect of nighttime temperatures. As a result, outdoor spaces become less comfortable, affecting human well-being, social interaction, and urban livability. Key factors include reduced vegetation, heat-retaining materials, and anthropogenic heat sources. Mitigation strategies like adding greenery, reflective surfaces, and better urban design can help improve comfort levels (Ng et al., 2012; Santamouris et al., 2015; Johansson et al., 2014).

3. Thermal Comfort:

3.1. Definitions of thermal comfort:

Thermal comfort is defined by the American Society of Heating, Refrigerating, and Air-Conditioning Engineers (ASHRAE) as the condition of mind that expresses satisfaction with the thermal environment and is assessed by subjective evaluation.

Thermal comfort is described as the state where the body's heat balance is achieved, with skin temperature and sweat rates maintained at levels within a comfortable range for the majority of individuals (Fanger, 1970).

Thermal comfort is "the condition of mind in which there is satisfaction with the thermal environment." This standard emphasizes the importance of maintaining a balance between heat production and loss in the human body. (ISO 7730, 2005)

Santamouris (2015) defines thermal comfort as "the condition in which individuals feel neither too hot nor too cold, with this sensation being affected by environmental modifications such as urban heat islands."

3.2. Definitions of outdoor thermal comfort:

ASHRAE Standard 55 (2020) notes that outdoor thermal comfort is influenced by factors such as solar heat gain, surface reflectivity, and wind patterns, and aligns with the same principle of subjective satisfaction with the thermal environment

Outdoor thermal comfort is tied to urban heat mitigation, is "the balance between microclimatic conditions and human physiological needs, aimed at creating comfortable outdoor spaces for social and economic activities." It stresses the role of urban design in improving comfort levels. (Santamouris, 2015).

Outdoor thermal comfort is "the state of satisfaction with the thermal environment in outdoor spaces, influenced by environmental parameters such as air temperature, solar radiation, wind speed, and humidity, as well as personal and psychological adaptation." (Nikolopoulou & Steemers, 2003).

3.3. Factors of outdoor thermal comfort:

A complex interplay of environmental, personal, and psychological factors influences outdoor thermal comfort. Environmental parameters such as air temperature, humidity, solar radiation, wind speed, and surface properties play a major role in shaping thermal perception in open spaces. In addition, personal attributes like clothing and activity levels (Figure 2.14), as well as psychological and cultural adaptations, influence comfort levels. Urban elements, including vegetation, building materials, and spatial design, further modify the microclimate, making

outdoor thermal comfort highly dynamic and contextual (Nikolopoulou & Steemers, 2003; Johansson & al, 2014).

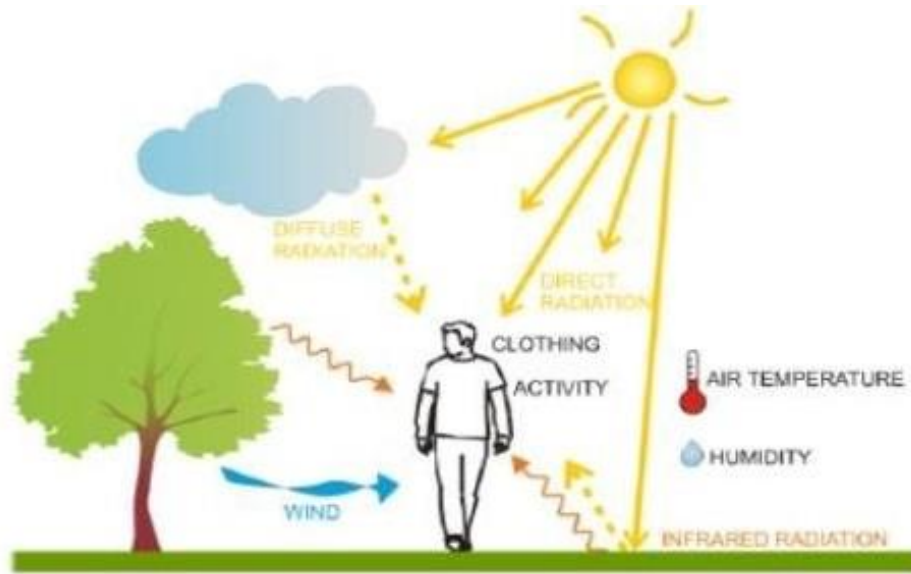


Figure 2.14. The Factors of outdoor thermal comfort

Source: Ridha. S et al, 2017.

3.3.1. Environmental Factors:

Research by Matzarakis & al. (2015) shows that air temperature, combined with humidity, wind speed, and radiation, determines the human energy balance and perceived thermal comfort.

- **Air Temperature (T_a):** Air temperature is the most fundamental factor in thermal comfort, is the ambient temperature of the surrounding air. Air temperature directly affects the sensation of heat or cold by determining the rate of heat exchange between the human body and the surrounding air. The World Meteorological Organization (WMO, 2018) defines outdoor air temperature as the temperature indicated by a thermometer exposed to the air in a position sheltered from direct solar radiation.
- **Mean Radiant Temperature (T_{mrt}):** Mean Radiant Temperature is defined as the uniform temperature of an ideal black enclosure that would yield equivalent radiative heat transfer with the human body as the actual environment, representing the spatially averaged radiant temperature of all surrounding surfaces, including buildings, pavements, vegetation, and the sky and integrates all short and long wave radiation fluxes to which a human body is

exposed (Figure 2.15), making it particularly crucial in outdoor thermal comfort assessment. T_{mrt} often has a more significant impact on outdoor thermal sensation than air temperature, especially in urban environments with complex radiation exchange patterns. (ISO 7726, 1998, Thorsson & al, 2007, Kántor & Unger, 2011).

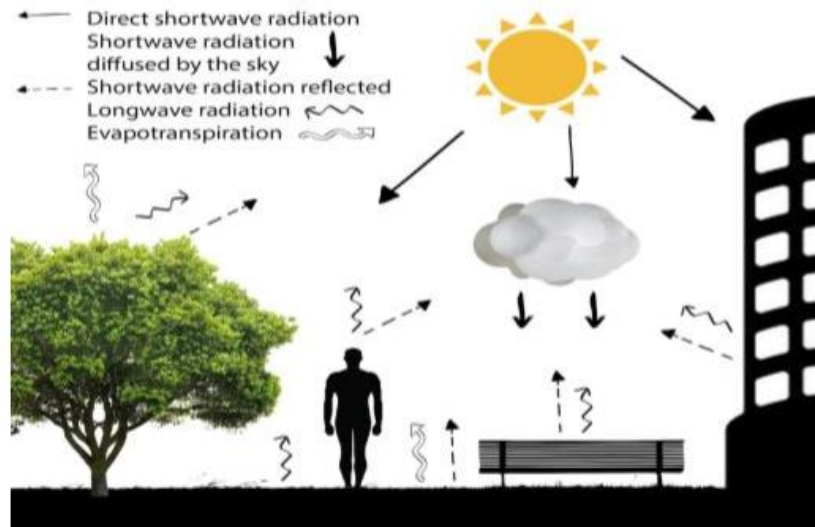


Figure 2.15. Relevant radiation fluxes and urban entities on the determination of outdoor MRT

Source: Naboni et al, 2019.

- **Relative Humidity (RH):** Relative Humidity it is the ratio of the partial pressure (or density) of water vapor in the air to the saturation pressure (or density) of water vapor at the same temperature and total pressure (ASHRAE, 2004).
- **Air Velocity (Va):** The movement of air in combination with air temperature will affect the rate at which hot air or vapour is ‘carried away’ from the body, thereby affecting body temperature and modify thermal sensation. The average air velocity, provides a commonly used overall value to represent this effect on the body (Badache H, 2021).

3.3.2. Personal Factors:

- **Metabolic Rate (M):** Metabolic rate (M) is the rate of transformation of chemical energy into heat and mechanical work by metabolic activities within an organism, usually expressed in terms of unit area of the total body surface area (Badache H, 2021). ISO 8996 (2004) defines it as the rate of energy production of the body, typically measured in met units (1 met = 58.2 W/m²).

- **Clothing Insulation (*I_{cl}*):** A body's heat must escape into the surrounding environment. If not, there will be a shift in body temperature. Clothing insulation is the primary factor influencing heat dissipation, which represents the thermal resistance provided by clothing ensembles and significantly influences heat exchange between the body and its environment (ISO 9920, 2007) and measured in clo units (1 clo = 0.155 m²K/W).

3.4. The outdoor thermal comfort indices:

Outdoor thermal comfort indices are tools developed to evaluate the thermal comfort of individuals in outdoor environments, considering the complex interaction of environmental and personal factors. The development of these indices has been crucial for urban planning, public health management, and climate-sensitive design, with widely adopted measures such as the Physiological Equivalent Temperature (PET), Universal Thermal Climate Index (UTCI), and Standard Effective Temperature (SET*) providing standardized approaches to thermal comfort assessment (Table 2.1) (Blazejczyk et al., 2012).

Table 2.1. Overview of Common Thermal Comfort Indices and Their Descriptions.

Source: Author.

Index	Description	Reference
PMV (Predicted Mean Vote)	Evaluates thermal comfort based on energy balance between the human body and the environment, considering variables like <i>T_{mrt}</i> , air velocity, <i>T_a</i> , and RH.	ISO 7730 (2005)
PPD (Predicted Percentage Dissatisfied)	Predicts the percentage of people dissatisfied with the thermal environment based on PMV.	ISO 7730 (2005)
UTCI (Universal Thermal Climate Index)	Estimates outdoor thermal comfort by integrating air temperature, wind speed, relative humidity, and radiation.	Fiala et al. (2012)
PET (Physiological Equivalent Temperature)	Assesses thermal comfort by comparing outdoor environments to a reference indoor setting.	Höppe (1999)
SET (Standard Effective Temperature)*	Incorporates thermal factors like clothing and activity to predict thermal comfort in outdoor and indoor settings.	Gagge et al. (1986)

HI (Heat Index)	Measures the perceived temperature by combining air temperature and relative humidity, commonly used for heat stress.	NOAA (National Weather Service)
WBGT (Wet Bulb Globe Temperature)	Evaluates heat stress by combining air temperature, humidity, radiant heat, and wind speed.	ISO 7243 (1989)

3.4.1. Predicted Mean Vote (PMV):

This is an index that predicts the average value of the votes of a large group of people on the seven points of the thermal sensation scale (ASHRAE, 2004), expressed from -3 to $+3$ corresponding to the categories: cold | cool | slightly cold | neutral | slightly warm | warm | hot (Figure 2.16). PMV calculation requires the following inputs: metabolic rate (Met), clothing insulation I_{cl} (clo), air temperature, air velocity, etc...

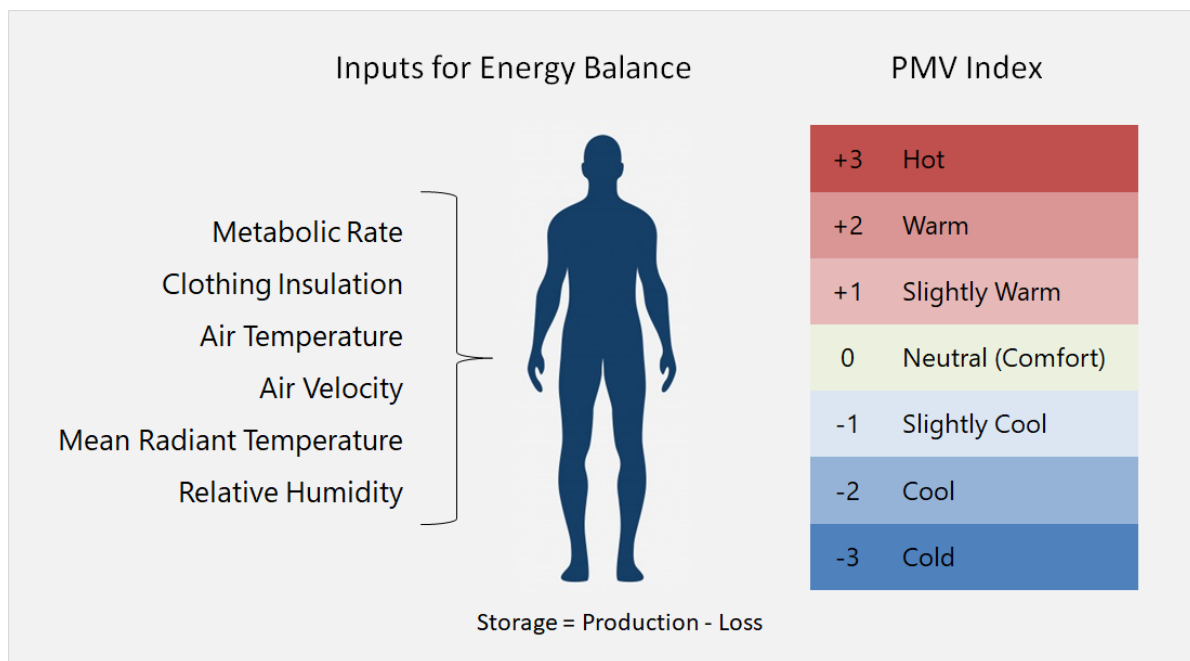


Figure 2.16. The PMV Thermal Comfort Scale.

Source: Jadhav, 2018.

3.4.2. Universal Thermal Climate Index (UTCI):

The UTCI provides a one-dimensional quantity reflecting the human physiological response to the multi-dimensional definition of actual thermal comfort. It adopts a multi-node model of human thermoregulation and an adaptive clothing model to simulate human reaction. UTCI is defined as

the air temperature (T_a) of the reference condition, which causes the same model response as the actual condition. These reference conditions include a person walking with a speed of 4 km/h (equivalent to a metabolic rate of 2.3 MET), a wind speed measured at a 10-m height following the meteorological convention of 0.5 m/s, a mean radiant temperature equaling air temperature, a relative humidity of 50% for $T_a \leq 29^\circ\text{C}$, and a vapor pressure of 20 hPa for $T_a > 29^\circ\text{C}$. The stress categories scale (Table 2.2) was developed on the basis of the simulated physiological and psychological response combined with the thermal physiological response of the human body (Di Zeng & al, 2020).

Table 2.2. Universal Thermal Climate Index (UTCI) equivalent temperatures categorized in terms of thermal stress and thermal perception.

Source: Di Zeng et al, 2020.

UTCI ($^\circ\text{C}$)	Stress Category	Thermal Perception
> 46	Extreme heat stress	Torrid
38–46	Very strong heat stress	Hottish
32–38	Strong heat stress	Hot
26–32	Moderate heat stress	Warm
9–26	No thermal stress	Comfortable
0–9	Slight cold stress	Cool
-13–0	Moderate cold stress	Coolish
-27–13	Strong cold stress	Cold
-40–27	Very strong cold stress	Chilly
< -40	Extreme cold stress	Freezing

3.4.3. Physiological Equivalent Temperature Index (PET):

Physiological Equivalent Temperature (PET) is another rational index. PET is defined as the air temperature at which, in a typical indoor environment, the heat balance of a human body is maintained by body and skin temperature under outdoor conditions (Table 2.3). PET is preferred over other indices, such as PMV, because of its unit of measurement ($^\circ\text{C}$), which makes it easier for urban planners and designers to interpret without the need for advanced meteorological or physiological knowledge (Badache H, 2021).

Table 2.3. Thermal perception classification according to PET values.**Source:** Matzarakis & Mayer.1996.

PET (°C)	Thermal Perception	Level of Physiological Stress
< 4	Very Cold	Extreme Cold Stress
4.1–8.0	Cold	Strong Cold Stress
8.1–13.0	Moderate Cold	Moderate Cold Stress
13.1–18.0	Slightly Cool	Slight Cold Stress
18.1–23.0	Comfortable	No Thermal Stress
23.1–29.0	Slightly Warm	Slight Heat Stress
29.1–35.0	Moderate Heat	Moderate Heat Stress
35.1–41.0	Warm	Strong Heat Stress

Conclusion:

The study of urban climatology is essential to comprehending and resolving the problems that metropolitan environments provide, particularly in regions with hot, dry weather. The significance of comprehending the urban heat island effect, the function of urban morphology, and the impact of human activity on urban climates was emphasized in the first section of this chapter. The chapter gives a thorough explanation of how urban climates are created and how they affect outside conditions by looking at these aspects. In the chapter's second section, outdoor thermal comfort is examined, along with the indices that are used to quantify these impacts and the elements that influence people's comfort in urban environments.

Improving the urban experience requires an understanding of outdoor thermal comfort, especially in hot and dry conditions. The models and indices covered in this chapter are useful resources for evaluating and improving outdoor areas to make sure people may use area comfortably. This chapter offers a basis for making well-informed decisions that can enhance the outdoor environment and make urban areas more livable by fusing the insights from urban climatology with the concepts of thermal comfort. The results highlight the necessity of a multidisciplinary approach to urban planning that combines human-centered design and climate science to build communities that are both heat-resilient and comfortable for their residents.

CHAPTER III: BUILDING MATERIALS AND CHARACTERISTICS: AN IN-DEPTH REVIEW OF MATERIAL THERMAL PROPERTIES

Introduction:

Building materials have an essential role in urban design and performance, particularly when it comes to improving outdoor thermal comfort in hot dry climates. The construction industry relies on natural resources such as wood, clay, and stone, as well as man-made materials such as concrete, steel, and composites (Hornbostel, 1991; Wang & Salmon, 2014). These materials' selection and use have a direct impact on urban thermal behavior, such as heat transfer, energy efficiency, and sustainability.

The evolution of building materials corresponds to advances in human civilization. From the use of natural resources in prehistoric shelters to the development of revolutionary materials like concrete in Roman architecture and, later, steel during the Industrial Revolution, construction techniques have been constantly transformed (Lancaster, 2005; Friedman, 2010). To address the challenges of climate change and resource conservation, the emphasis is now on sustainable materials such recycled composites and bio-based products (Pacheco & Jalali, 2011; Hanus & Harris, 2013). These innovations are especially important in hot, dry settings, where high temperatures necessitate materials that give thermal comfort while minimizing environmental impact.

Thermal properties of building materials emerge as an important focal point in this study. Researchers such as Al-Sanea and Zedan (2001) and Yilmaz (2007) have many research on how material properties such as thermal conductivity, emissivity, albedo, and thermal mass directly affect environmental performance. These qualities influence not only indoor comfort but also outdoor thermal environments, making material selection an important strategy for reducing urban heat island effects and improving microclimate conditions.

This chapter analyzes building materials in detail with emphasis on their definitions and classifications. and qualities. It begins by examining the evolution of materials over the time, focusing on important developments and how they have influenced construction practices. The chapter then investigates how materials are classified based on their composition, origin, and useful qualities. Materials' thermal properties, such as thermal mass, thermal resistance, and

thermal conductivity, are particularly important since they are critical for managing heat in outdoor conditions.

The format of this chapter reflects its principal goal: to lay the basis for the selection of materials optimal for thermal comfort in hot, dry regions. Understanding how materials interact with environmental elements like solar radiation and ambient temperature allows architects and engineers to make informed decisions that enhance energy efficiency and occupant comfort. This understanding is useful in promoting sustainable construction techniques, which align with the overarching goal of generating thermally adapted urban settings.

1. Building Materials:

1.1. Definitions and History:

Building materials are natural or manufactured substances and components that are used in the building and construction industry for creating structures, infrastructure, and architectural elements. These materials are selected and utilized based on their physical, mechanical, and chemical properties to meet specific engineering requirements, safety standards, and performance criteria for construction projects.

Based on number of studies and scientific works the building materials is: ‘Building materials are materials used for construction. Many naturally occurring substances, such as clay, sand, wood and rocks, even twigs and leaves have been used to construct buildings. Apart from naturally occurring materials, many man-made products are in use, some more and some less synthetic’ (Hornbostel, 1991) (Duggal, 2008). ‘Building materials in civil engineering are the materials used for construction that include natural substances, such as clay, sand, wood and rocks, as well as man-made products, such as concrete, steel, and polymer materials’ (Wang & Salmon, 2014). ‘Construction materials are the components used in the erection of structures. These materials can be natural, such as lumber and stone, or man-made, such as concrete and steel. The choice of materials for construction is based on cost, strength, durability, fire resistance and ease of use’ (Mamlouk & Zaniewski, 2011). The evolution of construction materials mirrors human civilization's progress. In prehistoric times, humans used natural materials like stone, wood, and clay for shelter (Addis, 2007). Ancient Egyptians mastered limestone and granite construction, as seen in the pyramids (c. 2700-2500 BCE) (Stocks, 2003), while Romans revolutionized architecture with concrete around 300 BCE (Lancaster, 2005). The Middle Ages saw the

refinement of stone masonry and timber framing, particularly in European cathedrals (Fitchen, 1961). The Industrial Revolution transformed construction with cast iron and steel, enabling bridges and skyscrapers. The invention of Portland cement in 1824 paved the way for modern concrete structures (Friedman, 2010) (Hewlett, 2003). The 20th century brought widespread use of reinforced concrete and advanced glass production for larger windows and curtain walls (Collins, 2004). Post-WWII construction incorporated plastics and engineered wood products. Recent decades have focused on high-performance and sustainable materials, including recycled materials and bio-based composites (Pacheco & Jalali, 2011). The 21st century has introduced smart materials and nanomaterials, enhancing construction efficiency (Hanus & Harris, 2013).

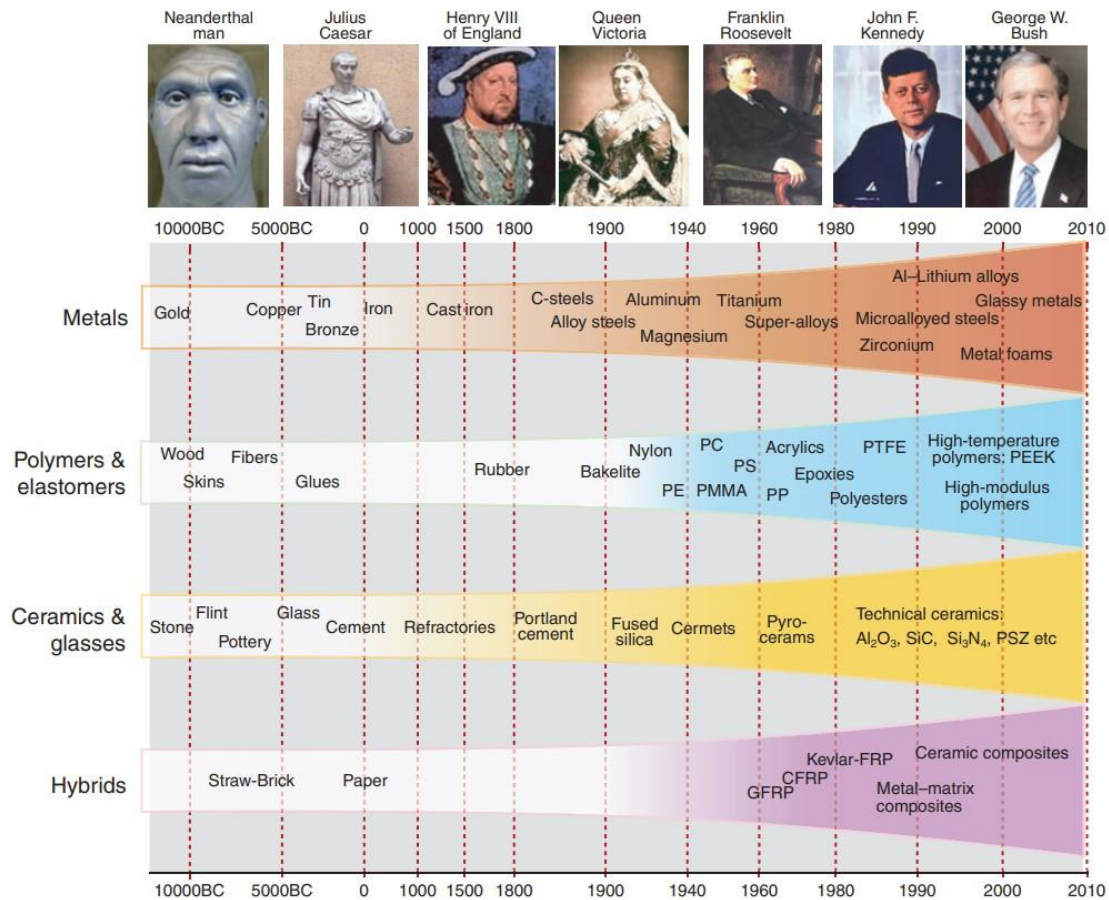


Figure 3.1. The development of materials over time.

Source: Ashby & al, 2007.

The development of materials over time. The materials of pre-history, on the left, all occur naturally; the challenge for the engineers of that era was one of shaping them. The development

of thermochemistry and later of polymer chemistry enabled man-made materials, shown in the colored zones (figure 1.1). Three-stone, bronze and iron-were of such importance that the era of their dominance is named after them (Ashby & al, 2007).

1.2. Classification of Building Materials:

Construction materials can be classified into various categories based on their origin, composition, usage, and properties. This classification helps architects, engineers, and builders select the appropriate materials for different construction purposes, ensuring optimal performance, durability, and sustainability. "Construction materials are the materials used in buildings and other civil engineering structures. They are generally classified into three major categories: general construction materials, auxiliary materials, and special materials" (Li, 2011). Each type of material, whether natural or manmade, organic or inorganic, load-bearing or insulating, has specific advantages and limits. Understanding the classification of construction materials is critical for making sound design and construction decisions that balance structural integrity, thermal comfort, and environmental effect.

Construction materials can be classified in several ways based on their origin, composition, and application (Table 3.1).

Table 3.1. Classification of building Materials.

Source: Ashby & Jones, 2012; Domone & Illston, 2010; Mamlouk & Zaniewski, 2011.

Classification Criterion	Category	Description	Examples
Origin	Natural Materials	Derived directly from nature, often with minimal processing.	Wood, stone, clay, sand
	Synthetic/Manufactured Materials	Produced by combining or modifying natural substances through various processes.	Concrete, steel, glass, plastic
Composition	Organic Materials	Contain carbon and typically derived from living sources.	Wood, bamboo, straw
	Inorganic Materials	Do not contain carbon, typically mineral-based or synthetic.	Cement, bricks, metals
Structure	Homogeneous Materials	Consist of one phase or uniform composition throughout.	Metals, plastics
	Composite Materials	Made of two or more different materials combined to improve strength or durability.	Reinforced concrete, fiber-reinforced polymer

Function	Load-Bearing Materials	Primarily used for structural support in buildings.	Steel, concrete, masonry
	Non-Load-Bearing Materials	Serve non-structural roles, often used for aesthetics or partitioning.	Glass, gypsum board
Thermal Properties	Insulating Materials	Reduce heat transfer and improve energy efficiency.	Fiberglass, foam, cellulose
	Thermal Mass Materials	Store heat and release it gradually, moderating indoor temperatures.	Concrete, brick, adobe

1.3. Building Materials Properties:

The classification and understanding of construction material properties are fundamental to their effective application in building and civil engineering projects. These properties determine not only the performance and durability of materials but also their suitability for specific construction applications. As Ashby and Jones (2021) note, "The systematic classification of material properties provides engineers with a framework for material selection and design optimization".

Construction material properties can be broadly categorized into physical, mechanical, chemical, and environmental characteristics. According to Domone and Illston (2022), "These properties interact in complex ways to determine the overall performance of materials in construction applications». The classification system helps engineers and architects make informed decisions about material selection based on project requirements and environmental conditions (Table 3.2).

Chemical properties focus on material stability and resistance to environmental factors. The International Council for Research and Innovation in Building and Construction (CIB, 2022) emphasizes that "understanding chemical properties is essential for predicting material durability and compatibility in various environmental conditions". Environmental properties have gained significance with increasing focus on sustainability, as "the environmental impact of construction materials throughout their lifecycle has become a critical consideration in material selection" (Pacheco-Torgal et al., 2023). Mechanical properties, including strength, elasticity, and hardness, "determine the material's ability to withstand loads and maintain structural integrity" (Mehta & Monteiro, 2021).

Physical properties of construction materials encompass fundamental characteristics that define their behavior and performance in construction applications. These properties, which include density, porosity, thermal characteristics, acoustic properties, and optical properties, are essential

for understanding material behavior and making informed decisions in construction design, among these physical properties, thermal characteristics play a crucial role alongside other properties. The interrelation between various physical properties, such as density, porosity, and thermal behavior, significantly influences material performance in building applications (Ashby and Jones, 2023).

Table 3.2. Classification of building Material Properties.

Source: Ashby & Jones, 2023; Mehta & Monteiro, 2021; Yilmaz, A. Z, 2007; ISO 10456.

Category	Property	Description	Example/Note
Physical	Density	Mass per unit volume, affects material weight and thermal mass.	e.g., Concrete: $\sim 2400 \text{ kg/m}^3$, Wood: $\sim 600 \text{ kg/m}^3$.
	Porosity	Proportion of void spaces, influencing insulation and permeability.	Brick has higher porosity than stone.
	Thermal Conductivity	Ability to conduct heat, critical for insulation and thermal management.	Low in wood ($\sim 0.1 \text{ W/m}\cdot\text{K}$), high in metals ($\sim 200 \text{ W/m}\cdot\text{K}$).
	Water Absorption	Amount of water absorbed, affecting durability and freeze-thaw resistance.	Clay bricks: $\sim 10\text{-}20\%$.
Mechanical	Compressive Strength	Maximum compressive load a material can bear.	Concrete: $\sim 20\text{-}40 \text{ MPa}$, Steel: $>200 \text{ MPa}$.
	Tensile Strength	Resistance to tension; indicates material flexibility and cracking behavior.	Steel has high tensile strength compared to concrete.
	Elasticity	Ability to deform under stress and return to original shape (modulus of elasticity).	Structural steel: $\sim 200 \text{ GPa}$.
	Hardness	Resistance to surface deformation or scratching.	Measured on Mohs scale, e.g., Granite $\sim 6\text{-}7$.
Chemical	Chemical Stability	Resistance to chemical reactions (e.g., corrosion, acid attack).	Aluminum resists oxidation better than iron.
	Fire Resistance	Ability to withstand high temperatures without significant degradation.	Concrete and gypsum-based materials perform well.
	Durability	Resistance to degradation over time due to environmental factors.	Depends on material and exposure.
	Reactivity	Tendency to react with other materials, influencing durability and compatibility.	Limestone reacts with acids.

Environmental	Embodied Energy	Total energy required to produce and transport the material.	High for aluminum (~200 MJ/kg), low for wood (~2 MJ/kg).
	Carbon Footprint	Total CO ₂ emissions associated with the material's life cycle.	Concrete emits ~0.9 kg CO ₂ /kg during production.
	Recyclability	Ability to be reused or recycled after its lifecycle.	Steel and aluminum are highly recyclable.
	Thermal Comfort Impact	Influence on indoor/outdoor thermal environments.	Light-colored surfaces improve reflectivity and outdoor thermal comfort in hot climates.

1.4. Thermal properties of materials:

The thermal properties of construction materials play a crucial role in building performance, energy efficiency, and occupant comfort. These properties significantly influence building thermal behavior, energy consumption, and sustainability aspects of construction projects. Understanding thermal properties is fundamental to achieving energy-efficient building design and meeting modern building energy codes (Desjarlais and Zarr ,2023).

Thermal properties encompass several key characteristics, including thermal conductivity, thermal resistance (R-value), thermal mass, specific heat capacity, and thermal expansion. These properties determine how materials store, transfer, and distribute heat, directly impacting building energy performance and indoor environmental quality (Clarke and Yaneske, 2022). The American Society of Heating, Refrigerating and Air-Conditioning Engineers emphasizes that proper selection of materials based on their thermal properties can reduce heating and cooling loads by 20-30% (ASHRAE, 2004).

Hall and Allinson (2009) and Sadineni and al (2011) study specialized uses, such as thermal mass for energy efficiency and latent heat in thermal energy storage systems. Al-Sanea and Zedan (2001) focus on properties like thermal inertia and thermal lag, which are key for adapting to hot climates, ensuring that buildings and outdoor spaces remain cooler during the day and warmer at night, while Yilmaz (2007) considers properties like emissivity and solar reflectivity, and heat absorbance is the combination of properties that determines how effectively materials can enhance comfort by preventing excessive heat buildup, and reducing energy consumption in urban environments (Table 3.3).

Table 3.3. Studies and Thermal Properties of Materials.

Source: Author.

Author/Study	Classification Method	Thermal Properties Identified	Sources
Ashby and Jones (2012)	Divided into intrinsic (material-dependent) and extrinsic (application-dependent) properties.	<ul style="list-style-type: none"> • Thermal conductivity. • Specific heat capacity. • Thermal expansion. • Thermal diffusivity. 	Ashby, M. F., & Jones, D. R. H. (2012). <i>Engineering Materials I: An Introduction to Properties, Applications, and Design</i> .
Mehta and Monteiro (2014)	Focused on concrete and cementitious materials, grouping properties by heat generation and transfer.	<ul style="list-style-type: none"> • Thermal conductivity. • Thermal diffusivity. • Heat capacity. • Heat of hydration. 	Mehta, P. K., & Monteiro, P. J. M. (2014). <i>Concrete: Microstructure, Properties, and Materials</i> .
Hall and Allinson (2009)	Grouped by energy efficiency relevance in buildings.	<ul style="list-style-type: none"> • Thermal mass. • Thermal conductivity. • Thermal diffusivity. • Specific heat • Emissivity. 	Hall, M., & Allinson, D. (2009). Assessing the moisture content of rammed earth walls using dynamic thermal properties.
Karlický and al. (2018)	Analyzed surface roughness using mesoscale atmospheric models (WRF and RegCM4) to assess urban parameterization effects.	<ul style="list-style-type: none"> • Roughness Length. • Thermal Conductivity. 	Karlický & al. (2018) <i>Atmospheric Chemistry and Physics</i>
Santamouris and al. (2018)	Investigated the impact of increasing urban albedo on mitigating the Urban Heat Island (UHI) effect in cities.	<ul style="list-style-type: none"> • Albedo • Reflectivity 	Santamouris & al. (2018) <i>Energy and Buildings</i>
Al-Sanea and Zedan (2001)	Classified by steady-state and dynamic conditions for hot climates.	<ul style="list-style-type: none"> • Thermal conductivity. • Thermal capacity • Thermal diffusivity, • Thermal inertia. • Thermal lag. 	Al-Sanea, S. A., & Zedan, M. F. (2001). <i>Effect of insulation location on thermal performance of building walls</i> .
Yilmaz (2007)	Focused on material categorization by response to environmental conditions.	<ul style="list-style-type: none"> • Thermal conductivity. • Thermal transmittance. • Specific heat. • Reflectivity. • Emissivity. 	Yilmaz, A. Z. (2007). <i>Materials of Construction</i> .
Sadineni and al. (2011)	Evaluated thermal performance of building envelope systems in energy-efficient construction.	<ul style="list-style-type: none"> • Thermal conductivity. • Thermal transmittance (U-value). • Specific heat. • Emissivity. • Solar reflectance. 	Sadineni, S. B., et al. (2011). Energy-efficient building envelope technologies. Renewable and Sustainable Energy Reviews.

The study of thermal properties of materials has been a major focus of research across numerous organizations and standards, reflecting its importance in building performance, energy efficiency, and occupant comfort (Table 3.4). Thermal qualities such as thermal conductivity, thermal resistance (R-value), specific heat capacity, and thermal transmittance (U-value) are classified by researchers and regulatory agencies according to their role in heat transport, storage, and environmental interactions.

The American Society of Heating, Refrigerating, and Air-Conditioning Engineers (ASHRAE) highlights practical metrics like U-values and R-values for energy-efficient building design and heat exchange between materials and the environment. In a similar way the International Organization for Standardization (ISO) offers a framework for both static and dynamic thermal behavior, taking into account moisture and layers of construction.

Regional frameworks, such as Algeria's Thermal Regulations for Residential Buildings (DTR C 3-2), adjust approaches to local climates, with a focus on heat loss, humidity, and material performance in real-world situations. The classifications are further refined into intrinsic and extrinsic properties, such as thermal inertia and thermal mass, which reflect the material's basic characteristics as well as its thermal behavior under use.

Table 3.4. Thermal Properties from ASHRAE, ISO, and DTR C 3-2.

Source: ASHRAE, 2021, 2019; ISO, 2005, 2014, 2017; DTR C 3-2, 1997.

Organization/Study	Classification Method	Thermal Properties Identified	Sources
ASHRAE	Practical metrics focused on building energy performance and system design.	<ul style="list-style-type: none"> • Thermal conductivity. • Thermal resistance (R-value). • Thermal transmittance (U-value). • Thermal mass. • Specific heat. 	ASHRAE (2021). <i>ASHRAE Handbook—Fundamentals</i> .
ASHRAE Standard 90.1	Establishes minimum energy efficiency requirements for building envelopes.	<ul style="list-style-type: none"> • U-value. • R-value. • Thermal bridging • Thermal mass. 	ASHRAE (2019). <i>ANSI/ASHRAE/IES Standard 90.1-2019: Energy Standard for Buildings Except Low-Rise Residential Buildings</i> .

ISO 10456	Standardized values for hygrothermal properties for construction materials.	<ul style="list-style-type: none"> • Thermal conductivity. • Thermal resistance (R-value). • U-value, • specific heat capacity. • Moisture interaction. 	International Organization for Standardization (2014). ISO 10456.
ISO 13786	Time-dependent and steady-state classifications for building envelopes.	<ul style="list-style-type: none"> • Thermal admittance. • Thermal delay. • Thermal transmittance, Thermal resistance (R-value). 	International Organization for Standardization (2017). ISO 13786.
ISO 6946	Layer-by-layer analysis of building elements.	<ul style="list-style-type: none"> • Thermal resistance (R-value) • Thermal transmittance (U-value) • Thermal bridging. 	International Organization for Standardization (2017). ISO 6946.
ISO 9869	On-site measurement of thermal properties for real-world validation.	<ul style="list-style-type: none"> • Thermal transmittance (U-value). • Thermal conductance (C-value). 	International Organization for Standardization (2014). ISO 9869-1.
ISO 15927	Examines thermal properties alongside moisture behavior.	<ul style="list-style-type: none"> • Thermal conductivity. • Water vapor permeability. • Thermal resistance (R-value). 	International Organization for Standardization (2005). ISO 15927-4.
Algeria's Thermal Regulations of Residential Buildings DTR C 3-2	Regulatory thresholds and steady-state calculations for residential energy performance in Algeria (DTR). Introduces dynamic simulation tools for variable environmental conditions.	<ul style="list-style-type: none"> • Thermal conductivity. • Thermal resistance (R-value) • Specific heat capacity. • U-value. • Thermal inertia. • Moisture effects. • Thermal delay 	Algeria's Thermal Regulations of Residential Buildings (1997). <i>DTR C 3-2: Réglementation Thermique des Bâtiments d'Habitation.</i>

2. Glossary of Thermal Properties of Materials:

2.1. The Albedo:

Albedo is the ratio of the reflected solar radiation to the incoming solar radiation on a surface. It is a unitless value ranging from 0 to 1, where 0 means no reflection (total absorption) and 1 means

total reflection. Higher albedo values indicate surfaces that reflect more sunlight, which helps keep surfaces cooler (Figure 3.2).

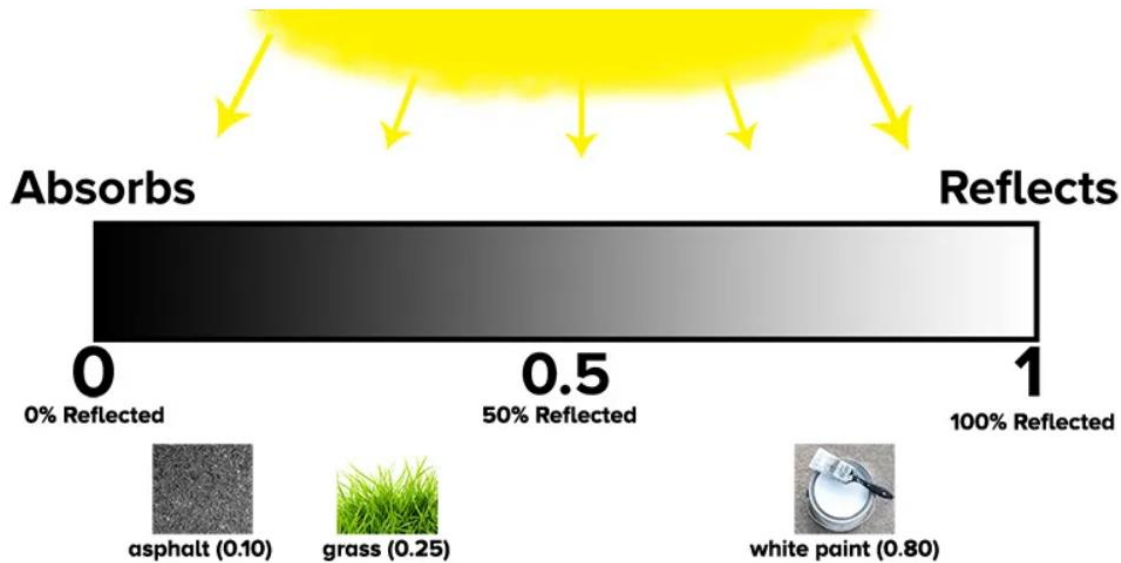


Figure 3.2. The difference between high albedo surface and low albedo surface.

Source: Hinkle k, 2016.

Low albedo materials, such as asphalt and dark-colored surfaces, can increase the urban heat island (UHI) effect due to their higher heat absorption and storage capabilities. In contrast, high albedo or reflective materials have been identified as an effective solution to mitigate the UHI effect (Mohajerani & al., 2017; Santamouris, 2014), as demonstrated by Akbari et al. (2005) who found that the use of high albedo roofing materials can reduce energy use and cooling loads in commercial buildings. By utilizing high albedo materials in the urban fabric, cities can combat the heat island phenomenon and lower surface temperatures.

2.2. Absorptivity (α):

Absorptivity is the fraction of incident radiation that a material absorbs. A material with high absorptivity will absorb more energy and may heat up quickly when exposed to sunlight or other sources of radiant energy.

2.3. Density (ρ):

Density is the mass per unit volume of a material. It is an essential property for thermal mass, as higher-density materials can store more heat energy due to their greater mass.

Example: Concrete, with a density around 2400 kg/m^3 , can absorb and store more heat than wood, which has a density of about 500 kg/m^3 .

$$\rho = \frac{m}{V} \quad (3.1)$$

Where:

- ρ = density (kg/m^3)
- m = mass of the material (kg)
- V = volume of the material (m^3)

2.4. Dry Density:

A physical property of a material that represents its mass per unit volume when it is completely dry. It is typically measured in kilograms per cubic meter (kg/m^3). It is the weight of the material's solid component (excluding water or moisture content) divided by the total volume it occupies.

2.5. Emissivity (ϵ):

Emissivity is the measure of a material's ability to emit thermal radiation relative to an ideal blackbody or perfect emitter. It ranges from 0 to 1, (Figure 3.3) where 1 represents a perfect blackbody. Higher emissivity values mean that a material can emit more energy, making it more effective at cooling through radiation.

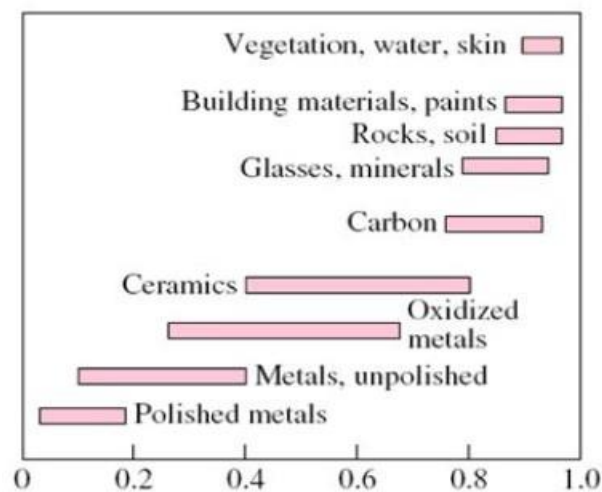


Figure 3.3. Typical ranges of emissivity of various materials.

Source: (Cengel, Y A, & al, 2008).

Metals like aluminum have low emissivity (about 0.05–0.1), which means they emit relatively little thermal radiation, while materials like concrete or brick have higher emissivity values (0.85–0.9), making them better at radiating heat away (Figure 3.3).

2.6. Reflectivity (ρ):

Reflectivity is the fraction of incident radiation that a material reflects. It varies with wavelength and angle of incidence, so reflectivity for visible light can differ from that for infrared radiation.

2.7. Roughness:

Roughness refers to the texture or surface irregularities of a material, which influence how it interacts with heat transfer mechanisms such as conduction, convection, and radiation.

Surface roughness impacts heat exchange with the surrounding air. Roughness is one component of the material's surface texture. It also significantly minimizes reflection due to the solar trapping effect. As a result, the surface temperature is observed to grow monotonically with roughness. (Guha and Chowdhuri, 1996).

2.8. Specific Heat Capacity (c):

Specific heat capacity is the amount of heat energy required to raise the temperature of one kilogram of a material by one degree Celsius (or Kelvin). It describes how much heat a material can store per unit of mass.

Example: Water has a high specific heat capacity (around 4186 J/kg·K), which makes it an excellent material for thermal storage systems compared to materials like metal, which have lower specific heat.

$$Q = m \cdot c \cdot \Delta T \quad (3.2)$$

Where:

- Q = heat energy stored or released (Joules, J)
- m = mass of the material (kg)
- c = specific heat capacity (J/kg·K)
- ΔT = temperature change (K or °C)

2.9. Thermal Bridging:

According to ASHRAE (2021), thermal bridging occurs when "highly conductive materials within the building envelope create a pathway for heat flow, bypassing insulation and increasing heat transfer."

ISO 10211:2017, the international standard for thermal bridges in building structures, defines it as a "part of the building envelope where the otherwise uniform thermal resistance is significantly reduced by full or partial penetration of the building envelope by materials with different thermal conductivities or by a change in thickness of the fabric."

2.10. Thermal Capacity:

Thermal capacity, also known as heat capacity, is the total amount of heat energy a material can store. It is the product of the material's density, volume, and specific heat capacity.

Example: Thick concrete walls (with high density and thickness) will have a higher thermal capacity than thinner, less dense walls, providing better temperature stability indoors.

$$C = \rho \cdot V \cdot c \quad (3.3)$$

Where:

- C = thermal capacity (J/K)
- ρ = density (kg/m³)
- V = volume of the material (m³)
- c = specific heat capacity (J/kg·K)

2.11. Thermal Conductance:

Conduction is the transfer of heat through a material without any movement of the material itself. Heat is transferred from molecule to molecule through direct contact.

Examples: Metals, ceramics, and other solid materials typically conduct heat via conduction.

2.12. Thermal Conductivity (k or λ):

Thermal conductivity (k -value) represents a material's ability to conduct heat. As Kumaran (2021) explains, "Materials with low thermal conductivity are essential for insulation applications, while materials with high thermal conductivity are crucial for heat dissipation".

$$q = -k \cdot A \cdot \frac{dx}{dT} \quad (3.4)$$

Where:

- q = the heat transfer rate (W),
- k = the thermal conductivity.
- A = the cross-sectional area through which heat is transferred (m^2),
- $\frac{dx}{dT}$ = the temperature gradient across the material.

Heat transfer in buildings may take place in four ways, by conduction, convection, radiation and evaporation (or condensation). Conduction is the flow of heat through a material by transfer from warmer to colder molecules in contact with each other. By convection, heat is transferred with the flow of molecules from one place to another with a change in their heat content. Radiation is the transfer of heat through space by electromagnetic waves. Evaporation and condensation involve changes of state (from liquid to gas and vice versa), which processes absorb or evolve heat (Givoni B, 1969).

2.13. Thermal Diffusivity (α):

Thermal diffusivity is a measure of how quickly a material can absorb heat from its surroundings and reach thermal equilibrium. It represents the ratio of a material's thermal conductivity to its volumetric heat capacity (Kumaran, 2023).

2.14. Thermal Effusivity (e):

Also known as thermal absorptivity, is a measure of a material's ability to exchange thermal energy with its surroundings. It represents the square root of the product of a material's thermal conductivity, density, and specific heat capacity (Li, 2023).

2.15. Thermal Inertia (I):

A thermal property that describes a material's ability to resist changes in temperature when subjected to thermal energy. It reflects the material's capacity to store heat and delay its transfer, playing a crucial role in thermal performance and energy efficiency in buildings.

the property of a material that expresses the degree of slowness with which its temperature reaches that of the environment (Ng and al, 2011)

Mathematically, thermal inertia is related to the product of three key thermal properties: thermal conductivity (k), density (ρ), and specific heat capacity (c):

$$I = k \cdot \rho \cdot c \quad (3.5)$$

Where:

- k = Thermal conductivity.
- ρ = Density (kg/m³)
- c = Specific heat capacity (J/kg·K)

2.16. Thermal Lag (Time Lag):

Thermal lag is the delay between the time when a material absorbs heat and when it releases it (Figure 3.4). This delay allows buildings to remain cooler during the day (by absorbing heat) and warmer at night (by gradually releasing the stored heat). In high thermal mass materials, thermal lag plays a key role in stabilizing indoor temperatures by offsetting peak heating and cooling needs (Figure 3.5).

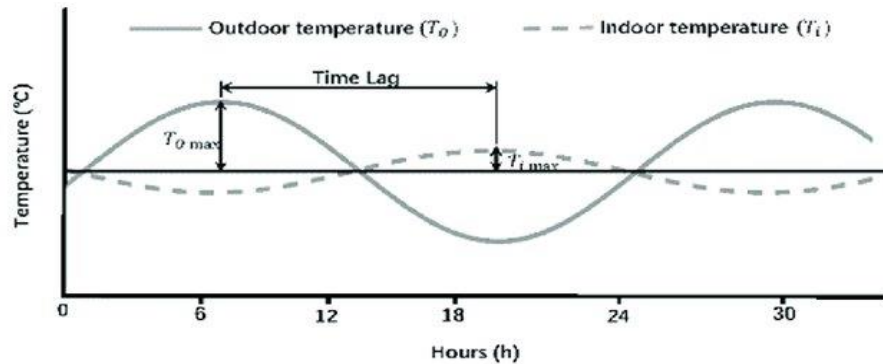


Figure 3.4. Thermal mass introduces a time lag.

Source: [Shenwei et al, 2022](#).

$$\Phi = t_{in(max)} - t_{out(max)} \quad (3.6)$$

Where:

- Φ = thermal lag (hours),
- $t_{in(max)}$ = time at which the maximum indoor temperature occurs (hours),
- $t_{out(max)}$ = time at which the maximum outdoor temperature occurs (hours).

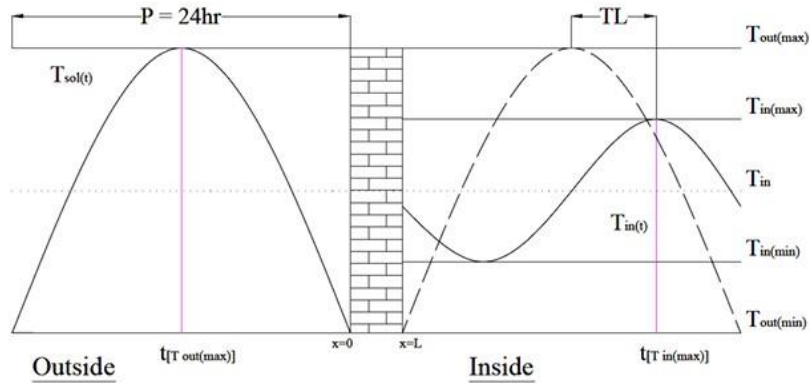


Figure 3.5. The schematic representation of time lag and decrement factor.

Source: Balaji et al., 2013.

Thermal lag is influenced by the thermal Diffusivity (α) and thermal Effusivity of the material, which combines thermal conductivity, density, and specific heat capacity.

2.17. Thermal Mass:

Thermal mass, characterized by specific heat capacity and density, influences a material's ability to store and release heat. Materials with high thermal mass can help regulate indoor temperature fluctuations and reduce peak heating and cooling loads. This property is particularly important in passive solar design and sustainable architecture (Hall and Allinson, 2023).

Thermal mass refers to a material's ability to absorb, store, and release heat over time. Materials with high thermal mass can stabilize indoor temperatures by absorbing heat during the day and releasing it at night.

$$Q = m \cdot c \cdot \Delta T \quad (3.7)$$

Where:

- Q is the amount of heat energy stored or released (J),
- m is the mass of the material (kg),
- c is the specific heat capacity of the material (J/kg·K),
- ΔT is the temperature change (K).

2.18. Thermal Radiation:

Radiation is the transfer of heat through electromagnetic waves (Figure 3.6), which can occur in a vacuum or through transparent media. It does not require a medium for heat transfer.

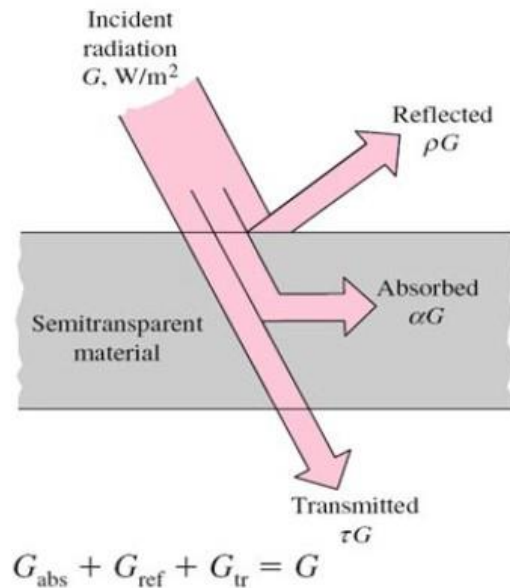


Figure 3.6. Behaviour of a semi-transparent material when receiving incident radiation **Source:** Cengel, Y A, et al, 2008.

Examples: The heat from the sun or a fireplace radiates through space.

$$q = \epsilon \cdot \sigma \cdot A \cdot (T^4 - T_s^4) \quad (3.8)$$

Where:

- q = heat transfer rate (W)

- ϵ = emissivity of the surface (dimensionless, between 0 and 1)
- σ = Stefan-Boltzmann constant
- A = surface area (m^2)
- T = absolute temperature of the radiating surface (K)
- T_s = absolute temperature of the surrounding environment (K).

2.19. Thermal Resistivity (R-value):

The thermal resistance (R-value), derived from thermal conductivity, provides a practical measure for comparing insulation materials and meeting building code requirements (Building Science Corporation, 2022)

Thermal resistivity is the measure of a material's resistance to heat flow. It is the inverse of thermal conductivity and indicates how well a material insulates.

$$R = \frac{d}{k} \quad (3.9)$$

Where:

- R is the thermal resistance ($\text{m}^2 \cdot \text{K}/\text{W}$),
- d is the thickness of the material (m),
- k is the thermal conductivity ($\text{W}/\text{m} \cdot \text{K}$).

2.20. Transmissivity (τ):

Transmissivity is the measure of how much radiant energy passes through a material. Materials with high transmissivity allow most incident radiation to pass through without significant absorption or reflection.

3. Thermal Properties According to Algeria's Thermal Regulations for Residential Buildings (CNERIB):

The following tables summarize the thermal properties of commonly used building materials, including their density, thermal conductivity, and specific heat capacity, Thermal Capacity. These properties are fundamental in assessing the thermal performance of materials, particularly in hot

and dry climates. The data presented in the (Tables 3.5) serves as a reference for selecting materials to optimize thermal comfort and reduce energy consumption.

Table 3.5. Thermal Properties of Buildings Materials as Defined by Algeria's DTR C 3-2.

Source: CNERIB, 1997.

Materials	Dry Density (kg/m ³)	Thermal Conductivity (W/m·°C)	Specific Heat Capacity (J/kg·°C)
Natural Stones			
Granites, Porphyries	2300–2900	3.0	936
Basalts	2700–3000	1.6	936
Andesites, Volcanic Tuffs	2000–2700	1.1	936
Sedimentary Rocks			
Quartzite Sandstones	2000–2800	2.6	792
Limestone Sandstones	2000–2700	1.9	792
Hard Limestones	2350–2580	2.4	936
Firm Limestones	1840–2340	1.4	936
Soft Limestones	1480–1830	1.0	936
Very Soft Limestones	1470	0.85	936
Metamorphic Rocks			
Marble	2590	2.9	936
Gneiss	2300–2900	3.0	936
Schists, Slates	2000–2800	2.2	936
Granular Materials			
Dry Sand	1300	0.6	823
Sand + Gravel	1800	1.2	792
Common Aggregate Concrete			
Solid Concrete	2200–2500	1.75	1080
Cavernous Concrete	1700–2100	1.4	1080
Dense concrete ("structural")	1600 to 1800	1.05	1080
Dense concrete	1200 to 1400	0.70	1080
Mortar (for coatings and joints)			
Cement mortar	1900	1.15	1080
Mixed mortar	2200	1.40	1080
Lime mortar	1800	0.87	1080
Plasters			
Dense plaster ("high strength")	1100 to 1300	0.50	936
Ordinary interior plaster	750 to 1000	0.35	936
Solid plaster tiles	900 to 1000	0.35	936
Silico-Calcareous Bricks			
Solid brick	1600 to 1800	0.80	936
Perforated brick	1400 to 1600	0.70	936

Wood (Flooring, Wall Coverings, etc.)			
Medium-density hardwoods (oak, fruit trees)	600 to 750	0.23	2160
Heavy softwoods	600 to 750	0.23	2160
Light hardwoods (lime, maple, soft beech)	450 to 600	0.15	2160
Medium-density softwoods (pine, maritime pine)	450 to 550	0.15	2160
Light softwoods (fir, spruce)	300 to 450	0.12	2160
Very light softwoods (poplar)	300 to 450	0.12	2160
Tiles	1900	0.80	936
Glass	2700	1.10	792
Asphalt	2100	0.70	1044
Bitumen (felt boards, impregnated flexible sheets)	1000-1100	0.23	1656
Earth (rammed, stabilized soil, compressed blocks, terracotta)	1700-2000	1.15	936
Wall and flora coverings			
Ceramic products (tiles and slabs)	1900	1.0	936
Marble mosaic tiles (granite-like)	2200	2.1	936
Metals			
Pure iron	7870	72	468
Steel	7780	52	468
Cast iron	7500	56	468
Aluminum	2700	230	936
Copper	8930	380	432
Lead	11340	35	468
Brass	8400	110	468

Table 3.6. Thermal Properties of common Buildings Materials as Defined by Algeria's DTR C 3-2. **Source:** CNERIB, 1997.

Material	Equivalent Conductivity (W/m°C)	Thermal Capacity (J/kg°C)	Density (kg/m³)
Hollow bricks	0.48	936	900
Hollow blocks			
Made of heavy aggregate concrete	1.10	1080	1300
Made of slag concrete	0.65	1080	1300

Floor with hollow clay blocks (ordinary concrete slab)			
Compression slab in ordinary concrete	1.45	1080	1450
Compression slab in expanded clay or shale concrete	0.98	1080	1340
Floor with hollow expanded clay or shale blocks			
Compression slab in ordinary concrete	1.04	1080	1200
Compression slab in expanded clay or shale concrete	0.81	1080	990
Floor with hollow terracotta blocks			
Compression slab in ordinary concrete	1.00	984	1150
Compression slab in expanded clay or shale concrete	0.70	984	1150

Conclusion:

The studies of building materials is critical to the creation of climate-responsive and sustainable urban environments. This chapter describes the historical evolution, classification, and qualities of construction materials, with a focus on their role in thermal management. Materials with suitable physical, mechanical, chemical, and environmental qualities can greatly increase outdoor thermal comfort, especially in the harsh conditions of hot, dry climes.

Mitigating the consequences of severe temperatures in metropolitan environments requires an understanding of the thermal behavior of materials, including their capacity to reflect, absorb, and retain heat. Material science innovations such as high-performance composites, phase-change materials, and nanotechnology provide new options to improve thermal efficiency while decreasing environmental impact.

Engineers and architects may combine comfort, sustainability, and performance by basing material choices on these ideas. This foundation not only encourages the creation of energy-efficient urban

designs, but it also discusses the critical need for resilient and adaptive construction techniques in the face of global climate change. As this thesis proceeds, these findings will serve as the foundation for creating ways to improve material selection for thermal comfort in hot, dry regions.

CHAPTER IV: LITERATURE REVIEW (PART A): A SYNTHESIS OF URBAN CLIMATE AND OUTDOOR THERMAL COMFORT

Introduction

In the face of unprecedented urbanization and escalating climate change, the creation of thermally comfortable urban environments has emerged as a critical challenge for city planners, architects, and policymakers worldwide. As cities continue to expand, the complex interplay between urban form, building materials, and local climate conditions increasingly influences the quality of life for billions of urban dwellers. This chapter presents a comprehensive review of the current state of knowledge regarding outdoor thermal comfort in urban settings, with a particular focus on the role of building materials in shaping these thermal environments.

The urgency of this topic cannot be overstated. The United Nations projects that by 2050, nearly 70% of the world's population will reside in urban areas (UN DESA reports, 2018), a trend that is reshaping landscapes and microclimates at an unprecedented rate. Concurrently, the Intergovernmental Panel on Climate Change (IPCC) warns of intensifying heat waves, rising average temperatures, and more frequent extreme weather events. These converging phenomena place immense pressure on urban infrastructure and human health, necessitating innovative approaches to urban design and material selection that can mitigate heat stress and enhance outdoor comfort.

The thermal properties of building materials play a pivotal role in this context. From the albedo of façades to the thermal mass of pavements, the choices made in urban construction have far-reaching implications for the thermal balance of city spaces. Recent advancements in material science offer new possibilities for heat mitigation, yet their effectiveness is deeply intertwined with the geometric complexity of urban canyons and the diverse climatic conditions across global cities. This review seeks to untangle these relationships, offering insights into how material properties interact with urban form to influence thermal comfort at the street level.

Moreover, this chapter explores the multifaceted nature of urban thermal comfort, acknowledging that it is not solely a matter of temperature control but a complex phenomenon involving radiative, convective, and conductive heat exchanges, as well as human physiological and psychological factors. By examining various thermal comfort indices and assessment

methodologies, we aim to provide a nuanced understanding of how different urban design strategies and material choices impact human thermal sensation in outdoor spaces.

This chapter extends beyond isolated material properties to consider the synergistic effects of multiple urban elements. We delve into the interactions between building materials, urban vegetation, and anthropogenic heat sources, recognizing that effective thermal comfort strategies often require integrated approaches that leverage the combined potential of grey and green infrastructure.

Importantly, this chapter acknowledges the context-specific nature of thermal comfort solutions. What works in the hot dry climate of North Africa may be unsuitable for the humid tropics or temperate regions. By examining case studies from diverse climatic zones, we aim to distill principles that can inform climate-responsive urban design while highlighting the need for localized research and tailored interventions.

As we search through the extensive body of literature, we also identify critical knowledge gaps and emerging research directions. The complex, multidisciplinary nature of urban thermal comfort presents both challenges and opportunities for future studies, particularly in developing holistic models that can accurately predict and optimize outdoor thermal environments in the face of changing climatic conditions.

Therefore, the chapter serves as a foundation for understanding the crucial role of building materials in shaping outdoor thermal comfort.

In this light, the literature review chapter is divided into two main parts: **(Part A)** which is representing the global literature about urban climate, outdoor thermal comfort and climate change studies through theoretical definitions; **(Part B)** which is representing the experimental methodologies and studies covering numerical software and field measurements protocols within different context.

[Part A.1]

Urban Climate & Outdoor Thermal Comfort Literature Overview

Bibliometric and clustering of concepts

Figure 4.1 shows a network of non-random structure with clear clustering. The presence of distinct clusters indicates specific sub-disciplines or topic areas within the broader research focus.

1. Cluster identification and topic analysis:

Four main clusters were identified, each potentially representing a distinct research topic:

- a) **Red cluster:** Dominated by terms related to urban environments and human mobility (e.g., ‘pedestrian,’ ‘street,’ ‘tourism’). This suggests a focus on urban studies or environmental psychology in public spaces.
- b) **Green cluster:** Contains terms associated with indoor environments and health concerns (e.g., ‘ventilation,’ ‘classroom,’ ‘health’). This cluster likely represents research on indoor environmental quality and its health implications.
- c) **Blue cluster:** Centered on physiological and environmental measurements (e.g., ‘skin temperature,’ ‘heart rate’). This cluster appears to focus on human biometrics in relation to environmental factors.
- d) **Yellow cluster:** Smaller and more isolated, with terms like ‘hutch’ and ‘calf’. This could represent a niche area, possibly related to agricultural or veterinary studies.

As lecture of the general network, the positioning and connections between clusters provide insights into interdisciplinary relationships. For instance, the blue cluster (physiological measurements) bridges the red (urban environment) and green (indoor environment) clusters, suggesting that human physiological responses are a connecting factor between indoor and outdoor environmental studies.

Terms like ‘performance,’ ‘subject,” and ‘building’ appear as larger nodes centrally positioned, indicating their role as key concepts or bridging terms across multiple research areas. This suggests that these concepts may be central to the overall research field represented.

The presence of both broad terms (e.g., ‘health’) and specific technical terms (e.g., ‘skin temperature’) indicates a field that spans from general concepts to specialized measurements and methodologies. The prominence of terms like ‘simulation,’ ‘prediction,’ and ‘measure’ suggests a strong emphasis on quantitative and modeling approaches within the field.

This network visualization represents a multidisciplinary research area intersecting environmental science, urban studies, and human health. The structure indicates a field that integrates studies of built environments (both indoor and outdoor) with human physiological responses and health outcomes. The connection between clusters implies that research in this field often crosses traditional disciplinary boundaries. The central positioning of performance-related terms suggests that much of the research may be oriented towards understanding or improving human performance in various environmental contexts.

2. Cluster identification and topic analysis:

On the other hand, Figure 4.2 employs a network analysis approach, based on co-occurrence of keywords. Nodes represent individual concepts, with their size indicating relative frequency or importance.

- a) ***Central Cluster (Red)***: Dominated by ‘humans’ and ‘temperature,’ indicating a core focus on human thermal behavior.
- b) ***Urban environment cluster (Yellow-Green)***: Features terms like ‘cities,’ ‘urban heat island,’ and ‘pedestrians,’ suggesting urban microclimate studies.
- c) ***Physiological response cluster (Pink)***: Contains ‘body temperature,’ ‘heat stress,’ and ‘adaptation,’ focusing on human physiological responses to thermal conditions.
- d) ***Indoor environment cluster (Light Blue)***: Includes ‘indoor climate,’ ‘air conditioning,’ and ‘air pollution,’ representing indoor environmental quality studies.
- e) ***Climate and seasons cluster (Green)***: Terms like ‘seasons,’ ‘cold climate,’ and ‘thermal history’ suggest research on climate-related thermal comfort.

2.1. Central concepts and bridging terms:

Therefore, ‘humans,’ ‘temperature,’ and ‘hot’ emerge as central, high-frequency terms, bridging multiple clusters. This centrality underscores the human-centric nature of the research field, with temperature as a key variable.

The network structure reveals strong interdisciplinary links. For instance, ‘air pollution’ connects urban environment studies with indoor air quality research, while ‘adaptation’ links physiological responses to broader climate studies.

The indication of location-specific terms (e.g., ‘India,’ ‘Australia,’ ‘Sweden’) indicates a global scope of research, potentially highlighting regional variations in thermal comfort studies. Terms such as ‘thermal index,’ ‘forecasting,’ and ‘radiometry’ suggest a range of quantitative and measurement-based methodologies applied in the field.

Smaller, peripheral nodes like ‘internet of things’ and ‘particle size’ may represent emerging research areas or methodologies within the field.

2.2. Quantitative Observations:

- a) **Node sizes:** ‘Humans,’ ‘temperature,’ and ‘cities’ appear as the largest nodes, indicating their high frequency or centrality in the research corpus.
- b) **Cluster density:** The central and urban environment clusters show the highest density of connections, suggesting these are well-established research areas.
- c) **Inter-cluster connections:** The physiological response cluster shows strong connections to both urban and indoor environment clusters, indicating its attaching role in the field.

Figure 4.2 represents research field at the intersection of human physiology, urban studies, environmental science, and building engineering, all focused on thermal comfort and environmental interactions. The structure suggests a mature field with well-defined sub-domains, yet with significant interdisciplinary overlap. The appearance of urban-related terms alongside physiological responses indicates a strong focus on understanding human thermal experiences in urban contexts, driven by urbanization policies and climate change concerns. The equal emphasis on indoor and outdoor environments suggests a holistic approach to thermal comfort studies. The inclusion of terms related to adaptation and various climates points to an evolving understanding of thermal comfort as a dynamic, context-dependent phenomenon rather than a universal standard. While Figure 2 provides valuable insights, it's important to note that the temporal dynamics are not captured; a time-based analysis could reveal evolving research trends. The relative importance of terms may be influenced by publication biases or database limitations. Quantitative analysis of node centrality and edge weights would provide more precise insights into term relationships.

Investigating emerging topics like ‘IoT’ integration in thermal comfort studies. Exploring the interplay between urban heat island effects and indoor thermal management strategies. Examining how physiological adaptation mechanisms relate to varying urban and building design approaches across different climatic regions.

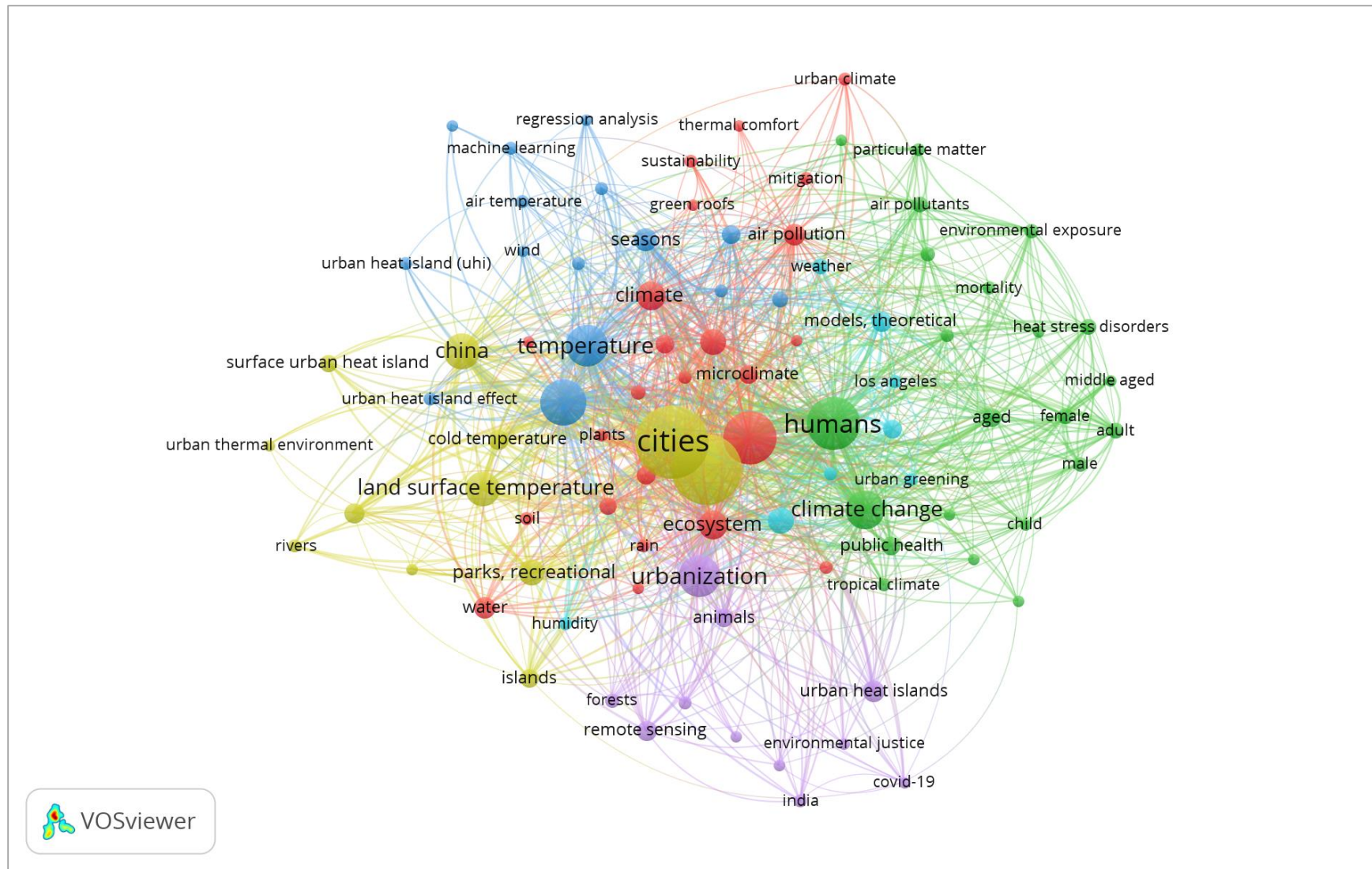


Figure 4.3. Literature review flowchart on the field of urban heat island (UHI) mitigation strategies between 2008 - 2023

Source: Author, 2023.

Figure 4.3 depicts a densely interconnected network with distinct clusters, indicating a multidisciplinary research field with several interrelated sub-domains. The network's structure suggests a mature field with well-established research areas and emerging connections between them.

3. Cluster identification and topic analysis:

- a) **Central cluster (Red):** Dominated by ‘cities,’ ‘temperature,’ and ‘climate,’ representing core urban climate research.
- b) **Human-environment interaction cluster (Green):** Includes ‘humans,’ ‘health,’ and ‘air pollution,’ focusing on human health in urban environments.
- c) **Urban Heat Island cluster (Yellow):** Features ‘land surface temperature,’ ‘urban heat island,’ and related terms, indicating a focus on urban thermal phenomena.
- d) **Environmental systems cluster (Blue):** Contains terms such as ‘ecosystem,’ ‘plants,’ and ‘water,’ suggesting research on urban greenery and natural systems within cities.
- e) **Methodology cluster (Light Blue):** Includes ‘machine learning,’ ‘regression analysis,’ and “models: theoretical,” representing analytical approaches used in the field.

Therefore, strong links are visible between clusters, particularly between urban climate (red) and human health (green) clusters, indicating the interdisciplinary nature of urban environmental research.

3.1. Emerging Topics:

Smaller nodes like ‘covid-19’ and ‘environmental justice’ suggest emerging research areas, potentially indicating new directions in the field.

3.2. Geographical Focus:

The appearance of ‘China’ and presence of ‘Los Angeles’ and ‘India’ indicate both global and location-specific research interests.

3.3. Quantitative Analysis:

- a. **Node Centrality:** Using visual estimation of node size as a proxy for centrality:
 - *Highest centrality:* ‘cities’ (largest node)
 - *Secondary centrality:* ‘humans,’ ‘temperature,’ ‘climate’

- *Tertiary centrality*: ‘climate change,’ ‘urban heat island,’ ‘air pollution’
- b. Cluster Density:** Estimating the number of nodes and connections within clusters:
 - *Highest density*: Central (red) and Human-Environment (green) clusters
 - *Medium density*: Urban Heat Island (yellow) cluster
 - *Lower density*: Methodology (light blue) and Environmental Systems (blue) clusters
- c. Inter-cluster Connections:** The strongest inter-cluster connections appear to be:
 - Between red (urban climate) and green (human-environment) clusters
 - Between yellow (urban heat island) and red (urban climate) clusters
- d. Term Co-occurrence:** High co-occurrence is visually apparent between:
 - ‘cities’ and ‘temperature’
 - ‘humans’ and ‘health’
 - ‘urban heat island’ and ‘land surface temperature’

3.4. Research Focus:

Figure 3 indicates a strong focus on urban climate and its impacts on human health and the environment. The centrality of ‘cities’ suggests that urban areas are the primary context for much of this research. The dense connections between clusters highlight the interdisciplinary nature of urban environmental research, integrating climate science, public health, ecology, and urban planning.

3.5. Methodological Approaches:

The presence of a distinct methodology cluster suggests a significant emphasis on advanced analytical techniques, including machine learning and theoretical modeling, in addressing complex urban environmental challenges.

3.6. Emerging Concerns:

The inclusion of terms such as ‘Covid-19’ and ‘environmental justice’ indicates that the field is responsive to current global challenges and social concerns. The prominence of specific locations

(China, Los Angeles, India) alongside global terms underscores the field's engagement with both local case studies and global phenomena.

3.7. Temporal Dynamics:

This static visualization doesn't capture the evolution of research topics over time. A longitudinal analysis could reveal trends and shifts in research focus. While visual estimation provides insights, precise quantitative analysis of node centrality, edge weights, and cluster modularity would offer more accurate results.

- Integrating more social science perspectives, particularly around environmental justice and urban governance.
- Exploring the interactions between climate change adaptation strategies and public health outcomes in cities.
- Investigating the role of emerging technologies (beyond machine learning) in urban climate research and management.
















These comprehensive three networks (Figures 1, 2, and 3) analysis provides a valuable overview of the current state of urban climate and environmental health research, highlighting key themes, methodological approaches, and potential areas for future investigation.

















[Part A.2]

Relevant Studies on Outdoor Thermal Indices and Heat Mitigation

Thermal indices comparison & development through articles

Table 4.1. Sample summary used of main recent literature about thermal comfort assessment and outdoor heat mitigation. **Source:** Author.

Aspects		Indicators	Based relevant and cited Articles and Books		Journals (Web of Science/ Scopus)	Publication year
Thermal Comfort (Outdoor)	Parameters	Individual (Human) Environmental	<ul style="list-style-type: none"> • Man, climate and architecture • Different aspects of assessing indoor and outdoor thermal comfort • Outdoor thermal comfort and outdoor activities: A review of research in the past decade • Instruments and methods in outdoor thermal comfort studies - The need for standardization 	   	Energy and buildings Cities Urban Climate	<ul style="list-style-type: none"> • 1969 • 2002 • 2012 • 2014
	Indices	PMV	<ul style="list-style-type: none"> • A new general formulation for the PMV thermal comfort index 		Buildings	<ul style="list-style-type: none"> • 2022
		PET	<ul style="list-style-type: none"> • A Simulation Study of the Impact of Urban Street Greening on the Thermal Comfort in Street Canyons on Hot and Cold Days • The impact of street geometry on outdoor thermal comfort within three different urban forms in severe cold region of China • Diurnal outdoor thermal comfort mapping through envi-met simulations, remotely sensed and in situ measurements • Thermal sensation and indices in the urban outdoor hot Mediterranean environment of Cyprus • Outdoor human thermal perception in various climates: A comprehensive review of approaches, methods and quantification 	    	Forests Building and Environment Atmosphere Theoretical and Applied Climatology Science of the total Environment	<ul style="list-style-type: none"> • 2023 • 2021 • 2023 • 2020 • 2018
		UTCI	<ul style="list-style-type: none"> • Improving the operational forecasts of outdoor Universal Thermal Climate Index with post-processing • How Can Street Interface Morphology Effect Pedestrian Thermal Comfort:A Case Study of the Old Town of Changsha, China • Comparing universal thermal climate index (UTCI) with selected thermal indices to evaluate outdoor thermal comfort in traditional courtyards with BWh climate • Spatiotemporal heterogeneity of street thermal environments and development of an optimised method to improve field measurement accuracy • The universal thermal climate index as an operational forecasting tool of human biometeorological conditions in Europe 	    	International journal of biometeorology SSRN Urban Climate Applications of the Universal Thermal Climate Index UTCI in Biometeorology (book chapter)	<ul style="list-style-type: none"> • 2024 • 2024 • 2024 • 2022

		COMFA	<ul style="list-style-type: none"> Outdoor human comfort and thermal stress: A comprehensive review on models and standards 		Urban Climate	<ul style="list-style-type: none"> 2016
		Other thermal indices	<ul style="list-style-type: none"> Microclimatic analysis of outdoor thermal comfort of high-rise buildings with different configurations in Tehran: Insights from field surveys and thermal comfort indices A review of outdoor thermal comfort indices and neutral ranges for hot-humid regions 	 	Building and Environment Urban Climate	<ul style="list-style-type: none"> 2023 2020
	Outdoor Thermal Comfort relationships	UHI (urban heat island)	<ul style="list-style-type: none"> Urban heat islands and their effects on thermal comfort in the US: New York and New Jersey Heat vulnerability and street-level outdoor thermal comfort in the city of Houston: Application of google street view image derived SVFs Urban Heat Island and Thermal Comfort Assessment in a Medium-Sized Mediterranean City Assessing urban heat islands and thermal comfort in Noida City using geospatial technology 	   	Ecological Indicators Urban Climate Atmosphere Urban Climate	<ul style="list-style-type: none"> 2023 2023 2022 2021
		Urban criteria	<ul style="list-style-type: none"> Urban design strategies for summer and winter outdoor thermal comfort in arid regions: The case of historical, contemporary and modern urban areas in Mashhad, Iran Influence of urban geometry on outdoor thermal comfort in a hot dry climate: A study in Fez, Morocco Effects of asymmetry, galleries, overhanging facades and vegetation on thermal comfort in urban street canyons 	  	Sustainable Cities and Society Building and Environment Solar Energy	<ul style="list-style-type: none"> 2023 2007 2006
		Building materials	<ul style="list-style-type: none"> Evaluation of outdoor thermal comfort under different building external-wall-surface with different reflective directional properties using CFD analysis and model experiment Exploration of the thermal behaviour and energy balance of urban canyons in relation to their geometrical and constructive properties Outdoor thermal comfort by different heat mitigation strategies- A review On the impact of innovative materials on outdoor thermal comfort of pedestrians in historical urban canyons 	   	Building and Environment Building and Environment Renewable and Sustainable Energy Reviews Renewable Energy	<ul style="list-style-type: none"> 2022 2021 2018 2018
		Vegetation	<ul style="list-style-type: none"> Outdoor thermal comfort enhancement using various vegetation species and materials (case study: Delgosha Garden, Iran) 		Sustainable Cities and Society	<ul style="list-style-type: none"> 2021
		Walkability	<ul style="list-style-type: none"> Pedestrians' behavior based on outdoor thermal comfort and micro-scale thermal environments, Austin, TX 		Science of the total Environment	<ul style="list-style-type: none"> 2022 2021



			• The Street Walkability and Thermal Comfort Index (SWTCI): A new assessment tool combining street design measurements and thermal comfort.						Science of the total Environment													
			<i>Citations</i>																			
			> 2000		> 20		> 400		> 25		> 350		> 180		> 130		> 700		> 20		> 40	

Table 4.1 presents a comprehensive overview sampling of studies examining the relationship between human, urban characteristics and thermal fluctuations across various climates. The research findings demonstrate that aspect ratio (H/W), street orientation, sky view factor (SVF), and overall city configuration significantly influence pedestrian thermal comfort, with effects varying based on local climate conditions. In hot-humid and hot-dry climates, increasing the aspect ratio generally leads to reduced air temperatures, with deep canyons showing better thermal conditions than shallow ones. Street orientation plays a crucial role, with N-S oriented streets typically offering better thermal comfort than E-W oriented ones, particularly in hot-dry climates. The impact of SVF varies; in humid continental climates, higher SVF values increase daytime temperatures while decreasing nighttime temperatures, whereas in hot-dry climates, high SVF values reduce both air temperature and pedestrian comfort. City configuration studies reveal that different urban layouts significantly affect wind velocity and mean radiant temperature. For instance, courtyard archetypes in oceanic climates and organic configurations with high shading in desert climates show improved thermal comfort, although the latter may have adverse effects on wind behavior in winter. These findings underscore the complex interplay between urban design elements and local climate in determining outdoor thermal comfort. The research highlights the need for climate-specific urban design strategies, as solutions effective in one climatic context may not be suitable in another. This complex understanding of how spatial characteristics influence thermal conditions is crucial for developing climate-responsive urban designs that enhance pedestrian comfort across diverse urban environments.

The urban environment significantly influences microclimates, especially in regions susceptible to extreme temperature fluctuations due to rapid urbanization and climate change. The topic of thermal comfort and heat mitigation in outdoor spaces has gained prominence as cities aim to enhance livability under changing environmental conditions. Researchers have focused on various indicators to evaluate outdoor thermal comfort, such as indices measuring thermal sensation and the relationship between urban geometry, building materials, vegetation, and urban heat islands (UHI). This review covers key methods and findings related to human and environmental factors that impact thermal comfort, providing insight into mitigation strategies based on recent literature. Thermal comfort is influenced by individual human characteristics and environmental factors. The studies summarized categorize their findings based on these two primary parameters:

1. ***Individual factors (Human):*** Studies focus on the physiological and psychological responses of individuals to thermal environments. This includes subjective thermal comfort experiences, thermal perception, and adaptation strategies to mitigate discomfort in extreme climates.
2. ***Environmental factors:*** Various environmental parameters such as air temperature, humidity, wind speed, and solar radiation influence outdoor thermal comfort. These studies often integrate simulations and field measurements to assess the thermal environments within urban settings.

A variety of thermal comfort indices are used to quantify human thermal comfort in outdoor environments. These indices are essential for assessing the thermal conditions in diverse climates and urban forms.

One of the well-established indices, PMV, has been used extensively in indoor environments and is adapted for outdoor assessments. Recent research, such as the study of Laouadi et al, 2022, introduced a general formulation for the PMV index, which has proven useful in simulating outdoor conditions.

The PET index, a crucial tool in evaluating outdoor thermal comfort, has been widely used in simulation studies. For instance, several studies explored the impact of urban street greening on thermal comfort in street canyons. The study of Jun-Ya Liu et al, 2023, which investigates how urban street greening affects thermal comfort in street canyons, and the study found that high tree

canopy density improves comfort on hot days and short hedges positively impact comfort during hot days using ENVI-met software. Other studies (Cheng Sun et al, 2022; Fiorillo et al, 2023; Pantavou et al, 2020; Potchter, 2018) have investigated the influence of street geometry, diurnal variations, and thermal sensation in different climatic regions, such as Cyprus and China. These findings highlight the versatility of PET in various urban forms and climates.

The UTCI is another widely adopted index that has been the subject of several recent studies. For example, research conducted by Kuzmanovic et al, 2024, has explored the effect of street morphology on pedestrian thermal comfort, while other studies assessed the operational forecasting capabilities of the UTCI. Comparisons between UTCI and other indices, such as COMFA, have revealed nuances in the assessment of outdoor thermal comfort, particularly in BWh (hot dry) climates (Zheng, 2024; Mahdavinejad et al, 2024; Xiong et al, 2022; Di Napoli, 2021).

Beyond the widely used PMV, PET, and UTCI, other indices such as COMFA have been utilized in specific contexts, particularly in hot-humid regions (Coccolo et al, 2016). A review of outdoor thermal comfort indices in Tehran, conducted through field surveys and simulations, demonstrates the breadth of research methodologies used to assess thermal environments in high-rise urban settings (Karimi et al, 2023; Binarti et al, 2020).

Urban heat islands exacerbate thermal discomfort in densely populated areas by amplifying local temperatures compared to surrounding rural areas. Several studies summarized in the table focus on the relationship between UHI and thermal comfort in cities like New York, Houston, and Mediterranean cities (Yin et al, 2023; Kalogeropolous et al, 2022; Sharma et al, 2021). Notably, the study of Kim et al, 2023 in Houston combined street-level thermal comfort assessments with Google Street View-derived sky view factors (SVFs) to evaluate heat vulnerability. These innovative methodologies integrate remote sensing and ground-level observations to provide more accurate representations of the UHI effect.

The spatial configuration of urban areas has a direct impact on outdoor thermal comfort. Several studies reviewed, such as those conducted in Mashhad (Darbani et al, 2023) and Fez (Johansson, 2006), examined how urban geometry, building configurations, and materials influence thermal environments. The study of Darbani et al, 2023 in Mashhad demonstrated that design strategies focusing on summer and winter thermal comfort could mitigate extreme

conditions in arid regions. The findings from these studies highlight the importance of thoughtful urban planning and architecture in enhancing outdoor thermal comfort.

The role of building materials in thermal regulation cannot be overstated, particularly in hot climates. Recent studies have examined how different reflective properties of building surfaces affect thermal comfort. For example, the study of Yuan et al, 2022 evaluated the thermal performance of building materials with varying directional reflectivity using computational fluid dynamics (CFD) analysis. This research is critical in identifying material properties that can mitigate heat retention and improve pedestrian thermal comfort in historical urban areas. Furthermore, the review of Taleghani, 2018 provided insights into various heat mitigation strategies, showcasing the potential of innovative building materials to enhance outdoor thermal environments.

Vegetation plays a pivotal role in cooling urban areas and improving thermal comfort through shading and evapotranspiration. Studies included in the table focus on the use of different plant species and vegetation arrangements to enhance outdoor thermal comfort. For instance, a case study conducted by Gachkar et al, 2021 in Delgosha Garden, Iran, demonstrated the effectiveness of specific vegetation types in reducing surface temperatures and enhancing the thermal comfort of outdoor spaces. These findings underline the importance of integrating green infrastructure in urban planning to counteract the UHI effect and improve the quality of life in cities.

Walkability is increasingly recognized as an important factor in urban design, directly linked to thermal comfort. Recent research has introduced tools such as the Street Walkability and Thermal Comfort Index (SWTCI), which combines street design measurements with thermal comfort assessments. A study conducted by Woong Kim and Brown, 2022 in Austin, Texas, explored pedestrian behavior in response to micro-scale thermal environments, revealing that thermal comfort significantly influences the walkability and usability of urban spaces.

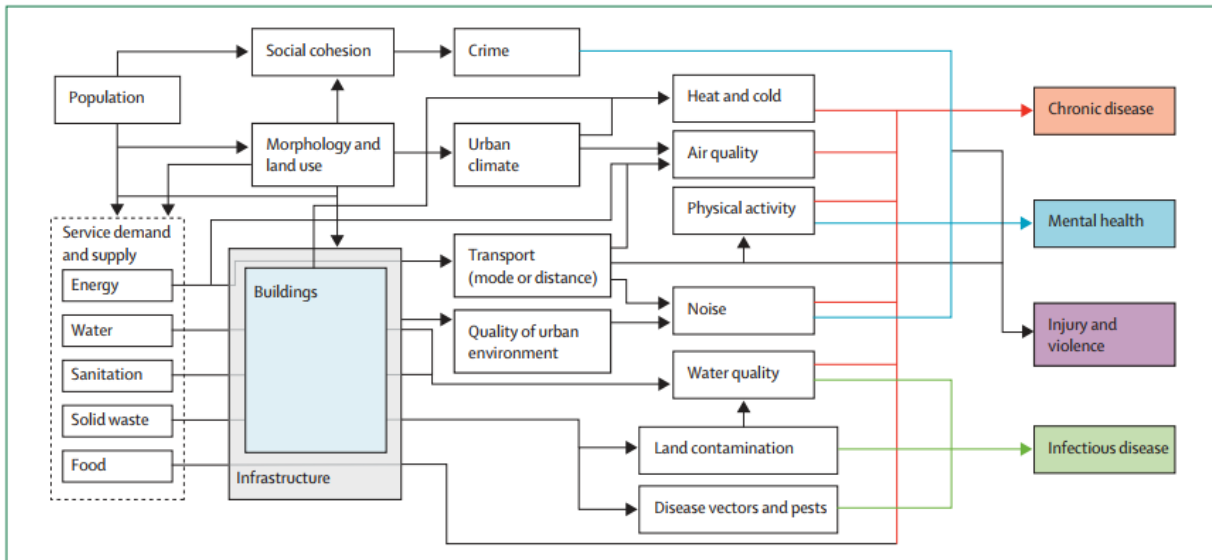
In our research, we focused on the intricate relationship between outdoor thermal conditions and building materials, particularly examining their combined impact on human thermal balance in extreme weather scenarios.

[Part A.3]

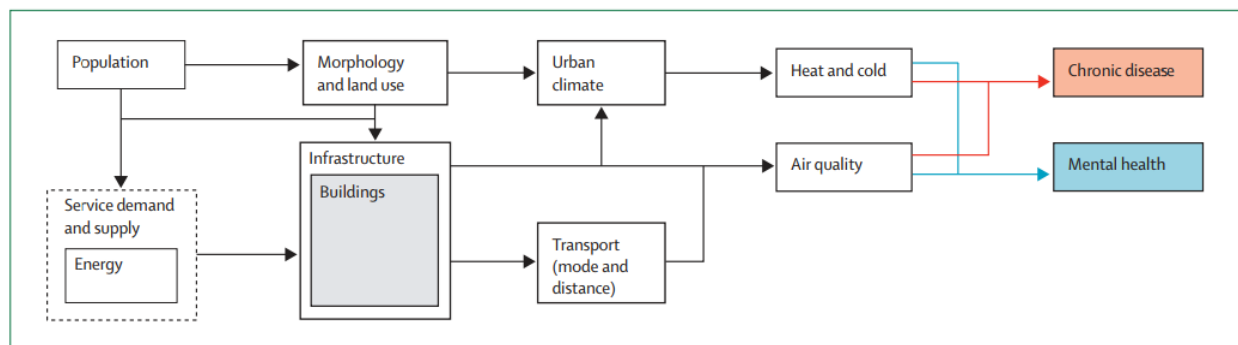
Relevant Studies about Outdoor Thermal Comfort and Urban Geometry

Insights & purposes

In the face of unprecedented global urbanization, there is an urgent imperative to create suitable living environments, infrastructures, and facilities to meet the burgeoning population's essential requirements. Kleerekoper et al, 2012 and Rydin et al, 2012, emphasize that global warming has rendered human comfort thresholds in urban areas increasingly vulnerable, leading to a spectrum of health issues. These range from cardiovascular diseases with heat stroke to cardiorespiratory ailments, significantly impacting public health.



(a)



(b)

Figure 4.4. Urban environment conditions' impact on human health and behavior: (a) Health outcomes and the urban environment: connections; (b) Connections of the urban heat island and health.

Source: Rydin, Y et al. (2012). Shaping cities for health: complexity and the planning of urban environments in the 21st century. The lancet.

Furthermore, Magli et al, 2015 and Pérez-Lombard et al, 2008 highlight a substantial surge in energy consumption for cooling purposes, exacerbating the environmental challenges faced by

urban centers. This multifaceted context, as noted by Santamouris, 2020, demands more effective, adaptive, and sustainable urban planning and development practices to enhance the quality of life for city dwellers while mitigating the adverse effects of climate change.

The strong relationship between urban morphology and thermal comfort has become a focal point of recent research. Studies have begun exploring the impact of urban fabrics and their building material characteristics on outdoor human thermal comfort and Urban Heat Island (UHI) effects. Darbani et al, 2023 and Ali-Toudert, 2021 have conducted comprehensive investigations in this domain, shedding light on the complex interplay between built environments and thermal dynamics. Complementing these efforts, Oke et al, 2017 provide a foundational understanding of urban climatology, emphasizing the need for interdisciplinary approaches in addressing urban thermal challenges.

However, Sharmin et al, 2017 point out that many previous studies have focused on single-factor groups to evaluate thermal comfort levels at different scales, without investigating the synergistic effects of multiple factors, particularly in building material characteristics. This gap in the literature underscores the need for more holistic research approaches that consider the interrelationships between various urban design elements.

Urban design strategies related to outdoor thermal comfort have been elaborated in diverse contexts and under various methodological approaches. Deng and Wong, 2020 investigated the impact of the H/W aspect ratio, the sky view factor (SVF), and urban canyon orientation as critical street geometry factors influencing microclimate variables at pedestrian levels in Nanjing City, China. Their results revealed that outdoor thermal comfort is significantly driven by solar access, which is determined by the canyon aspect ratio and orientation. Building on this, Jamei et al, 2016 emphasize the importance of integrating urban geometry considerations with vegetation strategies to optimize outdoor thermal environments.

In the context of hot dry climates, Johansson, 2006 conducted seminal research in Fez, Morocco. The study concluded that climate-conscious urban design should incorporate a compact urban form with deep street canyons to enhance outdoor thermal comfort. However, the researcher noted that cities with cold winters in similar climates should include wider streets for greater solar access, highlighting the need for climate-specific urban design solutions. Corroborating these findings, Ali-Toudert and Mayer, 2006 observed in Ghardaia City, Algeria, that the duration of

high thermal stress within a street canyon strongly depends on aspect ratio and street orientation. Their work underscores the importance of considering local climatic conditions in urban design decisions.

Expanding the geographical scope, Muniz-Gaal et al, 2020 found in tropical climates that canyons with a higher H/W aspect ratio increase wind speed and shading by buildings, thus improving thermal comfort at the pedestrian level, especially during summer.

To the best of our knowledge, the combination of street geometry aspects and building envelopes for outdoor thermal comfort has been very limited in previous research. This gap presents an opportunity for innovative studies that integrate multiple urban design elements to address thermal comfort challenges comprehensively.

Table 4.2. Summary of various studies about the relationships among the spatial characteristics within cities and the thermal fluctuations under different weather conditions.

Source: Jamei, E., et al. (2016). Review on the impact of urban geometry and pedestrian level greening on outdoor thermal comfort. Renewable and Sustainable Energy Reviews.

Reference	City	Climate	Results
<i>Summary of studies on the impact of aspect ratio (H/W) on pedestrian thermal comfort</i>			
Ahmed et al, 1994	Dhaka, Bangladesh	Hot-humid	4.5 K reduction in maximum air temperature by increasing the aspect ratio from 0.3 to 2.8
Johansson, 2006	Fez, Morocco	Hot-dry	6 K daytime air temperature difference between a deep and shallow canyon
Giannopolou et al, 2010	Athens, Greece	Mediterranean	Reduction of aspect ratio from 3 to 1.7 resulted in increased median (1.1 and 1.85 °C), maximum (0.57 and 0.86 °C), and minimum (1.5, 2.8 °C), values of cooling rates
Bourbia and Boucheriba, 2010	Constantine, Algeria	Semi-arid	Deep canyons presented lower values of air (3 - 6 C°) and surface temperature (12 °C), compared to shallow canyons
Bourbia and Awbi, 2004	El-Oued, Algeria	Hot-dry	The air temperature in wide canyons (H/W - 0.5) are 4 °C higher than the one in narrow canyons (H/W - 2)
Ali-Toudert and Mayer, 2007	Ghardaia, Algeria	Hot-dry	Increasing the aspect ratio from 1 to 2, contributed to up to 24 K improvement in PET values
<i>Summary of studies on the impact of street orientation on pedestrian thermal comfort</i>			
Nunez and Oke, 1977	Vancouver, Canada	Oceanic	Street orientation significantly affects the thermal balance in urban areas
Johansson, 2007	Fez, Morocco	Hot-dry	E - W oriented streets exhibit the worst thermal condition
Ali-Toudert, 2007	Ghardaia, Algeria	Hot-dry	N - S oriented streets recorded better thermal condition
Elnahas, 2003	Adelaide, Australia	Mediterranean	The effect of canyon orientation on comfort is more perceptible in deep canyons than in wide ones
Taleb and Taleb, 2014	Dubai, UAE	Desert	The acceptable range of comfort (PMV) is monitored in the orientations where in higher-level wind flow is promoted
<i>Summary of studies on the impact of sky view factor (SVF) on pedestrian thermal comfort</i>			

Yan et al, 2014	Beijing, China	Humid continental	Increasing SVF contributes to increased daytime and decreased night time air temperature
Bourbia and Awbi, 2004	El-Oued, Algeria	Hot-dry	High values of SVF reduce the air temperature and comfort at pedestrian level
Correa et al, 2012	Mendoza, Argentina	Mid latitude desert	Solar access and sky exposure ease the radiative cooling and affect the daytime and night time comfort respectively
Charalampopoulos et al, 2013	Athens, Greece	Mediterranean	Low SVF and dense green coverage resulted in 8.7 °C reduction in PET level
<i>Summary of studies on the impact of city configuration on pedestrian thermal comfort</i>			
Johansson et al, 2013	Sao Paulo, Brazil	Humid Subtropical	Significant differences in the wind velocity and mean radiant temperature were recorded in different urban configurations
Steemers et al, 1997	London, UK	Oceanic	The courtyard archetype is the most thermally comfortable urban configuration
Taleb and Abu-Hijleh, 2013	Dubai, UAE	Desert	Organic urban configuration with higher level of shading performed better in summer, but the impact on wind behavior was not beneficial in winter
Taleghani et al, 2014	Netherlands	Temperate	Duration of the exposure to direct sun and mean radiant temperature level are determinant factors in comfort level

Several noteworthy studies have explored the impact of street canyon geometries linked with building materials of external walls on the outdoor thermal environment. Ali-Toudert, 2021 found that differences in heat stress magnitudes depend on the aspect ratio due to different road and wall fractions, whereas thermal inertia and insulation lead to different shares of sensible versus storage heat throughout the day. This work is complemented by Oke et al, 2017, who provide a comprehensive framework for understanding the energy balance of urban canyons.

Wonorahardjo et al, 2020 referred to high-density walls such as brick and concrete storing heat, causing a significant increase in heat island intensity during the afternoon. Their findings align with those of Santamouris et al, 2011, who documented the thermal performance of various building materials in urban settings and their impact on the urban heat island effect.

In the field of innovative materials, Rosso et al, (2018) showed that cool materials can improve the microclimate without neglecting preservation constraints, setting the best thermal comfort scenarios by enhancing albedo on urban canyon surfaces. However, their application on the vertical surfaces of deep canyons can lead to increased thermal discomfort effects. This nuanced understanding is further developed by Santamouris et al, 2011, who explore the potential of advanced materials in urban heat mitigation strategies.

Schrijvers et al, 2017 found that the most effective strategy to minimize thermal stress inside urban canyons with aspect ratio $H/W=0.5$ is a uniform albedo of 0.2. For $H/W=1$, an albedo gradient from high at the bottom part to low at the top of the vertical walls of building envelopes showed the lowest thermal stress. These findings are supported by the work of Erell et al, 2014, who investigate the complex radiative interactions within urban canyons and their impact on pedestrian thermal comfort.

Table 4.3. Summary of characteristics of the studies on the thermal impact of a possible increase of urban albedo.

Source: Santamouris, M. (2013). Using cool pavements as a mitigation strategy to fight urban heat island - A review of the actual developments. Renewable and Sustainable Energy Reviews.

Reference	City	Initial albedo	Final albedo	Reduction of maximum ambient temperature (K)
Fang et al, 2011	Fresno, USA		Increase of albedo of the city because of cool pavements by 0.02	Reduction of the average ambient temperature by 0.2 K
Fang et al, 2011	Fresno, USA		Increase of albedo of the city because of cool pavements by 0.09	Reduction of the average ambient temperature by 0.8 K
Takahashi, 2011	Tokyo, Japan		Increase of the albedo by using cool pavements	Reduction of the average ambient temperature by 0.15 K
	Atlanta, USA	0.15	0.30	Negligible
	Atlanta, USA	0.15	0.45	2.5 K
IEC, 2007	Various Californian Cities	0.117 - 0.152	0.18 - 0.252	1.0 K
IEC, 2007	Various Californian Cities	0.117 - 0.152	0.199 - 0.374	2.0 K
EPA, USA	Los Angeles, USA	0.13	0.26	3.0 K
Taha, 2008	Huston, USA	0.08 for pavements; 0.1 for roofs; 0.25 for walls	0.2 for pavements; 0.3 for roofs; 0.3 for walls	0.5 K
Zhou and Shepherd, 2010	New York, USA	0.15	0.5	0.5 K
Rosenfeld et al, 1998	Los Angeles, USA	0.05 for pavements; 0.15 for roofs	0.3 for pavements; 0.5 for roofs	1.5 K
Millstein and Menon, 2011	Various US cities			Increase of albedo of pavements by 0.15, and of roofs by 0.25
Taha, 2008	Philadelphia, US			Increase of the global albedo by 0.1

Conclusion

The comprehensive literature review reveals that outdoor thermal comfort in urban environments is significantly influenced by the complex interplay between urban geometry, building materials, and local climate conditions. This relationship is particularly crucial in the context of rapid urbanization and climate change, which exacerbate thermal challenges in cities worldwide.

A key finding from the review is the critical role of building materials in shaping outdoor thermal environments. The thermal properties of materials used in urban construction, particularly in building envelopes and street surfaces, have a substantial impact on local temperature patterns and thermal comfort. Studies have shown that the selection of appropriate building materials can lead to significant improvements in outdoor thermal conditions. For instance, the use of high-albedo or ‘cool’ materials can mitigate heat stress by reflecting more solar radiation and reducing surface temperatures. However, the effectiveness of these materials varies depending on the urban context, particularly the geometry of street canyons.

The geometry of urban canyons, characterized by the height-to-width (H/W) ratio, emerges as a crucial factor in determining the performance of different building materials. Research indicates that in wide canyons ($H/W=0.5$), a uniform albedo of 0.2 is most effective in minimizing thermal stress. Conversely, in deeper canyons ($H/W=1$), an albedo gradient from high at the bottom to low at the top of vertical walls shows the best performance. These findings underscore the need for a complex approach to material selection that considers the specific geometric characteristics of urban spaces.

The review also highlights the importance of thermal inertia and insulation properties of building materials. Materials with high thermal mass, such as brick and concrete, can store significant amounts of heat, contributing to increased urban heat island intensity, particularly during afternoon hours. This phenomenon emphasizes the need for careful consideration of material thermal properties in urban design, especially in hot climates where heat storage can increase thermal discomfort.

CHAPTER V: LITERATURE REVIEW (PART B): A REVIEW OF MODELLING TECHNIQUES, CONTEXTUAL APPLICATIONS AND BUILDING MATERIALS

Introduction

This chapter provides an exploration of the numerical methodologies and experimental approaches in urban climate studies, focusing on their application to outdoor thermal comfort analysis and mitigation strategies.

The chapter delves into two major aspects: numerical modeling and field measurement techniques, highlighting the role of advanced tools and methodologies in understanding the relationship between urban morphology, building materials, and thermal behavior. Numerical simulation tools like ENVI-met, RayMan, and SOLWEIG are analyzed for their ability to model complex urban microclimates, providing detailed insights into radiation fluxes, thermal indices, and the impact of urban geometry on thermal performance. Experimental studies are discussed in the context of field measurement protocols, showcasing how empirical data on surface temperatures, albedo, and building envelope characteristics inform the development of climate-responsive design strategies.



The chapter bridges theoretical definitions with practical applications, emphasizing the importance of integrating numerical and experimental approaches to achieve sustainable urban environments. By exploring these methodologies, the chapter aims to provide a comprehensive understanding of how innovative tools and techniques can optimize thermal comfort and mitigate urban heat island effects in diverse climatic contexts.




[Part B.1]



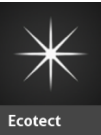
Numerical Modelling and Simulation Tools in Urban Area



Software from founders & users' visions

Table 5.1. Analysis of numerical tools for environmental and architectural simulation: a comparative overview. **Source:** Author.

Software	Definition	Characteristics and process	Inputs meteorological parameters	Outputs thermal indices	Main findings of studies about building materials and albedo impact on outdoor thermal comfort (Lam et al, 2021)
ENVI-met 	<ul style="list-style-type: none"> ENVI-met is a three-dimensional and CFD microclimate simulation software that enables the creation of sustainable living conditions in a constantly changing environment. The calculation modules of ENVI-met cover a wide range of scientific disciplines - from fluid dynamics and thermodynamics to plant physiology and soil science. ENVI-met is not recommended for Building Performance Simulation (BPS) analysis. However, with some effort, ENVI-met simulations can be run for a full year and these results can be used to support BPS. 	<ul style="list-style-type: none"> ENVI-met can simulate a specific meteorological for a specific planning scenario. The horizontal resolution is typically 1-10 m, with simulated periods ranging from 1 to 5 days. The size of the model domain is typically between 50×50 and 500×500 grid cells horizontally and 20-50 grid cells vertically. CPU: Intel Pentium D or AMD Athlon 64 X2 RAM: 8 GB OS: Windows 10 64-bit or higher VIDEO CARD: No specific requirements FREE DISK SPACE: more than 10 GB 	<ul style="list-style-type: none"> Tair, RH, Vair, Global radiation (optional), Precipitation (optional) 	<ul style="list-style-type: none"> PMV, PET, UTCI, SET* 	<ul style="list-style-type: none"> An increase of 0.4 in the ground surface albedo overall reduced thermal comfort. Asphalt could increase Ts by up to 4.7°C and Ta by up to 3.2°C. Observations yielded an average Ts of 64.6 °C for asphalt and 56.7 °C for concrete. The vegetation provided significant benefit to the environment. High albedo materials could ease the thermal load of the buildings but created a higher thermal stress for pedestrians. Low surface albedo (0.2) resulted in a 1.7 K reduction of PET, but high surface albedo (0.8) led to a 1.8 K increase of PET. Every surface albedo increment of 0.1 led to 1.2°C higher Tmrt, and consequently 0.8°C higher PET.
RayMan 	<ul style="list-style-type: none"> RayMan is a micro-scale model to calculate radiation fluxes in simple and complex environments. RayMan is one dimensional in space (all the calculations are performed for one point). It follows the diagnostic approach to be time-independent. 	<ul style="list-style-type: none"> RayMan allows the calculation of Tmrt, which is an important input parameter in the calculation of thermal biometeorological indices like PT, UTCI and PET. RayMan requires a limited number of meteorological input, and only common parameters RayMan determines the SVF. This can be done based on Fish-eye images. 	<ul style="list-style-type: none"> Tair, VP (or RH), Vair, fish-eye picture (optional) 	<ul style="list-style-type: none"> PET, PMV, SET*, UTCI, PT, mPET 	<ul style="list-style-type: none"> Increasing greenery cover improved thermal comfort during the whole study period. The Tmrt of grass cover and water element were around 48°C, compared with paving materials (72°C). Bare soil reduced Tmrt by up to 30 K, but impervious pavement (concrete) caused an increase in Tmrt of 16 K.

<p>SOLWEIG</p> 	<ul style="list-style-type: none"> SOLWEIG is a model that simulates spatial variations of 3D radiation fluxes and the Tmrt in complex urban settings. It is also able to model spatial variations of shadow patterns. In SOLWEIG, Tmrt is derived by modelling shortwave and longwave radiation fluxes in six directions. 	<ul style="list-style-type: none"> SOLWEIG requires meteorological forcing data (global shortwave radiation, air temperature (Ta), relative humidity (RH)), urban geometry (DSMs), and geographic information. It requires continuous maps of sky view factors to determine Tmrt. Both vegetation and ground cover information can be added to increase the accuracy of the model output. 	<ul style="list-style-type: none"> Tair, RH, Incoming shortwave radiation (W m²), Vair (optional) 	No	<ul style="list-style-type: none"> Compared with shadowing, changing ground surface materials was not as in reducing the radiant load during heat waves.
<p>Ansys FLUENT</p> 	<ul style="list-style-type: none"> Ansys FLUENT is a computational fluid dynamics (CFD) used for simulating fluid flow, heat transfer, and chemical reactions in complex systems. It is widely employed across various industries for engineering simulations that require the analysis of how fluids (liquids and gases) behave in different conditions. 	<ul style="list-style-type: none"> CPUs speed of 3.5 GHz or higher. At least 8 to 16 cores is recommended. CPUs with higher thread. 	<ul style="list-style-type: none"> Vair, Solar radiation, RH, VP, Turbulence, Pollutant, 	No	<ul style="list-style-type: none"> By reducing shortwave radiation reflected from the ground, it could lead to lower ground temperature and higher wall temperatures. Between small and large aspect ratio, the difference in the ground and wall temperature was smaller during daytime than night-time. This difference was also more noticeable when the bulk wind speed was smaller.
<p>Radiance</p> 	<ul style="list-style-type: none"> Radiance is a suite of programs for the analysis and visualization of lighting in design. The advantage of Radiance over simpler lighting calculation and rendering tools. 	<ul style="list-style-type: none"> Input files specify the scene geometry, materials, luminaires, time, date and sky conditions (for daylight calculations). Calculated values include spectral radiance (luminance + color), irradiance (illuminance + color) and glare indices. Simulation results may be displayed as color images, numerical values and contour plots. Additional tools: CAD or 3D modelling tools such as: AutoCAD, SketchUp, Rhino, or Blender. Processor: Intel Core i7/i9 with 6 to 8 cores, 3.0 GHz or higher. RAM: 16 GB or more. Storage: 512 GB. Graphics: Dedicated GPU. 	<ul style="list-style-type: none"> Solar radiation, Solar position, Sky conditions <p>Or:</p> <ul style="list-style-type: none"> EPW weather file TMY file 	No	-

<p>Grasshopper</p> 	<ul style="list-style-type: none"> Grasshopper is a cutting-edge parametric modelling tool which works with Rhino software to allow a powerful and efficient new way of designing. Grasshopper allows users to create complex and adaptable geometry through a node-based interface, enabling to generate forms and patterns through algorithmic design without needing to write traditional code. It's an environment and visual programming language that operates within the Rhinoceros 3D CAD. In an advanced level, Grasshopper is used in parametric modeling for architecture, structural engineering, fabrication, lighting performance analysis, and more. 	<ul style="list-style-type: none"> In Grasshopper, components are dragged onto the canvas, and programs are created. Grasshopper is usually used for creating a generative algorithm that is used for generative art. The types of algorithms may include audiovisual, textual, haptic applications, and numeric algorithms. Automation; Capsulize recurring tasks; Available modules in the plugin; Iterate faster; Community; facilitates integrating other software. Endless interface. High Single-Core Performance. Multiple Cores for Multithreading. 16 - 32 GB for RAM. High-Resolution Display. GPU: NVIDIA RTX 3060/3070 or AMD Radeon equivalent (6-8 GB VRAM) 	<ul style="list-style-type: none"> In Grasshopper, meteorological inputs are done in several plugins, such as Ladybug, Honeybee, and Dragonfly, which allow users to bring in environmental and climate data for advanced simulations. General weather file format is: EPW. 	No	-
<p>ArcGIS</p> 	<ul style="list-style-type: none"> ArcGIS is a comprehensive geospatial platform, and the leading geographic information system (GIS) technology. GIS is a proven IT technology that helps users understand patterns, relationships, and geographic context, providing a foundation for mapping and analysis. 	<ul style="list-style-type: none"> ArcGIS can do: <ol style="list-style-type: none"> Mapping: Understand data by mapping and visualizing it in 2D, 3D, and real time. Spatial analytics: Perform spatial modeling and analysis with data from any source, enriched by geography. Field operations. Data editing and management. Imagery and remote sensing 	<ul style="list-style-type: none"> Tair; RH; Vair; Solar radiation; VP ; Precipitation <p>in formats: Shapefiles (.shp); NetCDF; CSV; GRIB (.grb)</p>	No	-
<p>Ecotect</p> 	<ul style="list-style-type: none"> Ecotect is a comprehensive environmental building analysis software used for simulating and analyzing the performance of buildings in terms of energy, daylight, solar radiation, thermal comfort, and acoustics. In 2015, Ecotect was discontinued by Autodesk, and has been integrated into software, Autodesk Revit. 	<ul style="list-style-type: none"> Ecotect allows users to simulate and analyze a building's thermal behavior. It could model how heat would flow through different building materials and how internal temperatures would fluctuate in response to external weather conditions. It helps to estimate the energy consumption of a building based on its design, materials, and systems, allowing users to optimize for energy efficiency. 	<ul style="list-style-type: none"> Ecotect allows users to import weather data such as TMY or EPW files. 	No	-

		<ul style="list-style-type: none"> • Ecotect simulates daylight penetration and distribution within spaces. • The software allows for the analysis of solar radiation on building surfaces. 			
<p>TRNSYS</p> 	<ul style="list-style-type: none"> • TRNSYS is an extremely flexible graphically based software environment used to simulate the behavior of transient systems. • The vast majority of simulations are focused on assessing the performance of thermal and electrical energy systems. • TRNSYS has an extensive cross section of users worldwide that spans from researchers to consultants, engineers to building simulation experts, and students to architects. 	<ul style="list-style-type: none"> • TRNSYS is made up of two parts. The first is an engine (called the kernel) that reads and processes the input file, iteratively solves the system, determines convergence, and plots system variables. The kernel also provides utilities that determine thermophysical properties. • The second part of TRNSYS is an extensive library of components, each of which models the performance of one part of the system: TRNSYS3D; TRNBuild; TypeStudio; TRNEdit; TRNSED. 	<ul style="list-style-type: none"> • Weather files are often in specific formats like TMY (Typical Meteorological Year) or EPW (EnergyPlus Weather). 	No	-
<p>COSMO-CLM</p> 	<ul style="list-style-type: none"> • COSMO-CLM it is the climate version of the COSMO LM model, which is the operational non-hydrostatic mesoscale weather forecast model. • The mathematical formulation of COSMO CLM is based on the fluid dynamics equations for a compressible flow. • COSMO CLM is employed at spatial resolution between 1 and 50 km; these values are usually close to those requested by the impact modelers. 	<ul style="list-style-type: none"> • The prognostic variables are: horizontal and vertical Cartesian wind components, pressure perturbation, temperature, specific humidity, cloud water content, cloud ice content, turbulent kinetic energy and specific water content of rain, snow and graupel. 	<ul style="list-style-type: none"> • Tair; • RH; • Vair; • VP, 	No	-

In the evolving landscape of architectural and environmental design, various numerical tools have emerged to address the complex challenges of simulating and analyzing building performance, thermal comfort, and environmental conditions. As crucial step on our study methodology, Table 5.1 examines 10 prominent software solutions, each offering unique capabilities and applications in the field of environmental simulation and architectural design (Lam et al, 2021).

The analyzed software can be categorized into several functional groups. Microclimate simulation tools, such as *ENVI-met* (Bruse, 2004), provide sophisticated three-dimensional computational fluid dynamics (CFD) capabilities, enabling the simulation of sustainable living conditions in changing environments. These tools integrate multiple scientific disciplines, from fluid dynamics to plant physiology, offering comprehensive environmental analysis.

Thermal comfort analysis tools, i.e. *RayMan* (Matzarakis et al, 2007; 2010) and *SOLWEIG* (Lindberg et al, 2008; 2011), focus on calculating radiation fluxes and thermal indices. *RayMan*, while one-dimensional in space, excels in computing thermal biometeorological indices like PET (Physiological Equivalent Temperature), PMV (Predicted Mean Vote), and UTCI (Universal Thermal Climate Index). *SOLWEIG* specializes in simulating spatial variations of 3D radiation fluxes and mean radiant temperature in complex urban settings.

Advanced computational tools like *Ansys FLUENT* (Matsson, 2023) provide sophisticated CFD capabilities for simulating fluid flow, heat transfer, and chemical reactions in complex systems. These tools require significant computational resources but offer detailed analysis of fluid behavior under various conditions.

Parametric and lighting analysis tools, such as *Grasshopper* (Sadeghipour, 2013) and *Radiance* (Ward, 1994; Compagnon, 1997), focus on the analysis and visualization of lighting in design. *Radiance* offers advanced capabilities for spectral radiance and irradiance calculations, while *Grasshopper* provides a parametric modelling environment that enables algorithmic design through a node-based interface.

Geographic Information System (GIS) tools like *ArcGIS* (Scott and Janikas, 2009) offer comprehensive geospatial analysis capabilities, helping users understand patterns and relationships in geographic contexts. On the other hand, the building performance simulation software, such as

Ecotect (now integrated into Autodesk Revit) (Roberts and Marsh, 2001), focuses on analyzing building performance in terms of energy, daylight, and thermal comfort.

Furthermore, transient system simulation tools, represented by *TRNSYS* (Beckman et al, 1994), specialize in simulating the behavior of thermal and electrical energy systems over time. Climate modelling software like *COSMO-CLM* (Rockel et al, 2008) provides capabilities for mesoscale weather forecasting and climate simulation.

The comparison reveals varying input requirements across software, with most tools requiring basic meteorological parameters such as air temperature (t_{air}), relative humidity (RH), and wind speed (V_{air}). Output capabilities also differ, with some tools focusing on thermal indices while others provide broader environmental analysis.

Key findings from studies using these tools highlight the significant impact of building materials and surface albedo on outdoor thermal comfort. For instance, research has shown that increasing ground surface albedo can affect thermal comfort, with high albedo materials potentially creating higher thermal stress for pedestrians despite reducing building thermal load.

This diverse system of numerical tools reflects the complexity of environmental and architectural design challenges. Each software solution offers specific strengths and limitations, emphasizing the importance of selecting appropriate tools based on project requirements, computational resources available, and the specific aspects of environmental or architectural analysis needed.

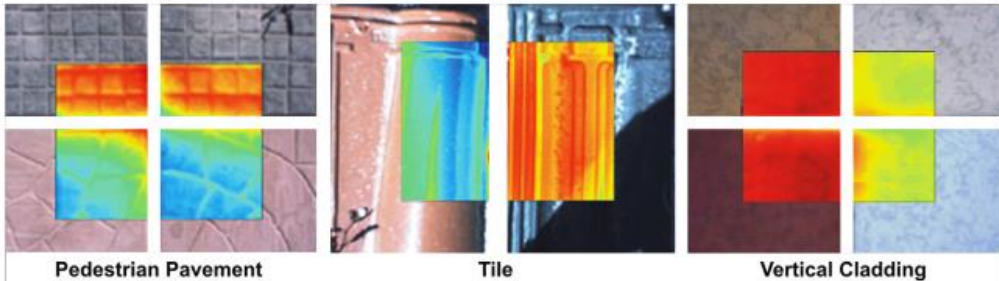
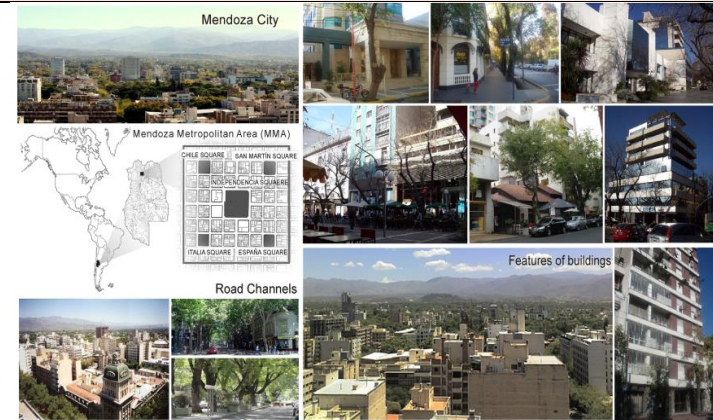

As main analysis and overview throughout the literature review and the objectives of the current research, we found that ENVI-met presents the favorable software for our study concerns in modelling, validation and simulations.

[Part B.2]

Most Relevant Studies on the Relationships between Building Envelop and Outdoor Thermal Behavior

Field measurement methodologies

Table 5.2. Summary of some relevant studies regarding relationships between buildings external envelopes and outdoor thermal fluctuations based on field measurements.

Articles	Building Materials and Outdoor Thermal Heat Assessment
<p>Classification of building materials used in the urban envelopes according to their capacity for mitigation of the urban heat island in semiarid zones</p> <p>Energy and Buildings 2014</p> <p>Noelia J. Alchapar</p> <p><u>Location</u> Mendoza, Argentina</p> <p><u>The climate</u> BWk climate zone</p> <p>Citations: 121</p>	<p>Figure: Examples of thermal images, and Solar Reflectance Index (SRI) values.</p>  <p>Figure shows thermal images and SRI values for Pedestrian Pavement, Tile, and Vertical Cladding. The images are arranged in a grid, with thermal images on the left and SRI values on the right. The labels 'Pedestrian Pavement', 'Tile', and 'Vertical Cladding' are at the bottom of each column.</p> <p>Location of the study context_ Country and city</p>  <p>Location map of Mendoza City and the Mendoza Metropolitan Area (MMA). The map shows the city's location in Argentina, with a detailed inset of the MMA area. Labels include 'Mendoza City', 'Mendoza Metropolitan Area (MMA)', 'CHILE SQUARE', 'SAN MARTIN SQUARE', 'INDEPENDENCIA SQUARE', 'ITALIA SQUARE', 'ESPINOSA SQUARE', and 'Road Channels'.</p>  <p>Thermal and optical evaluation of materials in the study site. The image shows a large array of material samples laid out on a flat surface, with thermal and optical evaluation data overlaid on the samples.</p> <p>Thermal and optical evaluation of materials in the study site.</p> $\text{Solar Reflectance Index (SRI)} = 100 \times \frac{T_b - T_s}{T_b - T_w}$ <p>where:</p> <p>T_b = black pattern temperature, K</p> <p>T_w = white pattern temperature, K</p> <p>T_s = steady-state surface temperature, K</p> <p>By means of Equation, the superficial temperatures of the patterns are calculated under local environmental conditions, according to regulations.</p> <p>Results:</p> <ol style="list-style-type: none"> 1) The classification of urban envelope materials, such as pavements, facades, and roofs, using the Solar Reflectance Index (SRI) to assess their capacity to mitigate UHI effects. 2) By correlating (SRI) values with various material characteristics, including color, composition, and texture, the study offers insights into how these factors influence thermal performance. 3) The alarming trend of increasing energy consumption due to higher cooling demands in urban areas, which is exacerbated by the UHI effect. 4) The study provides empirical data showing that a significant percentage of evaluated materials have low SRI values, indicating that many existing urban materials may not be effective in mitigating heat gain.

On the impact of innovative materials on outdoor thermal comfort of pedestrians in historical urban canyons

Renewable Energy
2017

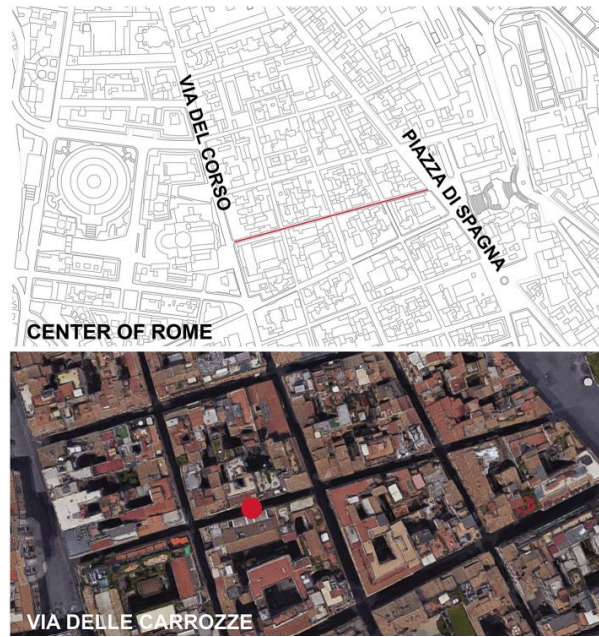
Federica Rosso

Location
Rome, Italy

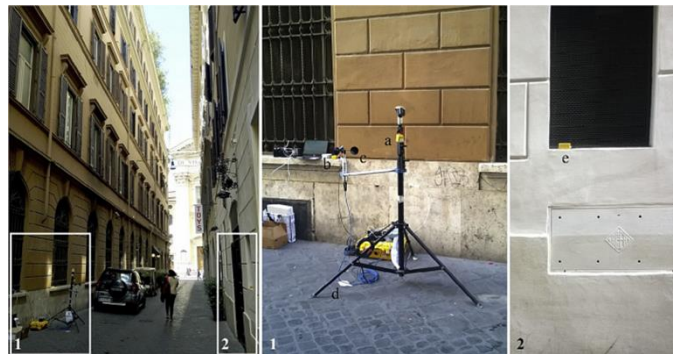
The climate
Csa climate zone

Citations: 115

Via delle Carrozze (red line), view from Google Maps



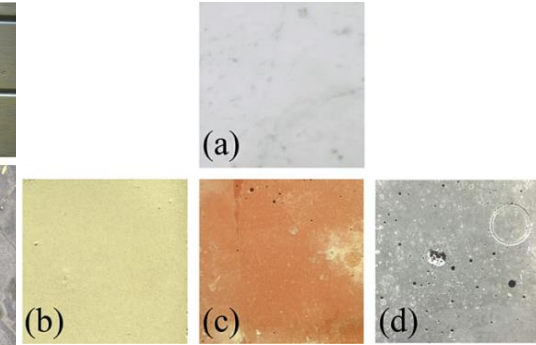
Monitoring setup in the urban canyon.



1)



2)



- 1) On the left (I), sanpietrini paving, light stone basement and reddish mortar; on the right, light ochre mortar (III) and sanpietrini paving (II).
- 2) Considered cool materials: (a) Bianco Carrara marble and IR colored mortar, (b) white, (c) red and (d) gray

Table: Urban Canyons' material investigated combinations.

Combination	Surface	Traditional mortar	Traditional stone paving	(a) Marble	IR mortar		
					(b) White	(c) Red	(d) Gray
Case R (Reference)	Envelope Paving	X	X				
Case 1	Envelope Paving		X	X			
Case 2	Envelope Paving			X			X
Case 3	Envelope Paving		X			X	
Case 4	Envelope Paving					X	X
Case 5	Envelope Paving		X		X		
Case 6	Envelope Paving				X		X
Case 7	Envelope Paving			X		X	

Using advanced cool materials in the urban built environment to mitigate heat islands and improve thermal comfort conditions

Solar Energy
2011

Matthaïos
Santamouris

Location
Greece

The climate
Csa climate zone

Citations: 1158

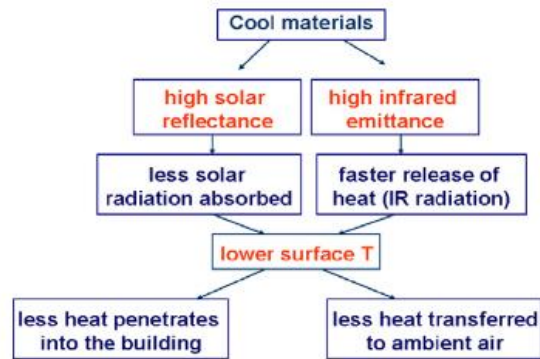
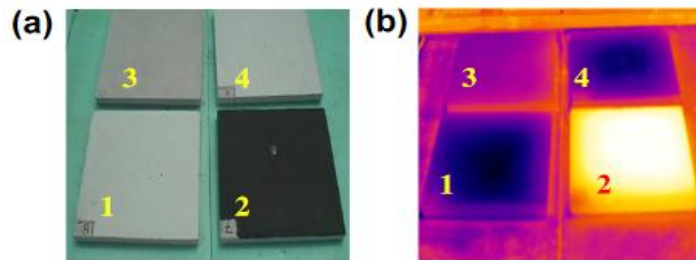


Fig. 1. The basic principles of cool materials.



Visible and infrared images of four concrete tiles painted with cool white coatings.

Methods

- The initial phase involves the creation of light-colored materials that exhibit high reflectivity and emissivity.
- The second phase focuses on the development of colored materials that maintain high near-infrared reflectance while appearing visually appealing.
- The final phase addresses the development of dynamic cool materials that can change their optical and thermal properties in response to environmental conditions.

Results:

Table: Values of measured solar reflectance and infrared emittance of commonly using roofing material.

Material	Solar reflectance	Infrared emittance	Solar reflectance index
Coatings	0.70 - 0.85	0.80 - 0.90	84 - 113
White	0.20 - 0.65	0.25 - 0.65	-25 to 72
Conventional black	0.04 - 0.05	0.80 - 0.90	-7 to 0
Cool black	0.20 - 0.29	0.80 - 0.90	14 - 31
Conventional dark colored coatings	0.04 - 0.20	0.80 - 0.90	-7 to 19
Cool dark colored coatings	0.25 - 0.4	0.80 - 0.90	21 - 45
Asphalt shingles			
White asphalt shingle	0.20 - 0.30	0.80 - 0.90	15 - 28
Black	0.04	0.80 - 0.90	-7 to -1
Dark colored conventional asphalt shingles (using a two-layer process)	0.05 - 0.10	0.80 - 0.90	-6 to 6
Cool colored asphalt shingles (using a two-layer process)	0.18 - 0.34	0.80 - 0.90	11 - 37
Tiles			
Terracotta ceramic tile	0.25 - 0.40	0.85 - 0.90	23 - 45
White clay tile	0.60 - 0.75	0.85 - 0.90	71 - 93
White concrete tile	0.60 - 0.75	0.85 - 0.90	71 - 93
Grey concrete tile	0.18 - 0.25	0.85 - 0.90	14 - 25
Dark colored concrete tile	0.04 - 0.40	0.85 - 0.90	-4 to 45
Cool dark colored concrete tile	0.40 - 0.60	0.85 - 0.90	43 - 72
Membranes			
White membrane	0.65 - 0.85	0.8 - 0.90	76 - 107
Black	0.04 - 0.05	0.8 - 0.90	-7 to 0
Metal roof			
Unpainted	0.20 - 0.60	0.05 - 0.35	-48 to 53
Painted white	0.60 - 0.75	0.8 - 0.90	69-93
Dark conventionally colored	0.05 - 0.10	0.8 - 0.90	-6 to 6
Dark cool colored	0.25 - 0.70	0.8 - 0.90	21 - 86
Build up roof			
With asphalt	0.04	0.85 - 0.90	-4 to -1
With dark gravel	0.08 - 0.20	0.8 - 0.90	-2 to 19
With white gravel	0.30 - 0.50	0.8 - 0.90	27 - 58
With white coating	0.75 - 0.85	0.8 - 0.90	93 - 113
Modified bitumen			
White mineral surface capsheet	0.10 - 0.20	0.85 - 0.95	4 - 21
White coatibg over mineral surface	0.60 - 0.75	0.85 - 0.95	71 - 94

Characterising thermal behaviour of buildings and its effect on urban heat island in tropical areas

International Journal of Energy and Environmental Engineering 2020

Surjamanto Wonorahardjo

Location Indonesia

The climate Af climate zone

Citations: 74

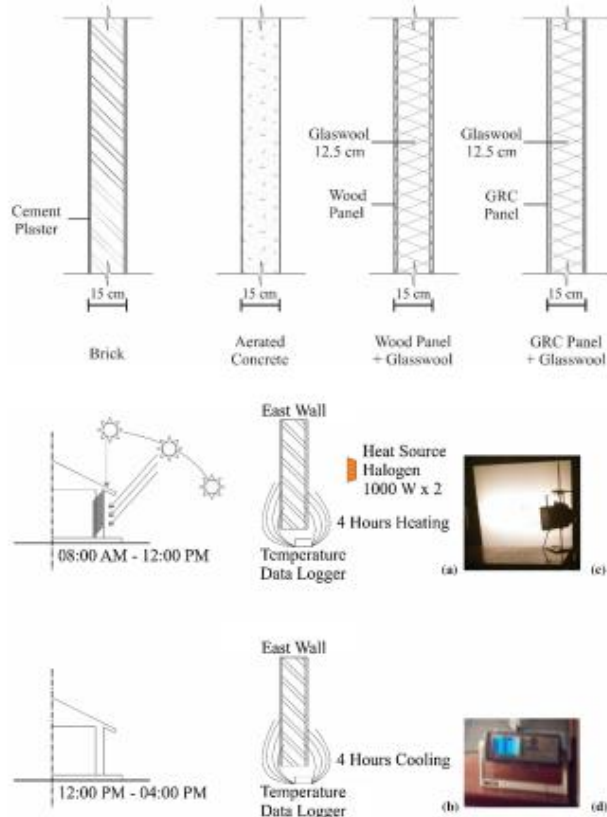
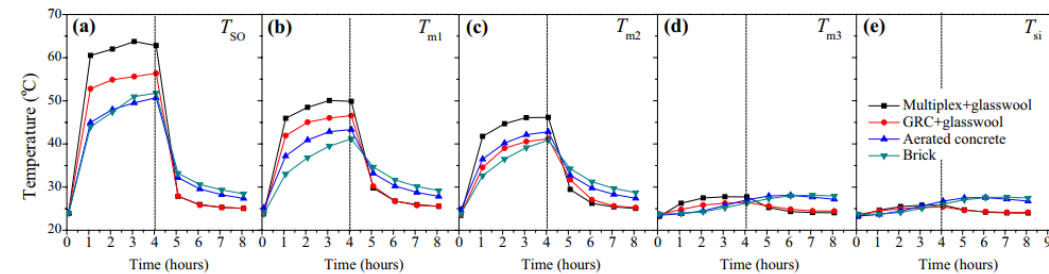


Figure: The wall temperature measurement.

Methods

- The study utilizes a direct temperature measurement method, which captures not only the surface temperature but also the internal temperatures of the wall materials.
- Mathematical and digital modeling is conducted using Energy2D software to simulate heat flow and validate the experimental results.

Results:



Temperatures evolution during the heating and cooling process.

- The analysis reveals that the block wall (BW) type, which includes brick and aerated concrete, exhibited a higher indoor air temperature, specifically 0.32 °C higher than the insulated sandwich wall (ISW) type, which comprises wood and GRC with glass-wool insulation.
- The ISW type, while showing a higher HII of 0.74 °C compared to the BW type, demonstrates better insulation properties that can mitigate heat transfer to the interior, thus providing a cooler indoor environment.
- The findings indicate that the choice of materials significantly influences both the thermal comfort of residents and the overall energy consumption associated with cooling in urban areas.

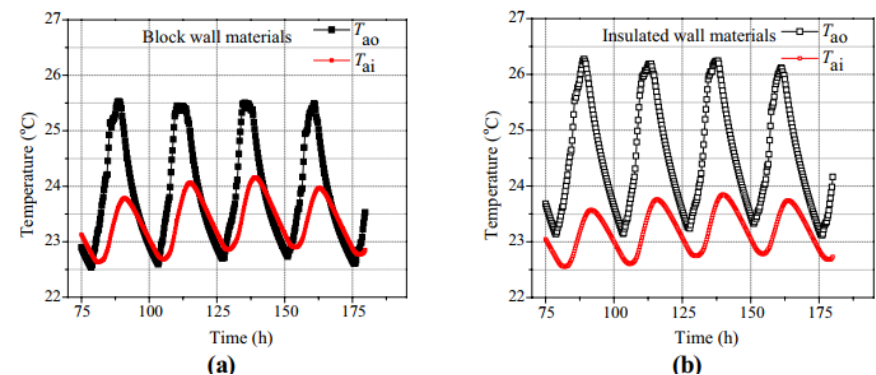


Figure: Simulation process of urban space, using a block wall type and insulated wall materials.

Passive cooling of outdoor urban spaces. The role of materials

Solar Energy
2004

L. Doulos

Location
Greece

The climate
Csa climate zone

Citations: 678

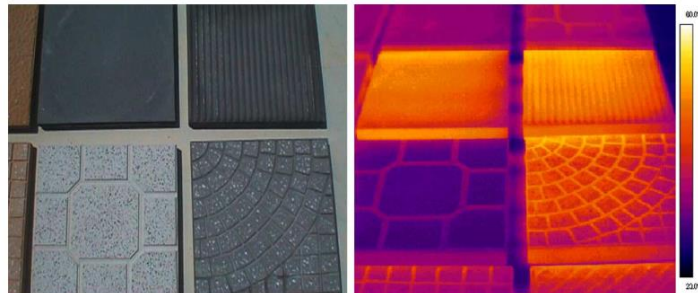


Figure: Visible and Infrared image of selected building materials.

Methods

- A total of 93 materials were selected for this study, which were analysed through both theoretical and experimental approaches.
- An experimental campaign was conducted in Athens during August 2001.
- This involved the use of infrared (IR) thermography to measure the surface temperatures of the selected materials.

Results:

- One of the key findings was the classification of materials into 'cool' and 'warm' categories based on their thermal performance.
- The analysis revealed that materials with lighter colors and smoother surfaces generally exhibited lower surface temperatures compared to darker and rougher materials.
- The study highlighted the impact of surface roughness and size on temperature distribution.

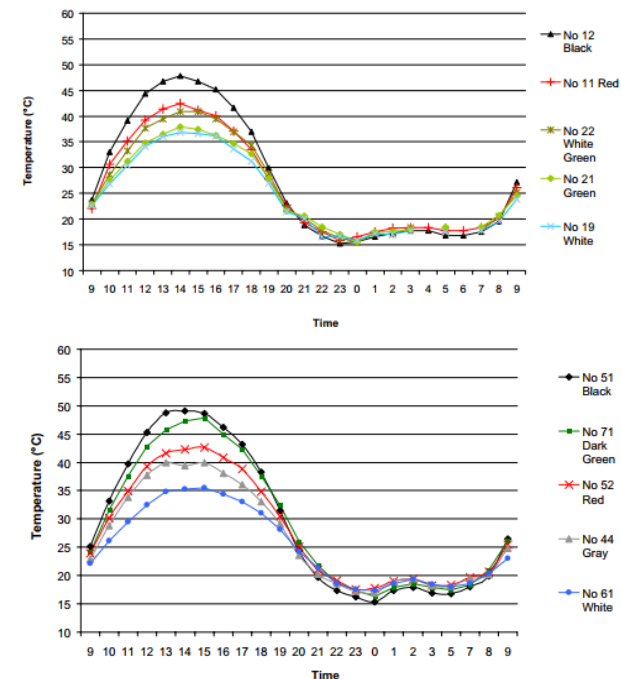


Figure: Distribution of hourly surface temperatures.

- The study's results contribute to a better understanding of how different materials can be utilized in urban planning to enhance outdoor thermal comfort and reduce energy consumption in buildings.

Conclusion

Innovative materials and surface treatments have shown promise in improving outdoor thermal comfort. Cool pavements, for instance, have been found to reduce average ambient temperatures by up to 0.8 K in some urban areas. Similarly, advanced façade materials and coatings can significantly mitigate the thermal behavior of building envelopes, influencing both indoor and outdoor thermal environments. However, the review also cautions that the application of highly reflective materials on vertical surfaces in deep canyons may accidentally increase thermal discomfort due to increased reflected radiation at the pedestrian level.

The interaction between building materials and other urban elements, such as vegetation, is another critical aspect highlighted in the literature. Green infrastructure, including street trees and vertical greenery, can enhance the thermal performance of building materials by providing shade and evaporative cooling. This synergy between green and grey infrastructure presents opportunities for integrated approaches to urban thermal comfort management.

The review underscores the need for climate-specific solutions in material selection and application. Strategies that are effective in hot-dry climates may not be suitable for hot-humid or cold climates. For instance, the optimal material properties for enhancing thermal comfort in the arid climate of Biskra City, may differ significantly from those suitable for a humid subtropical climate. This variability necessitates context-sensitive research and design practices that account for local climatic conditions, urban morphology, and cultural factors.

Despite the extensive research in this field, significant gaps remain in our understanding of the combined effects of urban geometry and building materials on outdoor thermal comfort. Many studies have focused on single-factor analyses, leaving the synergistic effects of multiple urban design elements relatively unexplored. This gap presents an opportunity for future research to develop more holistic models that integrate various aspects of urban form and material properties to predict and optimize outdoor thermal comfort.

The implications of building material choices on energy consumption and sustainability are also noteworthy. Improving outdoor thermal comfort through appropriate material selection can lead to reduced energy demand for cooling in adjacent buildings, contributing to more sustainable

urban development. This connection between outdoor thermal environments and building energy performance highlights the broader impact of material choices in urban design.

In conclusion, the literature review demonstrates that building materials play a pivotal role in shaping outdoor thermal comfort in urban environments. Their impact is modulated by urban geometry, climate conditions, and interactions with other urban elements such as vegetation. Future research should focus on developing integrated approaches that consider the complex interplay between these factors, aiming to create more resilient, comfortable, and sustainable urban spaces. As cities continue to grow and face increasing thermal challenges, the thoughtful selection and application of building materials will be crucial in creating livable urban environments adapted to local climatic conditions and resistant to the impact of climate change.

CHAPTER VI: METHOD AND MATERIAL: METHODOLOGY, DATA COLLECTION, AND ANALYTICAL TECHNIQUES

Introduction

This chapter focuses on the methodological framework employed to address the challenges of urban design in hot dry climate, particularly regarding outdoor thermal comfort. This methodological chapter presents a structured approach to understanding how external building materials can impact thermal comfort, within the city of Biskra, Algeria, as a case study.

The chapter employs a combination of empirical measurements, numerical modeling, and simulation analyses. Continuous meteorological field measurements were conducted in 2021 within a selected urban reference canyon representative of Biskra's residential neighbourhood. These measurements represent the main data for evaluating the correlation among the height-to-width (H/W) ratio, street orientation, and the thermal properties of construction materials. Using ENVI-met software, the chapter models 24 scenarios encompassing diverse urban geometries, building materials, and orientations, enabling a comprehensive analysis of their impact on outdoor thermal comfort.

A critical feature of this chapter is its focus on methodological approach in calibrating and validating numerical models. Field data were systematically compared to simulation results to ensure accuracy, employing statistical metrics such as Root Mean Square Error (RMSE) and Mean Bias Error (MBE). This methodological step ensures the reliability of the analysis and supports robust conclusions regarding the thermal implications of different urban configurations.

Additionally, the methodology incorporates a historical dimension, tracing the evolution of building materials and their adaptation to Biskra's climate over time. From traditional adobe and palm fronds to modern concrete and ceramic finishes, the chapter provides context for material selection in thermal performance studies.

Overall, this methodological chapter establishes a replicable framework for evaluating urban design strategies aimed at enhancing thermal comfort in arid climates, offering valuable tools for researchers and practitioners in urban climate studies.

1. Research method

The current research used three main methods including continuous field measurements, numerical modelling and simulations. Accordingly, to determine urban design guidelines that couple the urban canyon geometry with the building's external envelopes in relation to human outdoor thermal comfort, we followed an empirical approach.

Figure 6.1 illustrates the study's conceptual framework, outlining the main steps, from site data collection to numerical model-ing and simulation data processing. The following subsections provide a detailed explanation of the research methodology.

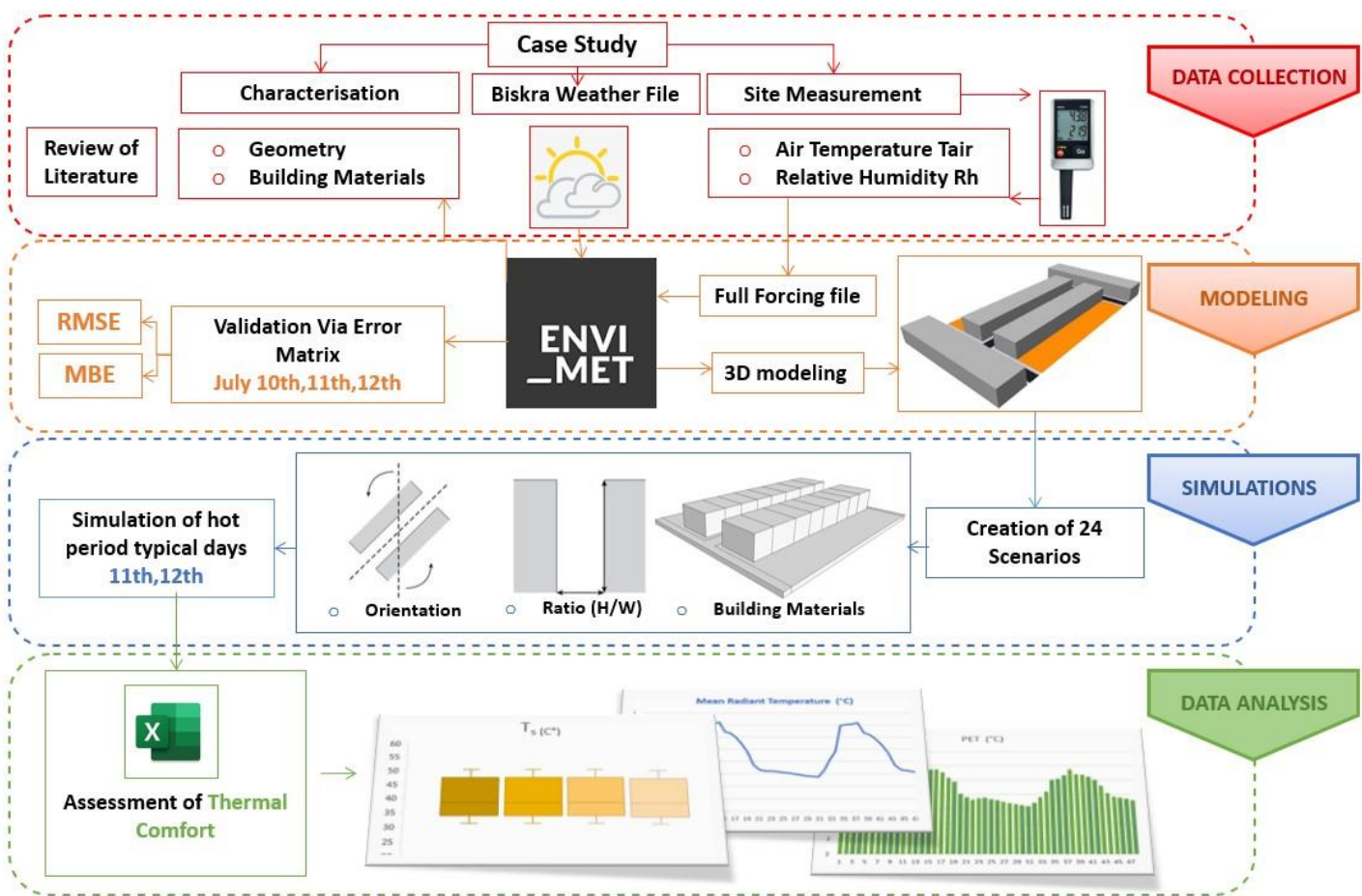


Figure 6.1. Research Study Conceptual Framework from the data collection, modeling, simulations, and data analysis.

Source: Author, 2023.

2. Case study

2.1. General climate conditions of the study context

The study area of Biskra region falls under the BWh category (hot desert climate) according to Köppen-Geiger classification. Climate data analysis from 1958 to 2021 reveals an annual mean temperature of 22.4°C, with significant seasonal variations. Temperature extremes range from a recorded maximum of 41.9°C to a minimum of 6.4°C (Center for the Built Environment (CBE), 2021). The annual temperature cycle reaches its peak in July, when temperatures can climb to 45°C, while January represents the coldest month, with temperatures occasionally dropping to 1°C. Atmospheric humidity levels remain generally low throughout the year, with an average relative humidity of 47%. There is notable seasonal variation in humidity, from a peak of 65% in December to a minimum of 28.3% during the hottest months of July and August. Precipitation in the region is minimal and unpredictable, with an annual average of only 126 mm. The past decade has been marked by severe drought conditions, with some years experiencing virtually no rainfall. This pattern of limited and unreliable precipitation, combined with high temperatures and low humidity, underscores the region's arid desert characteristics.

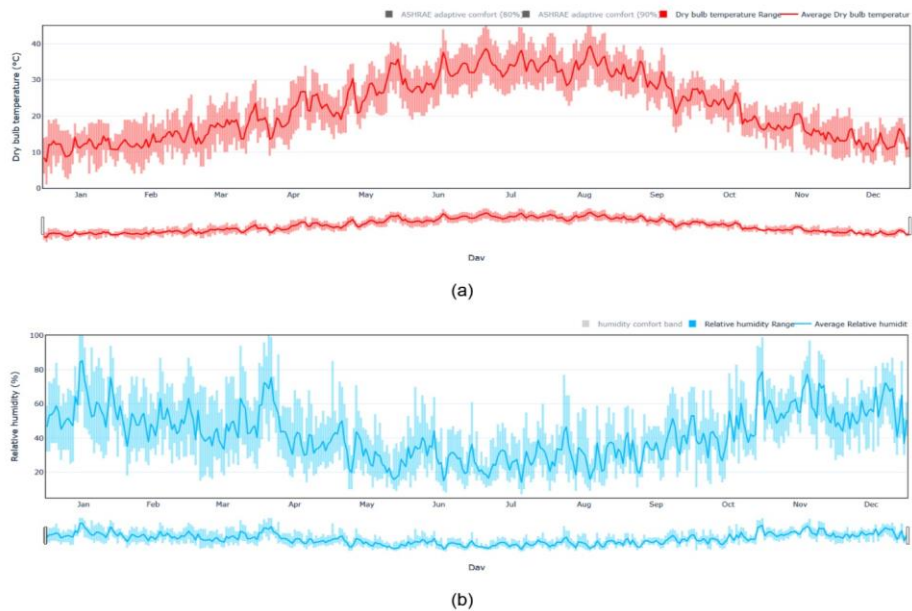


Figure 6.2. Climatic conditions of the study context: (a) air temperature; (b) relative humidity.

Source: CBE Clima Tool, Berkeley University, USA, 2023.

2.2. Characterization of Biskra city housing sector

Biskra occupies a strategically significant position as a gateway to the Algerian Sahara, owing to its vital geographical location at the transition between the Atlas Mountains and the desert. Due to this strategic importance, the city has been home to numerous civilizations throughout its history. The urban evolution of Biskra can be traced through four distinct and significant periods: the precolonial (Ottoman) period, the colonial period (French occupation), the post-colonial period, and the contemporary period. Each of these historical phases has left an indelible mark on the city's urban fabric, architecture, and cultural landscape, contributing to its rich and layered urban heritage. The transitions between these periods were marked by significant changes in urban planning, architectural styles, and the social organization of space, reflecting the different approaches and priorities of each era.

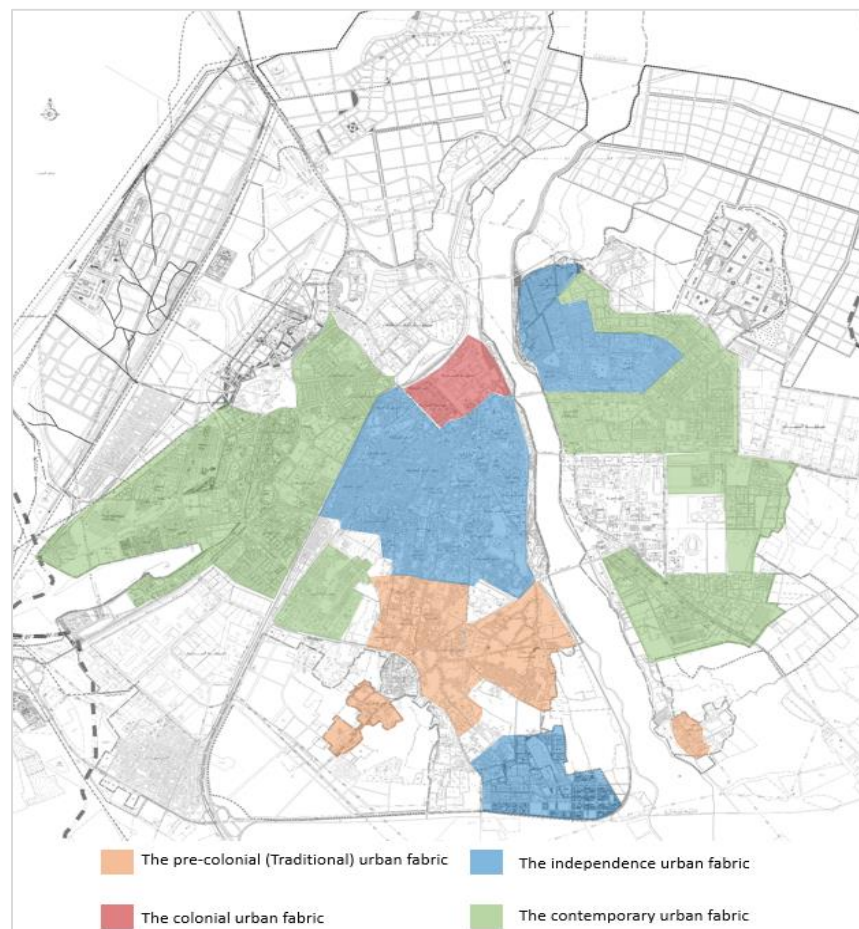


Figure 6.3. Different urban fabrics distribution within Biskra city, from precolonial tissue to contemporary period.

Source: Author, 2021.

The urban landscape of Biskra has undergone significant transformations over centuries, shaping its development through diverse urban fabrics and housing typologies. The current city's residential architecture can be broadly categorized into two main categories: individual housing and collective multi-family housing, with distinct variations across different neighborhoods. The analysis of the city's building composition reveals that new individual housing dominates the urban fabric, accounting for 76% of all residential structures. Collective and semi-collective multi-family housing shares an equal proportion with traditional individual housing, each representing 11% of the total housing stock. The remaining 2% consists of precarious individual housing, which is primarily distributed along the city's periphery in the form of rural dwellings and self-constructed units. This distribution reflects the evolution of Biskra's urban form, illustrating a clear preference for individual housing while maintaining a mix of housing types to accommodate different socio-economic needs and cultural preferences. The relatively low percentage of collective housing suggests an urban development pattern that favors lower density, individual residences over high-density apartment buildings, possibly influenced by local cultural norms and available land resources.

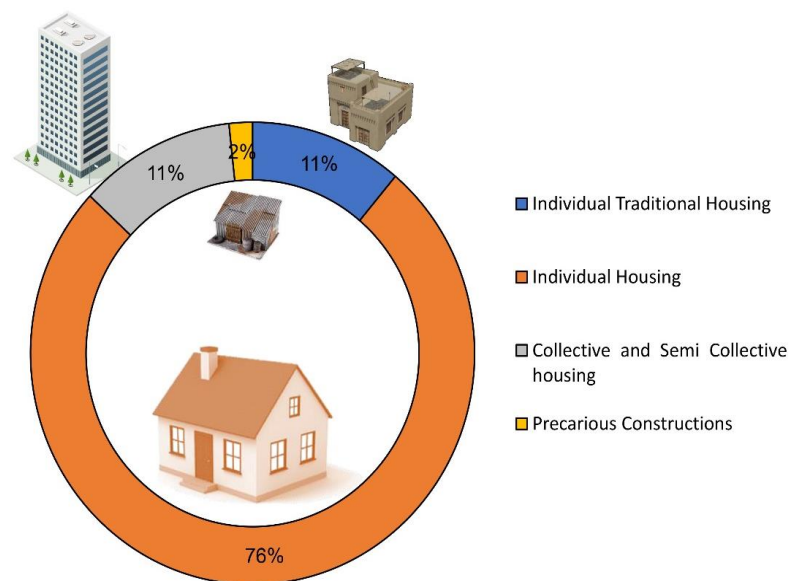


Figure 6.4. Housing typology in the city of Biskra 2018 (Algerian National Statistics Office, 2018).

Source: Author, 2023.

2.3. Building materials envelopes' use within Biskra city over the history

2.3.1. Precolonial era (before 1848):

Biskra city during the precolonial period was dominated by vernacular built-up in Toub (Figure 6.5), and characterized by compact urban form and distributed in the palm grove.



Figure 6.5. Adobe blocks implemented for walls in old houses throughout ancient urban fabrics in Biskra city.

Source: Author, 2022.

Therefore, the main used building materials during this era were:

- ***Earth and adobe:*** the primary material for constructing homes, walls, and other structures. Earth was a prevalent material due to its availability and low cost, often used in the form of adobe bricks. Mud bricks were made from a mixture of clay, sand, and straw, molded and left to dry in the sun (Izemmorena & Guettala, 2014).
- ***Local stones:*** the stones were used for foundations and in certain cases for building walls, enhancing structural integrity and aesthetic appeal in traditional dwellings (Naidja et al., 2022).
- ***Palm tree trunks:*** palm tree trunks were used as support beams, particularly in roofing. Palm wood was locally available and used for load-bearing structures.
- ***Palm fronds:*** in some constructions, palm fronds were utilized for roofing and shading, reflecting the integration of local flora into building practices (Hamouda & Outtas, 2011).

- **Clay Plaster:** applied to the surfaces of mud-brick walls to smooth and protect the structure from weathering. Clay Plaster helped seal the structure and provided an additional layer of thermal insulation.
- **Lime mortar:** used as binder in masonry and for coating walls, lime improved the durability of the structures and acted as a sealant to prevent water infiltration.

2.3.2. The colonial era (1848 - 1962):

French colonial architecture in Biskra, combined native local elements with European design principles. The buildings featured large windows and doors, often with shutters to regulate sunlight and airflow and sloped tiled roofs (Figure 6.6).



Figure 6.6. Stone blocks in the French buildings' typologies covering the external envelopes.

Source: Author, 2022.

Otherwise, the main used building materials during this era were:

- a. Local building materials adapted to French architecture:
 - **Clay and adobe:** one of the most common traditional materials in Biskra, was extensively used for walls.
 - **Stone and Limestone:** locally sourced stone was used in more important buildings, especially public and civic structures like government offices, schools, and churches.
 - **Wood:** the wood was important for structural elements like beams and, more prominently in the construction of balconies, shutters, and decorative lattices or wooden windows.

b. French new introduced building materials:

- ***Concrete and cement:*** concrete became more popular, particularly in urban buildings, military institutions and new construction projects. Concrete and cement enabled more sophisticated, durable, and multi-story structures.
- ***Terracotta roof tiles:*** were used extensively for roofing.
- ***Plaster:*** used to finish the exterior walls of buildings, giving them a smooth, whitewashed appearance, and helped to reflect sunlight and reduce heat absorption.

2.3.3. After independence (after 1962):

In the sixtieth, the houses in popular neighborhoods were originally built using local materials such as bricks for walls and mortar for floors. Improvements have been made, including the addition of interior and exterior flooring and improved fixture durability. The flat roof design, typical in desert architecture in post-independence housing.

On other hand, the used building materials during this era were:

- Concrete and cement.
- ***Prefabricated concrete:*** in some housing developments, prefabricated concrete panels were employed to quickly construct multi-story apartment buildings.
- ***Reinforced steel:*** along with concrete, steel reinforcement was employed in the construction of major residential complexes and public structures. In comparison to traditional mudbrick and stone structures, the adoption of modern construction techniques, such as steel frames, enabled taller and higher buildings.

2.3.4. The contemporary period (nowadays):

During the 1970s, Biskra quickly experienced large urban planning changes, with the implementation of the New Urban Habitat Zone (ZHUN) by the government giving rise to planned subdivisions. The implementation of the governmental urban planning instruments such as: the Urban Development Master Plan (PDAU) and the Land Occupancy Plan (POS), involved the simultaneous creation of housing (collective, semi-collective or individual), equipment and infrastructure.




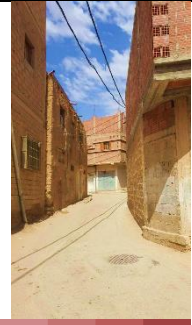




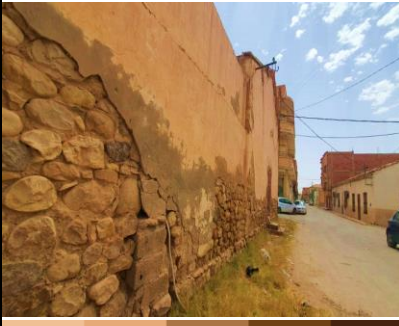

Otherwise, the used building materials were more developed and varied:









- **Concrete:** concrete is the primary building material in contemporary Biskra. It is used extensively in the construction of residential, commercial, and public buildings due to its durability, cost effectiveness, and ease of availability.
- **Reinforced concrete:** reinforced concrete (with steel) is commonly used for structural components such as columns, beams, and foundations, especially in multi-story apartment buildings.
- **Precast Concrete:** Precast concrete panels are often used in housing estates for standardized construction.
- **Hollow concrete blocks:** concrete blocks are widely used for walls in both residential, administrative and commercial buildings. These blocks are easy to produce, and suitable for the hot and dry climate of Biskra (Rahmani et al., 2022).
- **Hollow bricks:** commonly used due to their availability and cost effectiveness, hollow bricks are utilized for their structural properties but require careful consideration regarding thermal comfort (Rahmani et al., 2022).
- **Structural steel:** used extensively for reinforcement in concrete structures, but it is also employed in modern buildings for constructing frameworks, particularly in high-rise apartments and commercial structures.
- **Ceramics:** the introduction of ceramic as finishes of building external envelopes and façades. The use of ceramics was amplified for the esthetic and insulation needs.
- **Glass:** a new material as glass was introduced for the external buildings' envelopes and new architecture design.

As synthesis of the most used building materials in Biskra city, Table 1 shows various urban fabrics of the city with distinct external envelopes, colors and textures. Although, Table 6.1 illustrates the development of housing typologies over time.

Table 6.1. Overview of distinct neighbourhoods containing various building materials characteristics in Biskra city: from the oldest to the recent.

Source: Author, 2021.

Site	Location	Site description	Building materials, colors and textures: Wall (S); Soil (S)		
1. Al-Mecid		<ul style="list-style-type: none"> Traditional urban fabric integrated within the palm grove Irregular and linear street geometry Dense, compact urban form featuring narrow streets (less than 3 m wide) (H/W) ratio of approximately 2.3, with building height of 7 m at max Moderate vegetation coverage at 30% 			
			Limstone (W) + asphalt (S) Rough texture	Concrete (W) + asphalt (S) Rough texture	Hollow Brick (W) + asphalt (S) Rough texture
2. Feliache		<ul style="list-style-type: none"> Traditional urban fabric integrated within the palm grove Irregular and linear street geometry similarly to old neighbourhoods (H/W) ratio of above 2.0 Less vegetation coverage at 20% 			
			Limstone (W); Palm trees + land (S) Rough texture		
3. Station neighbourhood		<ul style="list-style-type: none"> Individual colonial housing Regular block geometry with similar typology housing Large streets compared to traditional urban fabrics with 8 m wide Uniform orientation streets Very Less vegetation coverage at 10% 			
			Stone & concrete (W) + asphalt (S) Rough texture	Stone, brick & concrete (W) + asphalt (S) Rough texture	

<p>4. Independence neighbourhood</p>		<ul style="list-style-type: none"> • Individual governmental family housing • Regular small blocks geometry with similar typology housing • Very narrow streets with less than 3 m wide • Uniform orientation streets • Very Less vegetation coverage at 5% 	 <p>Hollow Brick & concrete (W) + asphalt (S)</p> <p>Smooth texture</p>
<p>5. Villas Cadres</p>		<ul style="list-style-type: none"> • Individual family housing • Regular geometry with similar typology housing • Large streets • Very Less vegetation coverage at 3% 	 <p>Hollow Brick & concrete (W) + asphalt (S)</p> <p>Smooth texture</p>
<p>6. West urban extension</p>		<ul style="list-style-type: none"> • Governmental Collective family housing • Regular blocks geometry • Isolated blocks • Opened streets • No vegetation cover 	 <p>Hollow Brick & concrete (W) + asphalt (S)</p> <p>Rough texture</p>
<p>7. Individual housing development El Alia (reference study area)</p>		<ul style="list-style-type: none"> • Individual family housing • Regular geometry with distinct typology housing • Medium streets • Very Less vegetation coverage < 5 % 	 <p>Hollow Brick & concrete (W) + asphalt (S)</p> <p>Rough & smooth textures</p> <p>Hollow Brick, concrete & ceramics (W) + asphalt (S)</p> <p>Rough & smooth textures</p>

3. Continuous field measurement and model validation:

3.1. Field measurement protocol:





At first, the research is mainly based on hourly continuous measurements within a selected street canyon (reference study area in Table 6.1) between the period of 25 March and 25 November 2021 to characterize the effect of the thermal behavior of external walls during a long period.

Table 2 reveals the monitoring data logger Testo 175 H1 characteristics, measuring the air temperature (T_{air}) and relative humidity (RH). It is necessary to indicate that the data logger was installed 30 cm away from a building's external wall, at a height of 1.4 m from the ground, to avoid any heat exchange from external lighting during the night or humidity generated by the nearby trees and grass. Harrison, 2014 has further discussed the measurement and data logger installation protocols.

Table 6.2. The details of the monitoring device used for this study.

Source: Author, 2021.

Variable	Device	Dimensions	Unit	Accuracy	Range
Air temperature (T_a)	Testo 175 H1 0572 1754	149 x 53 x 27 mm	$^{\circ}\text{C}$	$\pm 0.4\text{ }^{\circ}\text{C}$	- 20 to + 55 $^{\circ}\text{C}$
Relative humidity (RH)			%	$\pm 1.0\%$	0 to 100 %

The data logger records 144 values per day, equivalent to one measurement every 10 minutes. To manage the device's recorded datasets, a complementary software tool 'Comfort Software Basic 5.0' is required, which is specifically designed to be compatible with the instrument. This software provides comprehensive data management capabilities, allowing users to download, view, and analyze recorded data through various visualization options including graphs and tables. It supports data export to common formats like CSV or Excel for further analysis. The software enables configuration of data logger settings, including measurement intervals, start/stop times,

and alarm thresholds if applicable. Running on Windows 10 or higher, with minimum system requirements of 4GB RAM and 500 MB free disk space, Comfort Software Basic 5.0 offers key features such as real-time data monitoring (when supported by the logger), multiple dataset comparison, and basic statistical analysis. The user-friendly interface includes automatic file naming based on recording date, data backup capabilities, and customizable display options, making it an essential tool for efficient data handling and analysis of the logger's measurements.

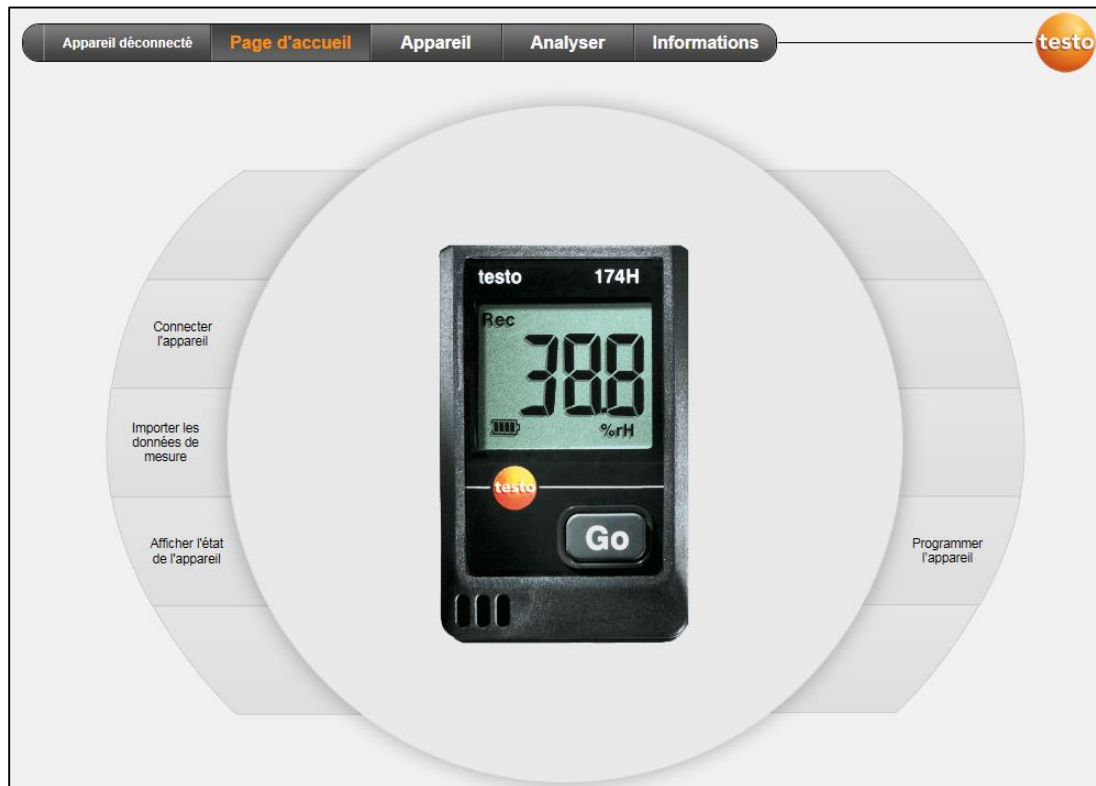


Figure 6.7. Testo Comfort Software Basic Interface: data logger configuration and data import.

Source: Author, 2021.

3.2. Sample selection:

The study area was meticulously selected based on specific criteria related to the housing typology which are (i) predominance of individual housing constitutes 76 % of the city built environment, representing the dominant residential typology (ii) A medium urban density identifying a balanced spatial configuration that typifies contemporary urban development in the region (iii) and a regular urban geometry for the total tissue, which demonstrates a consistent and

orderly spatial layout, enabling systematic urban analysis and providing a representative urban morphological structure.

In this light, following the selection of the city of Biskra as study context, among various sites our research identified a specific reference study area street-house (Table 6.1), as representative sample for our investigation. The selected street and house were strategically chosen to facilitate the implementation of the monitoring instrument while ensuring complete security and optimal research conditions.

Therefore, the research focused mainly on urban canyon located within a regular individual residential neighborhood (reference study area in Table 6.1) in the southeast of Biskra city. The canyon extends approximately 90 m in length, with buildings averaging 10 m in height. The canyon has an aspect ratio (H/W) of 1 and is oriented along an East-West axis (Figure 6.8). All external walls in the studied buildings are 30 cm thick, constructed with hollow bricks layered with 20 mm of plaster and finished with a 30 mm mortar coating.



Figure 6.8. The location of the site in Biskra City.

Source: Author, 2023.

3.3. Field measurement:

In Figure 8, the temperature curve (red) exhibits a clear seasonal pattern. From March to the mid-year period, there is a gradual increase in temperature, peaking during the summer months of

July and August. The peak summer season temperatures range between 30°C to 35°C, consistent with the measurement period shown in the graph. Following the summer peak, temperatures appear to decrease steadily towards the end of the recorded period. The data shows diurnal temperature variations, with daily peaks and troughs clearly visible throughout the timeline. The lowest temperatures in the dataset appear to be around 15°C, though without the full annual cycle visible in this graph. The temperature fluctuations shown are typical of the regional climate, demonstrating significant variation between daytime highs and nighttime lows, as well as a gradual seasonal shift over the recorded period.

In contrast, the relative humidity curve (blue) exhibits an inverse relationship with temperature. During the colder months, the relative humidity is higher, often exceeding 50%. This pattern reflects the ability of cooler air to retain more humidity. However, as the temperature increases during summer months, the relative humidity drops significantly, frequently falling below 20% during the hottest periods. This decrease in humidity during the summer is due to the elevated temperatures, which lead to greater evaporation and a reduction in the moisture content of the air. The fluctuations in humidity, particularly during the transitional seasons of spring and fall, indicate rapid weather changes or possibly the influence of short-term atmospheric phenomena such as winds or local convective activities.

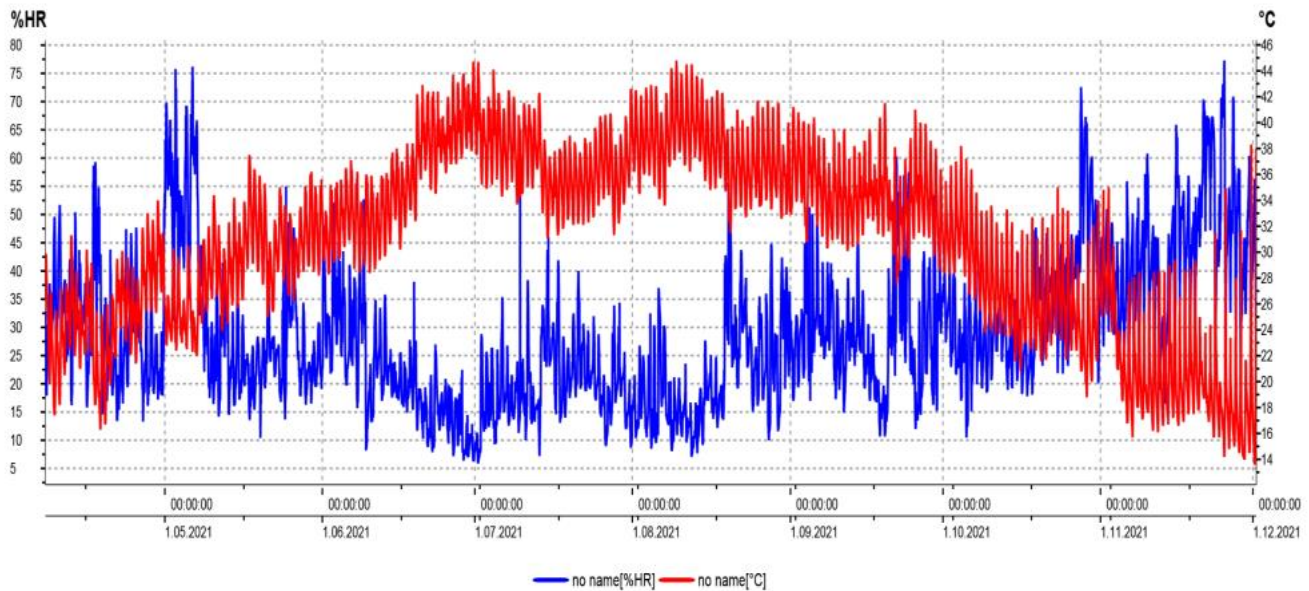


Figure 6.9. The field measurements of air temperature (Tair) and relative humidity (RH).

Source: Author, 2023.

3.4. Validation and calibration of ENVI-met model:

The study employs numerical models, referred to as scenarios, and developed using the latest version of ENVI-met CFD software. These scenarios incorporate various parameters related to the built environment and microclimatic conditions.

The validation of the field measurement and simulation results was performed using two key statistical metrics: Root Mean Square Error (RMSE) and Mean Bias Error (MBE), which quantified the differences between measured and simulated data for the baseline street scenario against a reference station. The analysis revealed that for the baseline condition, the RMSE value was 1.34 (corresponding to 5.08%) and the MBE value was 0.76 (equivalent to 2.88%) (Table 6.3). These results demonstrate strong agreement between the model simulations output and field measurements, as both values fall well within the acceptable limits established by ASHRAE Standard 14-2002, which specifies thresholds of $\pm 30\%$ for RMSE and $\pm 10\%$ for MBE. The relatively low RMSE percentage indicates good overall prediction accuracy, while the small positive MBE suggests a minimal systematic bias in the model's predictions, with a slight tendency to overestimate values compared to the reference station. Given these statistical outcomes, the validation process effectively confirms the model's reliability for the study conditions, providing a solid foundation for subsequent analyses of outdoor thermal comfort and the impacts of different building materials. The high level of agreement between simulated and measured data ensures that the model can be confidently used to evaluate various urban design scenarios and their effects on the local thermal environment.

$$\text{RMSE} = \sqrt{\frac{1}{n} \cdot \sum_{i=1}^n (\text{Sim}_i - \text{Obs}_i)^2} \quad (1)$$

$$\text{MBE} = \frac{1}{n} \cdot \sum_{i=1}^n (\text{Sim}_i - \text{Obs}_i) \quad (2)$$

Table 6.3. Statistical metrics for the validation of the numerical models.

Source: Author, 2023.

Street	Indices	Reference station	
Baseline	RMSE	1.34	5.08 %
	MBE	0.76	2.88 %

4. Development of the Analysis Model:

4.1. Developing based-criteria:

Based on the precedent criteria, the analysis model was developed on its representation of typical housing characteristics in Biskra city, specifically considering the following parameters:

- a) Individual housing typology (regular shape).
- b) Building materials characteristics (variable).
- c) Street aspect ratio (H/W) (variable).
- d) Street orientation (variable).

These criteria ensure that the selected urban canyon exemplifies the predominant residential construction patterns in the region. As well as for the development for the analysis model (following section).

4.1.1. Height-to-width (H/W) ratio variable:

To develop the analysis model (unified model design), which is designed mainly on two building bars (linear blocks), the study incorporates specific street canyon characteristics (between linear blocks) designed basically on the (1) **height-to-width (H/W) ratio**, resulting in three main distinct street geometries:

- a) **Deep canyon:** (H/W = 1.25).
- b) **Regular canyon:** (H/W = 1.00).
- c) **Shallow canyon:** (H/W = 0.62).

These ratios were carefully determined based on actual building heights (reference study area), with corresponding adjustments to street widths.

4.1.2. Street orientation variable:

The study design also considers (2) **street orientation** as a critical parameter, with canyons aligned along two principal axes:

- a) North-South (N-S).
- b) East-West (E-W).

This strategic orientation arrangement ensures comprehensive analysis of solar radiation exposure throughout the day, accounting for the sun's path and its impact on different building façades.

4.1.3. Building materials variable:

The (3) **building materials** used in this study, were detailing within their multi-layer compositions and thermo-physical characteristics. All building materials comply with the Algerian thermal guidelines established by the Algerian Centre for Building Integrated Studies and Research (CNERIB) 2016, ensuring adherence to required thermal standards and promoting energy-efficient, sustainable building practices.

In this light, the principal modeling scenarios are categorized into four types based on wall construction (Table 6.4):

- Wall 1 (BR):** Hollow brick (baseline scenario).
- Wall 2 (CN):** Concrete hollow block.
- Wall 3 (AD):** Adobe brick.
- Wall 4 (ST):** Limestone.

After all, the development of the analysis model based on the previous criteria: height-to-width (H/W) ratio; street orientation; and building materials parameterization, generated a total of 24 plots (scenarios) in Figure 6.10.

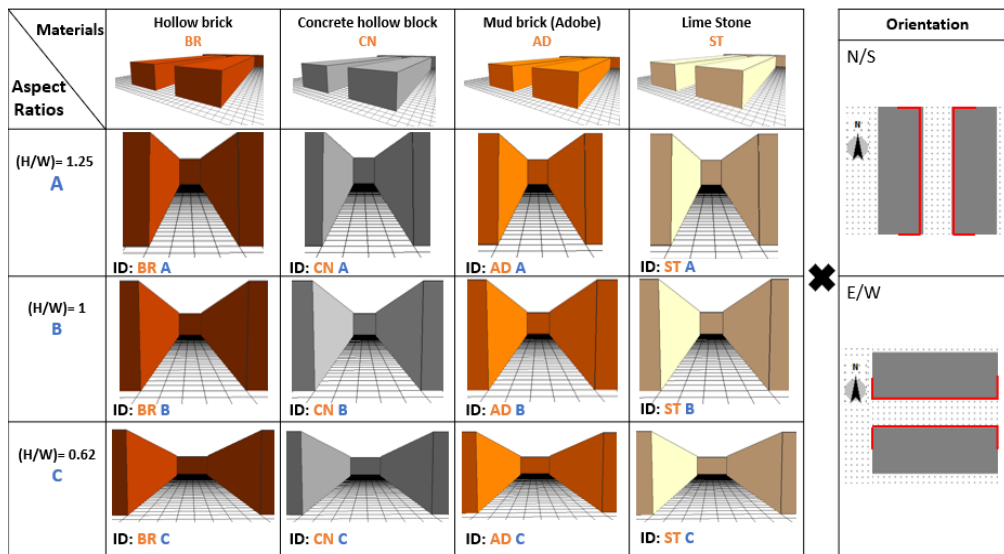


Figure 6.10. The developed scenarios based on: geometry, orientation and building materials.

Source: Author, 2023.

5. Numerical modelling Inputs and simulation via ENVI-met:

As discussed previously, the modeling encompasses 24 distinct scenarios, primarily focusing on building material characteristics, including external walls, soils, and pavements. ENVI-met is a prognostic, three-dimensional, grid-based microclimate model designed to simulate complex surface-vegetation-air interactions in urban environments. The software is widely used to assess the impacts of various urban geometries on outdoor thermal comfort and to predict the thermal effects of different mitigation strategies. It provides comprehensive tools for simulating and analyzing local microclimates and thermal comfort conditions.

The ENVI-met database manager tool was used to set and customize surface and building material parameters, ensuring accurate simulations for outdoor thermal comfort analysis. This comprehensive dataset was compiled and saved as a software library, facilitating easy access for current modeling and future research applications. Otherwise, the building materials used in this study, were designed based on external envelops layers and their thermo-physics characteristics (Table 6.4), including:

- a) Thermal conductivity.
- b) Specific heat capacity.
- c) Emissivity.
- d) Albedo.
- e) Absorption.

Table 6.4. Thermal properties of building materials used within the studies scenarios.

Source: Author, 2023.

Construction Materials	Layers (Outside to Inside)	Composition	Thickness (m)	Thermal conductivity (W/ m-K)	Specific heat capacity (J/kg K)	Density (kg/ m3)	Albedo	Emissivity	Absorption
Wall 1 (Reference)	Layer 1	Mortar	0.02	1.40	1080	2200	0.30	0.84	0.50
	Layer 2	Hollow brick	0.15	0.48	936	900	0.34	0.9	0.66
	Layer 3	Air cavity	0.05	0.024	1000	1.22	-		-
	Layer 4	Hollow brick	0.10	0.48	936	900	0.34	0.9	0.66
	Layer 5	Plaster	0.02	0.35	936	800	0.93	0.91	0.07
Wall 2	Layer 1	Mortar	0.02	1.40	1080	2200	0.30	0.94	0.50
	Layer 2	concrete hollow block	0.20	1.10	1080	1300	0.30	0.92	0.80
	Layer 3	Plaster	0.02	0.35	936	800	0.93	0.91	0.07

Wall 3	Layer 1	Mortar	0.02	1.40	1080	2200	0.30	0.94	0.50
	Layer 2	Mud brick (Adobe)	0.50	0.81	1075	2500	0.33	0.85	0.69
	Layer 3	Plaster	0.02	0.35	936	800	0.93	0.91	0.07
Wall 4	Layer 1	Mortar	0.02	1.40	1080	2200	0.3	0.94	0.50
	Layer 2	Lime Stone	0.60	2.40	936	2400	0.4	0.95	0.50
	Layer 3	Plaster	0.02	0.35	936	800	0.93	0.91	0.07
Roof	Layer 1	Concrete	0.05	0.46	1080	1200	0.30	0.94	0.50
	Layer 2	Concrete slab (hollow block)	0.16	1.45	1080	1450	0.30	0.92	0.80
		Mortar							
	Layer 3		0.02	1.40	1080	2200	0.30	0.94	0.50
Street floor		Concrete pavement	0.01	-	-	-	0.50	0.90	-
		Asphalt	0.10	-	-	-	0.20	0.90	-
		Loamy Soil	-	-	-	-	-	0.90	-

The 24 scenarios (Figure 6.10) present a systematic matrix of urban canyon configurations. Utilizing four distinct building materials (Table 6.5): hollow brick (shown in orange/red), concrete hollow block (gray), mud brick or Adobe (orange), and lime stone (light yellow/beige). As mentioned previously, these materials are examined across three different aspect ratios (H/W), creating a total of 12 unique geometric configurations. The aspect ratios progress from a deep canyon ($H/W = 1.25$) at the top row, labeled as 'A', through a regular canyon ($H/W = 1.0$) in the middle row, labeled 'B', to a shallow canyon ($H/W = 0.62$) in the bottom row, named 'C'. Each configuration is assigned a unique identifier 'ID' combining the material abbreviation (BR for hollow brick, CN for concrete block, AD for Adobe, and ST for lime stone) with the aspect ratio letter (A, B, or C). For instance, BR A represents a hollow brick canyon with an H/W ratio of 1.25. The study further incorporates two street orientations: North-South (N/S) and East-West (E/W), effectively doubling the number of scenarios to 24 total configurations. This comprehensive approach allows to analyze accurately the effects of individual parameters (building material, geometry, orientation) while holding others constant, enabling a thorough investigation of their impacts on urban microclimate and outdoor thermal comfort.

The initial scenario serves as the baseline model and reference point for the study area. This baseline accurately represents all current urban geometry and building material characteristics specific to the reference study area. The streets in the baseline model are oriented East-West, with walls and external pavements constructed from brick, asphalt, and concrete.

The second step, to quantitatively evaluate the impact of building materials on outdoor thermal comfort, this study utilizes the Physiological Equivalent Temperature (PET) index, a widely recognized thermal comfort measure derived from the Munich Physiological Heat Balance (MEMI) model. The PET index offers several advantages for urban climate studies: it is universally applicable and unaffected by variables such as clothing values and metabolic activity; it is founded on thermo-physiological principles, providing an accurate representation of human climate sensations; it operates objectively, without requiring subjective evaluations; and it demonstrates sensitivity to windy environmental conditions. As a thermal measure, the PET index employs a specific scale based on criteria related to the physical environment and human body. In this study, outdoor thermal comfort assessment follows the adapted PET scale for arid climate (BWh), as established by Cohen et al. (2019).

The comprehensive modelling process employs ENVI-met software and incorporates field measurements conducted within the street canyon over one year, from April 10, 2021, to April 9, 2022. The software implements these field measurement datasets using the full forcing method and converts all weather data inputs into CSV files. The summer typical days chosen for the study were July 10, 11, and 12, 2021, representing the extreme weather period typical of North African arid lands. Furthermore, the validation of numerical model results typically involves comparing simulation outcomes with in-situ measurement data. According to Liu et al. (2021), 92.59% of previous studies employed air temperature (T_a) as the primary validation variable, followed by relative humidity (RH) at 27.78% and mean radiant temperature (T_{mrt}) at 12.96%. Other parameters such as surface temperature (T_s), air velocity (V_{air}), solar radiation (SR), and longwave radiation (LR) were used in less than 10% of validation studies. In this context, the current study's validation was performed using air temperature (T_a), employing root-mean-square error (RMSE), mean bias error (MBE), and linear regression (R^2) as statistical metrics. The evaluation of outdoor thermal comfort primarily relies on two meteorological variables: mean radiant temperature (T_{mrt}), which is significantly impacted by factors including spatial configuration, shading effects, and the exposure of the human body to shortwave and longwave

radiation fluxes, and surface temperature (T_s), which accounts for the direct and indirect effects of surrounding building materials.

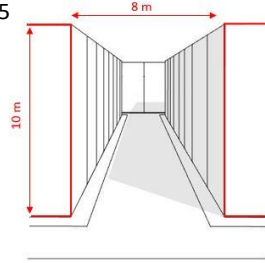
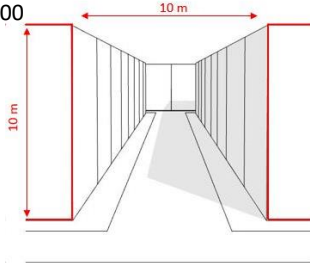
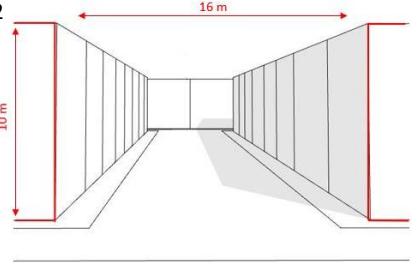
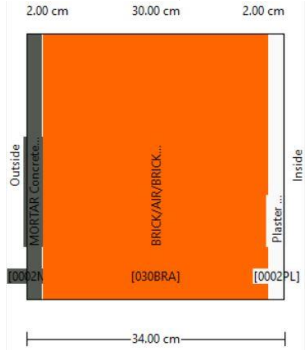
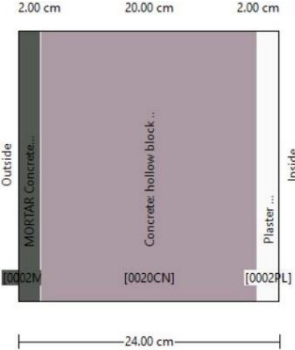
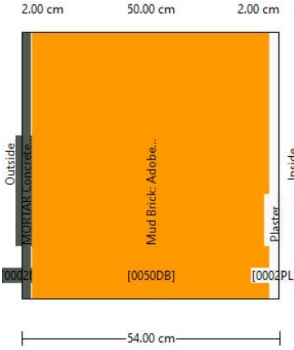
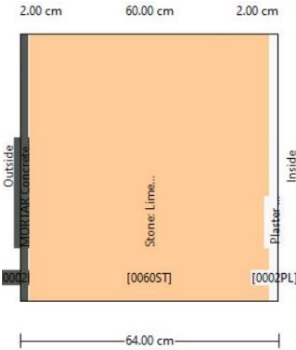
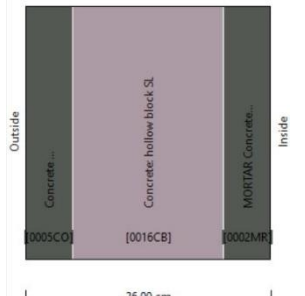
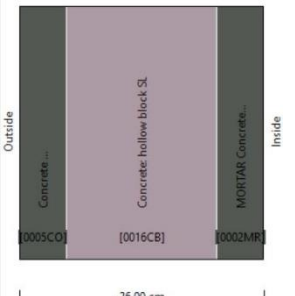
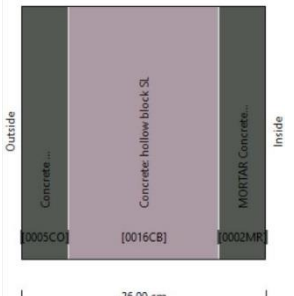
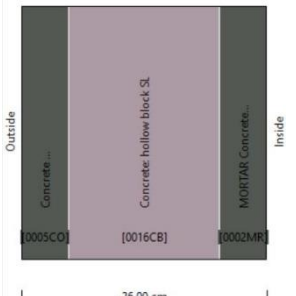
On the other hand, thermal comfort indices were calculated using BIO-met, a specialized post-processing tool designed for computing human thermal comfort indices using simulated datasets from the ENVI-met model. BIO-met adheres to ISO 7730 specifications, which define the 'Standard Human,' ensuring reliable and precise evaluation of individual thermal comfort levels. The tool can calculate various thermal indices, including Dynamic Thermal Comfort (dPET) and classic static indices such as PET, Standard Effective Temperature (SET), and Universal Thermal Climate Index (UTCI). For this study, the subject parameters in BIO-met were set to a 35-year-old male weighing 75 kg, with a height of 1.75 m, static clothing insulation of 0.90 clo, and a total metabolic rate of approximately 86.21 W/m² in a standing position.

The simulation protocol was meticulously designed to ensure accurate and comprehensive results. The process identified various spatial characteristics, including location coordinates, detailed model geometry, and specific construction materials for all surfaces within the study area (Table 6.5). The model domain was carefully configured to represent the actual urban environment, with particular attention paid to building heights, street widths, and the arrangement of urban features. Grid resolution was set to provide a balance between computational efficiency and accuracy, with a finer resolution used in areas of particular interest or where significant thermal gradients were expected. The simulation runtime was 48 hours, starting from July 10, 2021, to ensure thermal stability and to account for the diurnal cycle of heat storage and release in urban materials. This duration allowed for a 24-hour spin-up period, ensuring that the model reached equilibrium before the analysis period began. All simulated output variables were consistently measured at the standardized pedestrian height of 1.4 meters above ground level, following established protocols for urban comfort studies. The simulation time step was carefully selected to capture rapid changes in environmental conditions while maintaining computational efficiency.

Table 6.5. ENVI-met modelling inputs parameters: space geometry, model geometry, construction material, and simulation.

Source: Author, 2023.

Space geometry				
Street orientation	E-W N-S	E-W N-S	E-W N-S	E-W N-S
Longitude (°)	5.73	5.73	5.73	5.73
Latitude (°)	34.85	34.85	34.85	34.85

Aspect Ratio (H/W)	A=1.25	B=1.00	C=0.62	
				
Model geometry				
Grid size	100 m × 70 m x ...	100 m × 70 m x ...	100 m × 70 m x ...	100 m × 70 m x ...
dx = size of X grid	dx = 2.00	dx = 2.00	dx = 2.00	dx = 2.00
dy = size of Y grid	dy = 2.00	dy = 2.00	dy = 2.00	dy = 2.00
dz = size of Z grid	dz = 2.00	dz = 2.00	dz = 2.00	dz = 2.00
Construction material				
Building material	Walls: - Created wall: Mortar; (Hollow brick/ Air/ Hollow brick); Plaster	Walls: - Created wall: Mortar; Concrete hollow block; Plaster	Walls: - Created wall: Mortar; Mud brick (Adobe); Plaster	Walls: - Created wall: Mortar; Lime Stone; Plaster
				
	Roofs: Created roof: Concrete; Concrete slab (hollow block); Mortar	Roofs: Created roof: Concrete; Concrete slab (hollow block); Mortar	Roofs: Created roof: Concrete; Concrete slab (hollow block); Mortar	Roofs: Created roof: Concrete; Concrete slab (hollow block); Mortar
				
Soil	Concrete pavement Asphalt Road Loamy soil	Concrete pavement Asphalt Road Loamy soil	Concrete pavement Asphalt Road Loamy soil	Concrete pavement Asphalt Road Loamy soil
Simulation				
Start Date	10.07.2021	10.07.2021	10.07.2021	10.07.2021
Start time	23h00	23h00	23h00	23h00
Total simulation time	48h	48h	48h	48h

Type of meteorological boundary conditions	Full forcing - CSV	Full forcing - CSV	Full forcing - CSV	Full forcing - CSV
--	--------------------	--------------------	--------------------	--------------------

Conclusion:

The chapter provides a robust methodological framework for analyzing outdoor thermal comfort in hot dry climate, within Biskra, Algeria, as a case study. It integrates continuous field measurements, numerical modeling, and simulation with ENVI-met software to evaluate how building materials, and street geometry impact thermal conditions. The validation of simulation models with empirical data ensures reliability, supported by statistical metrics like RMSE and MBE.

Historical analysis contextualizes material use, tracing its evolution from traditional adobe to modern concrete. Scenarios include varying height-to-width ratios, street orientations, and material compositions, resulting in 24 configurations analyzed for their microclimatic effects. The study's use of the PET index for thermal comfort assessment ensures objective and precise evaluations, offering replicable methodologies for sustainable urban design in hot dry climate.

CHAPTER VII: RESULTS AND ANALYSIS: PRESENTATION AND INTERPRETATION OF FIELD MEASUREMENTS AND SIMULATION RESULTS

Introduction

This chapter presents a comprehensive analysis of microclimatic parameters in urban settings, focusing on 24 different scenarios simulated during typical summer days in July 2021. The study examines three key variables: Mean Radiant Temperature (T_{mrt}), Surface Temperature (T_s), and Physiological Equivalent Temperature (PET) index. These scenarios explore various combinations of street orientations (East-West and North-South), height-to-width ratios ($H/W = 1, 1.25, \text{ and } 0.62$), and building materials (brick, concrete, adobe, and limestone). The research aims to understand how these different urban design elements influence thermal comfort in arid climates, with particular attention to the interaction between street geometry and building envelope materials.

1. Assessment of the Mean Radiant Temperature (T_{mrt}):

Figure 7.1 displays the profiles of hourly average, maximum, and minimum T_{mrt} (Mean Radiant Temperature) values obtained from measuring points in different representational scenarios over a 48-hour period, comparing East-West (left) and North-South (right) street orientations with varying height-to-width (H/W) ratios: (a) $H/W = 1$, (b) $H/W = 1.25$, and (c) $H/W = 0.62$. All scenarios exhibit consistent bi-modal daily patterns, with temperature values ranging between approximately 2.0°C and 4.0°C , showing distinct peaks in the early morning hours (around 02:00-04:00) and afternoon (approximately 14:00-16:00), while temperature minimums occur between peaks at roughly 08:00 and 20:00. E-W orientation scenarios demonstrate slightly more pronounced temperature fluctuations compared to N-S orientations, with Scenario B ($H/W = 1.25$) showing the highest peaks in both orientations, while Scenario C ($H/W = 0.62$) displays somewhat moderated peaks, particularly in the E-W orientation. N-S oriented streets exhibit more rapid temperature changes during transition periods, especially noticeable in the steeper slopes of the warming and cooling phases. The thermal amplitude between daily maximum and minimum temperatures ranges from approximately 1.5°C to 2.0°C across all scenarios, with the E-W orientation generally showing greater thermal stress due to extended exposure to direct solar radiation. The data reveals a slight temporal shift in peak temperatures between orientations, with N-S streets typically reaching maximum temperatures about 1-2 hours later than E-W streets,

likely due to differences in solar exposure patterns. The consistent repetition over 48 hours indicates reliable diurnal and nocturnal cycling, with geometry playing a crucial role in modulating the thermal environment, clearly demonstrating how street orientation and aspect ratios influence the temporal distribution and intensity of thermal conditions in urban settings, with implications for urban heat island mitigation strategies and pedestrian thermal comfort planning.

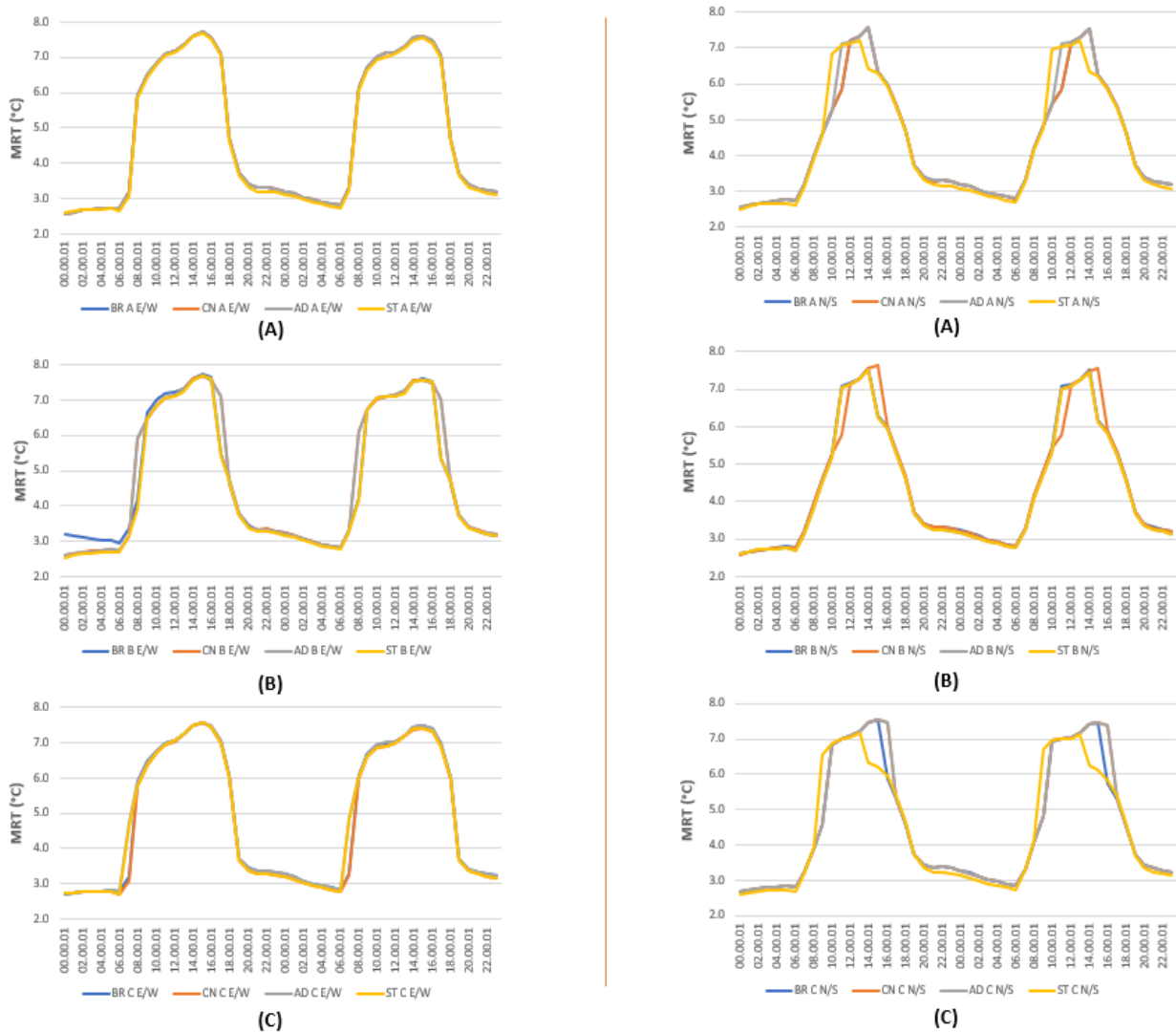


Figure 7.1. Hourly mean radiant temperature (MRT) values for the 24 scenarios, E-W (left) for the (A, B, C) ratio. N-S (right) for the (A, B, C) ratio.

Source: Author, 2023.

Notably, in the N-S orientation, the limestone (ST) scenarios in both A and C configurations showed slightly lower T_{mrt} average values during peak hours (around 14:00-16:00). However,

this same material exhibited a more rapid temperature increase compared to other materials during morning hours, typically starting from 9:00 to 10:00, across all street geometries. In the E-W street orientation with the B aspect ratio ($H/W = 1.25$), both brick (BR) and limestone (ST) scenarios demonstrated marginally cooler temperatures, with T_{mrt} values approximately $0.2-0.3^{\circ}\text{C}$ lower than concrete (CN) and adobe (AD) during peak hours. The temperature differences between materials were most pronounced during the warming and cooling phases, with variations of approximately 0.5°C observed during these transition periods.

The minimum T_{mrt} values were recorded during nighttime hours, reaching approximately 2.0°C across all scenarios in both E-W and N-S orientations. Temperature gradients show a consistent pattern, decreasing gradually after 18:00 to reach minimum values around 05:00 the next morning. Several factors contribute to the variations in T_{mrt} among different scenarios. The deeper street canyons (configurations A and B) within the N-S orientation tend to be slightly cooler, particularly where brick and limestone walls are used. This effect is likely due to the higher aspect ratios providing more shading, while the thermal properties of lighter materials result in reduced heat absorption and retention. Additionally, the E-W street orientation experiences more direct solar radiation during the daily cycle, leading to slightly higher T_{mrt} values, whereas the N-S orientation benefits from reduced solar exposure and increased shaded surfaces, resulting in marginally lower temperature fluctuations.

2. Assessment of the Surface Temperature (T_s):

The simulation results for surface temperatures (T_s) of walls at 1.4 m height across different modeled scenarios are presented in box plots (Figures 7.2, 7.3), revealing distinct patterns between E-W and N-S street orientations. The results shows median T_s values ranging between 40°C - 42°C for most scenarios, with variations observed between different building materials and aspect ratios. In E-W oriented streets (Figure 7.2), all configurations (A1-C1) demonstrate relatively consistent temperature distributions, with median values around 40°C for all material types (BR, CR, AD, and ST). The interquartile ranges typically span $31-50^{\circ}\text{C}$, with maximum values reaching approximately 50°C across all scenarios. On the other hand, the N-S oriented streets (Figure 7.3) exhibit slightly higher temperature variations, with median values around 41°C - 42°C and notably higher maximum temperatures reaching 61°C - 63°C in configurations A2 and B2. Limestone (ST) shows marginally lower temperatures in some configurations, though the difference is minimal

(approximately 1°C) compared to other materials. Contrary to expected thermal behavior, the aspect ratio ($H/W = 1, 1.25, \text{ and } 0.62$) appears to have limited impact on surface temperatures, with all configurations showing similar median values and temperature distributions. This indicates that street geometry may have less influence on surface temperatures than anticipated. The data indicates that building material choice (between BR, CR, AD, and ST) has minimal effect on overall thermal performance, with all materials showing similar temperature distributions within each configuration. The higher maximum temperatures in N-S orientations, particularly evident in the whiskers of the box plots, suggest these façades experience more intense solar exposure during peak hours despite potentially having longer periods of shade.

Therefore, this comprehensive analysis indicates that street orientation has a more significant impact on surface temperature extremes than either building materials or canyon geometry, with N-S orientations experiencing higher maximum temperatures despite similar median values to E-W orientations.

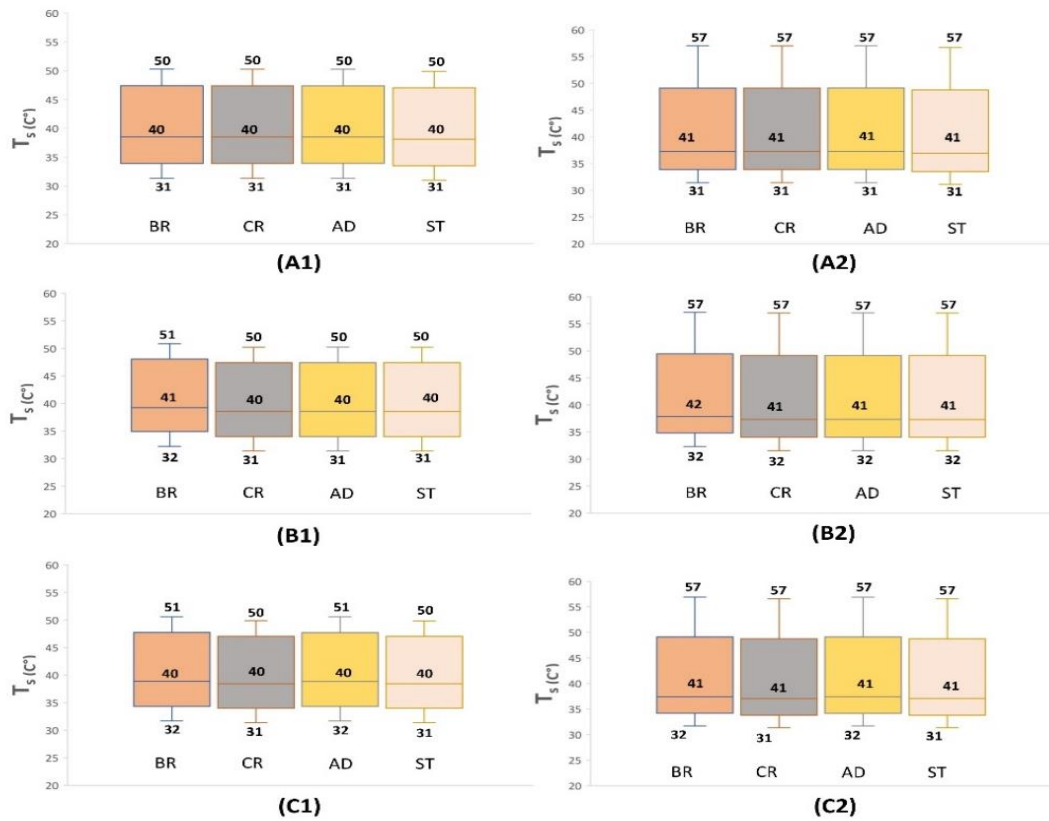


Figure 7.2. Box plots of surface temperatures (T_s) values: E-W orientation for the (A, B, C) ratios, (1) north side, (2) south side.

Source: Author, 2023.

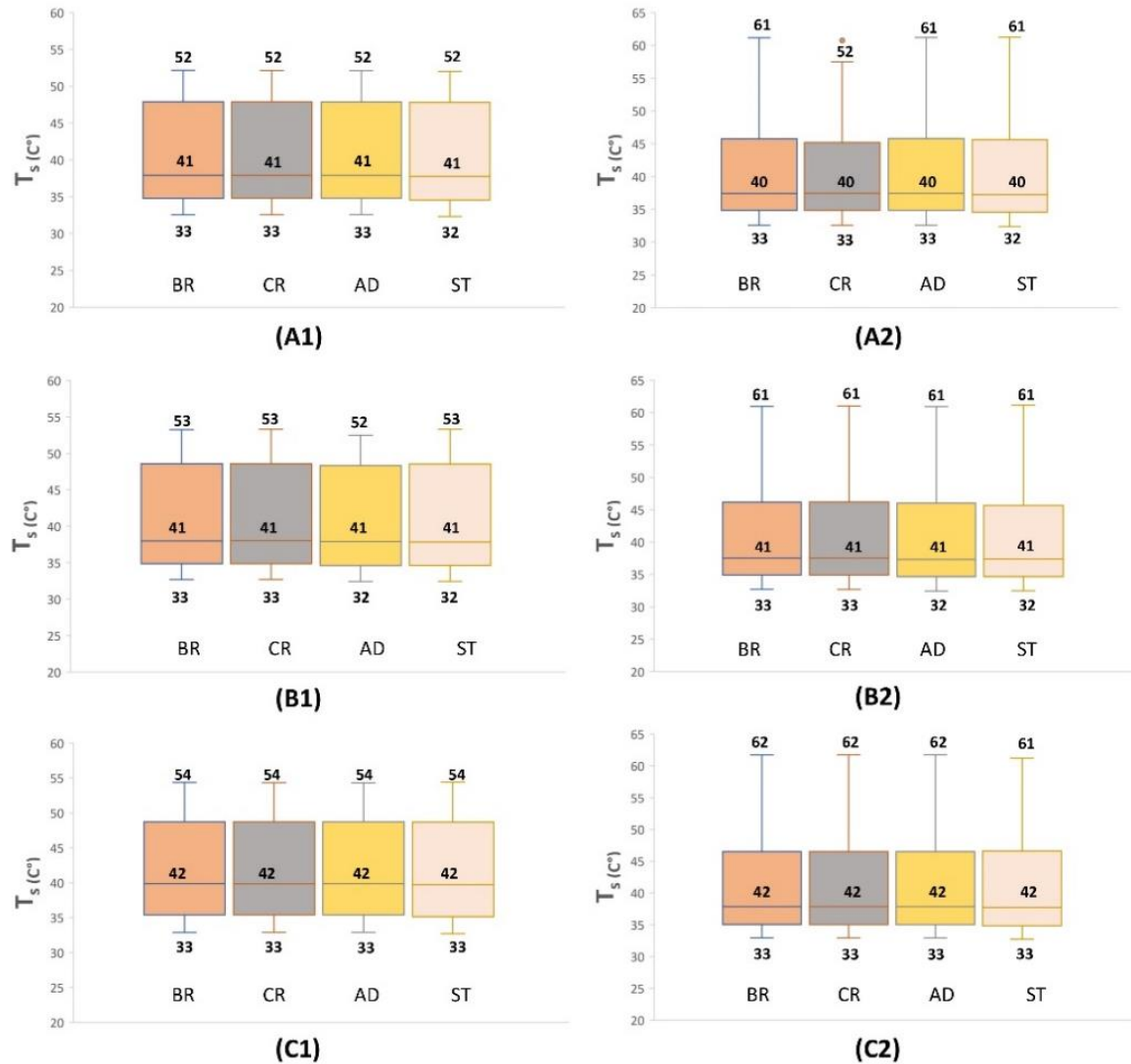


Figure 7.3. Box plots of surface temperatures (T_s) values: N-S orientation for the (A, B, C) ratios (1) east side, (2) West side.

Source: Author, 2023.

2.1. Thermal mapping of the surface temperature (T_s) by Leonardo interface:

As shown in Figures 7.4 and 7.5, the results of the surface temperature (T_s) analysis reveal crucial insights into the thermal behavior of urban street canyons in hot dry climate, with significant variations observed across street orientations, height-to-width (H/W) ratios, and building materials.

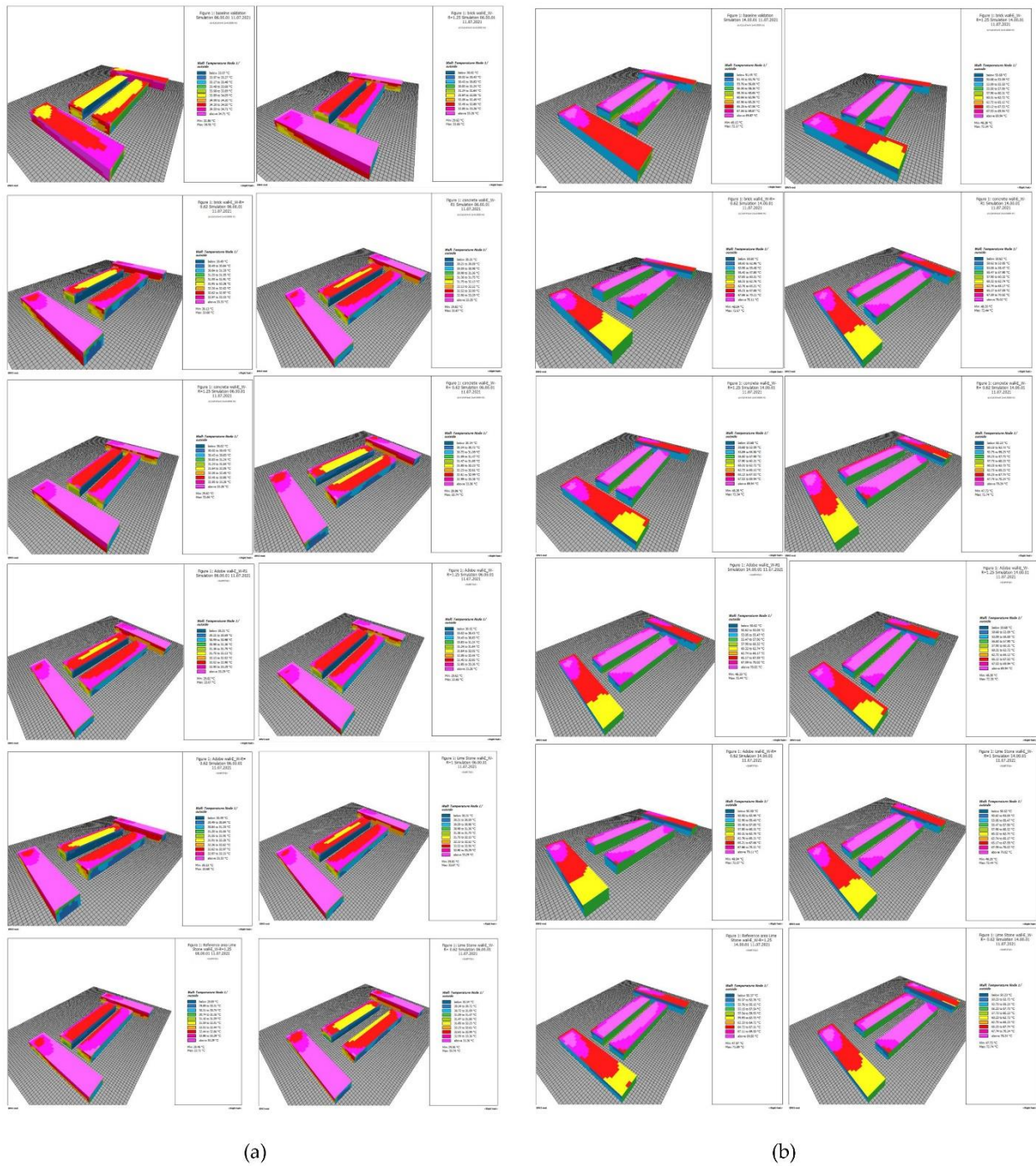


Figure 7.4. Surface temperature (T_s) values within E-W orientation, by Leonardo interface..

Source: Author, 2023.

East-West (E-W) oriented streets exhibit the highest thermal stress, with surface temperatures peaking at approximately 60°C during midday (14:00–16:00), driven by prolonged

solar exposure aligned with the sun's trajectory. The thermal mapping highlights how shallow canyons ($H/W = 0.62$) experience the greatest thermal stress due to limited shading and extensive exposure of canyon walls, particularly on façades oriented perpendicular to the solar path.

The wide spacing between buildings allows sunlight to penetrate deep into the canyon, leaving a large proportion of walls and ground surfaces exposed to direct radiation. This lack of shading results in surface temperatures that remain elevated for longer periods, contributing to a delayed cooling phase during the evening. Conversely, intermediate ($H/W = 1.0$) and deep canyons ($H/W = 1.25$) show a degree of thermal mitigation, with deeper canyons performing significantly better. In deep canyons, the increased height of buildings provides enhanced shading to canyon walls and ground surfaces, reducing the magnitude of solar heat gain. However, even in these configurations, the E-W orientation still exhibits higher peak T_s values compared to N-S streets, underlining the inherent thermal challenges associated with this orientation. The thermal behavior of building materials further amplifies the variations in surface temperatures observed in E-W streets. Among the materials analyzed, limestone (ST) demonstrates the most effective thermal performance, with slightly lower T_s values compared to other materials due to its high albedo, which reflects a significant proportion of incoming solar radiation. Adobe (AD) also performs moderately well, though its thermal efficiency is somewhat reduced due to its moderate heat retention properties. Brick (BR) and concrete (CN), on the other hand, exhibit the poorest thermal performance in E-W streets. Their high thermal mass causes them to absorb and retain large amounts of heat during the day, resulting in elevated surface temperatures and a slower cooling phase in the evening. This heat retention is particularly problematic in shallow and intermediate canyons, where the prolonged solar exposure exacerbates the thermal load on these materials.

A distinctive characteristic of E-W streets is the bimodal pattern of surface temperature variations throughout the day. The first temperature peak occurs in the morning (approximately 9:00 - 11:00) when east-facing walls are exposed to direct sunlight, while the second peak is observed in the afternoon (14:00 - 16:00) as solar radiation shifts to west-facing walls. This pattern highlights the dynamic nature of thermal stress in E-W streets, with alternating periods of intense heating on opposite canyon walls. Additionally, the ground surfaces in E-W streets experience consistent solar exposure throughout the day, contributing to elevated overall T_s values. The thermal behavior of the ground is critical, as it serves as a heat reservoir that radiates absorbed

energy back into the canyon, further increasing the thermal stress on canyon walls and surrounding pedestrian areas.

Overall, the results underscore the inherent thermal challenges of E-W oriented streets, which are predominantly driven by prolonged solar exposure and limited shading. The thermal mapping data clearly highlights the critical role of canyon geometry and material properties in modulating surface temperatures within these streets. While deep canyons and reflective materials can mitigate some of the thermal stress, the fundamental alignment of E-W streets with the sun's path remains a significant factor contributing to elevated T_s values.

In contrast, the North-South (N-S) oriented streets display more moderate thermal stress patterns, with lower peak T_{mrt} values that are approximately 5°C - 10°C lower than the E-W orientations during the hottest hours. Additionally, the N-S configurations exhibit more rapid transitions between temperature levels, particularly during the morning and evening hours.

The analysis of surface temperature (T_s) in North-South (N-S) oriented streets highlights their elevated thermal efficiency compared to East-West (E-W) streets, primarily due to the orientation's ability to minimize direct solar exposure on building façades and ground surfaces during peak hours. In N-S orientations, the alignment of the street axis perpendicular to the sun's path ensures that the canyon walls experience limited direct radiation throughout the day. This results in reduced heat accumulation on vertical surfaces, which is particularly advantageous for thermal comfort in urban environments. Surface temperature peaks in N-S streets are consistently lower, ranging between 50°C and 55°C , compared to the 60°C observed in E-W streets. This reduction is particularly significant during the afternoon hours, where the shading provided by the canyon walls in N-S streets prevents excessive solar heating.

One of the key factors contributing to the improved thermal performance of N-S streets is the role of shading. The orientation naturally favors alternating periods of shade on opposite canyon walls, as sunlight moves from east to west over the course of the day. This dynamic shading creates cooler microclimates within the canyon, particularly in configurations with higher height-to-width (H/W) ratios. Deep canyons ($H/W = 1.25$) perform particularly well in N-S orientations, as the taller buildings provide extended shading for both the ground and opposite walls.

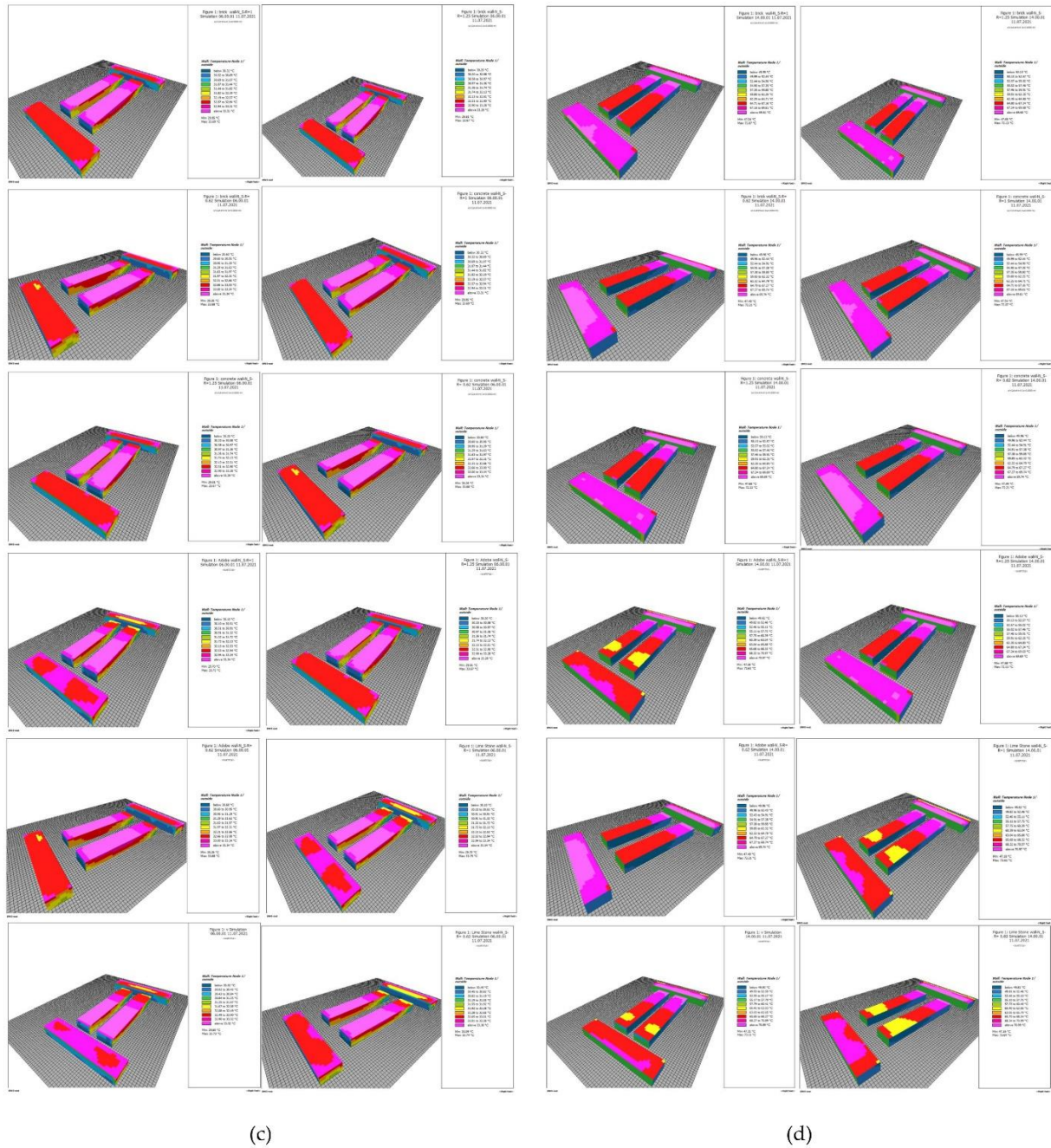


Figure 7.5. Surface temperature (Ts) values within N-S orientation, by Leonardo interface..

Source: Author, 2023.

This effect reduces direct solar radiation exposure and lowers the overall surface temperature of the urban canyon. Shallow canyons ($H/W = 0.62$), while less effective in providing shade, still

perform better in N-S orientations than their E-W counterparts, as the perpendicular alignment minimizes prolonged exposure to direct sunlight on the vertical surfaces.

The material properties of building façades and ground surfaces further influence T_s variations in N-S streets. Limestone (ST) consistently emerges as the most effective material for thermal regulation in this orientation. Its high albedo reflects a substantial portion of incoming solar radiation, reducing heat absorption and subsequent surface temperatures. Additionally, limestone's low heat retention allows it to release absorbed heat quickly, further enhancing cooling efficiency during the evening hours. Adobe (AD), while not as reflective as limestone, also performs well in N-S orientations due to its moderate thermal mass, which helps to balance heat absorption and dissipation. In contrast, brick (BR) and concrete (CN) demonstrate higher surface temperatures due to their greater thermal mass and lower reflectivity, which lead to prolonged heat retention and delayed cooling. This behavior is particularly evident in shallow canyons, where these materials exacerbate the thermal stress despite the orientation's inherent advantages.

The ground surfaces in N-S oriented streets also benefit from the dynamic shading provided by the canyon geometry. Unlike in E-W streets, where ground surfaces are exposed to direct sunlight for most of the day, N-S streets experience alternating periods of shade as the sun moves across the sky. This shading reduces the overall heat load on the ground, contributing to cooler surface temperatures and improved thermal comfort for pedestrians. In configurations with deeper canyons, the ground receives even less solar radiation, further enhancing the cooling effects. However, in shallow canyons, ground surfaces still experience higher temperatures, underscoring the importance of incorporating additional cooling strategies, such as reflective paving materials or vegetative cover, to mitigate thermal stress.

The thermal mapping of N-S streets reveals distinct diurnal patterns in surface temperature variations. Unlike the bimodal pattern observed in E-W streets, N-S streets exhibit a more gradual increase in T_s during the morning hours, followed by a steady peak in the early afternoon (around 12:00 - 14:00), and a rapid decline as the sun moves west and shade cover the canyon walls. This pattern reflects the orientation's ability to moderate solar heating and promote efficient cooling during the transition periods. Moreover, the thermal behavior of N-S streets is less influenced by seasonal variations compared to E-W streets, as the perpendicular alignment ensures consistent shading effects throughout the year, even in climates with high solar angles during summer.

Despite their overall superior thermal performance, certain challenges remain in optimizing the design of N-S streets. In shallow canyons, the limited height of buildings reduces the shading potential, leading to higher surface temperatures on both walls and ground surfaces. This underscores the importance of prioritizing deeper canyons ($H/W \geq 1.25$) in urban designs, as they provide more effective thermal mitigation. Additionally, while high-albedo materials like limestone perform exceptionally well, the benefits can be further enhanced by integrating vegetative elements, such as green façades and tree canopies, which not only provide additional shading but also contribute to evaporative cooling.

In N-S streets, the orientation's ability to maximize shading and minimize direct solar exposure results in lower thermal stress levels, making it a preferred design choice for hot dry climate. This orientation provides a more thermally stable environment, reducing the need for active cooling measures and supporting sustainable urban planning objectives. Incorporating reflective materials, optimizing H/W ratios, are essential components of a holistic approach to enhancing thermal comfort in N-S streets.

3. Evaluation of the Physiological Equivalent Temperature Index (PET):

The analysis of the Physiological Equivalent Temperature (PET) index reveals distinct thermal stress patterns across a 48-hour cycle (Figure 7.6), encompassing three thermal stress zones: warm, hot, and very hot, based on criteria established for arid (BWh) climates. The results demonstrate clear diurnal variations across all scenarios, with significant differences between East-West (E-W) and North-South (N-S) street orientations.

In E-W orientations, all scenarios exhibit a pronounced bi-modal pattern with two daily peaks, reaching maximum values of approximately 60°C during peak hours (around 14:00 - 16:00) with a $PET_{\text{maxE-W}} = 60.6^{\circ}\text{C}$. The street canyon geometry, defined by height-to-width ratios ($H/W = 1, 1.25$, and 0.62 for configurations A, B, and C respectively), shows minimal impact on peak PET values, though slight variations are observed during transition periods. The average values of PET were 47.7°C with extreme hot stress. All configurations maintain relatively consistent patterns, with the nighttime (00:00 - 06:00) PET values remaining in the warm stress range (approximately 35°C - 40°C).

On the other hand, the N-S orientations display more moderate thermal stress patterns, with lower peak values and less pronounced bi-modal distribution. The maximum PET values in N-S orientations are approximately 5°C - 10°C lower than in E-W orientations during peak hours. Additionally, N-S configurations show more rapid transitions between stress levels, particularly during morning and evening hours.

Across all scenarios, the period between 09:00 and 19:00 consistently falls within the very hot thermal stress category, with PET values exceeding 55°C during peak hours. Although, the results show a gradual decrease in PET values after 19:00, reaching minimum values (around 35°C) in the early morning hours (04:00 - 06:00) before beginning to rise again with the next day's solar cycle.

The consistency of patterns across different canyon geometries suggests that street orientation has a more significant impact on thermal stress than the height-to-width ratio, particularly in determining peak PET values and the duration of extreme heat stress conditions. This analysis indicates that E-W street orientations experience more severe and prolonged thermal stress compared to N-S orientations, with implications for urban design and thermal comfort strategies in hot dry climate.

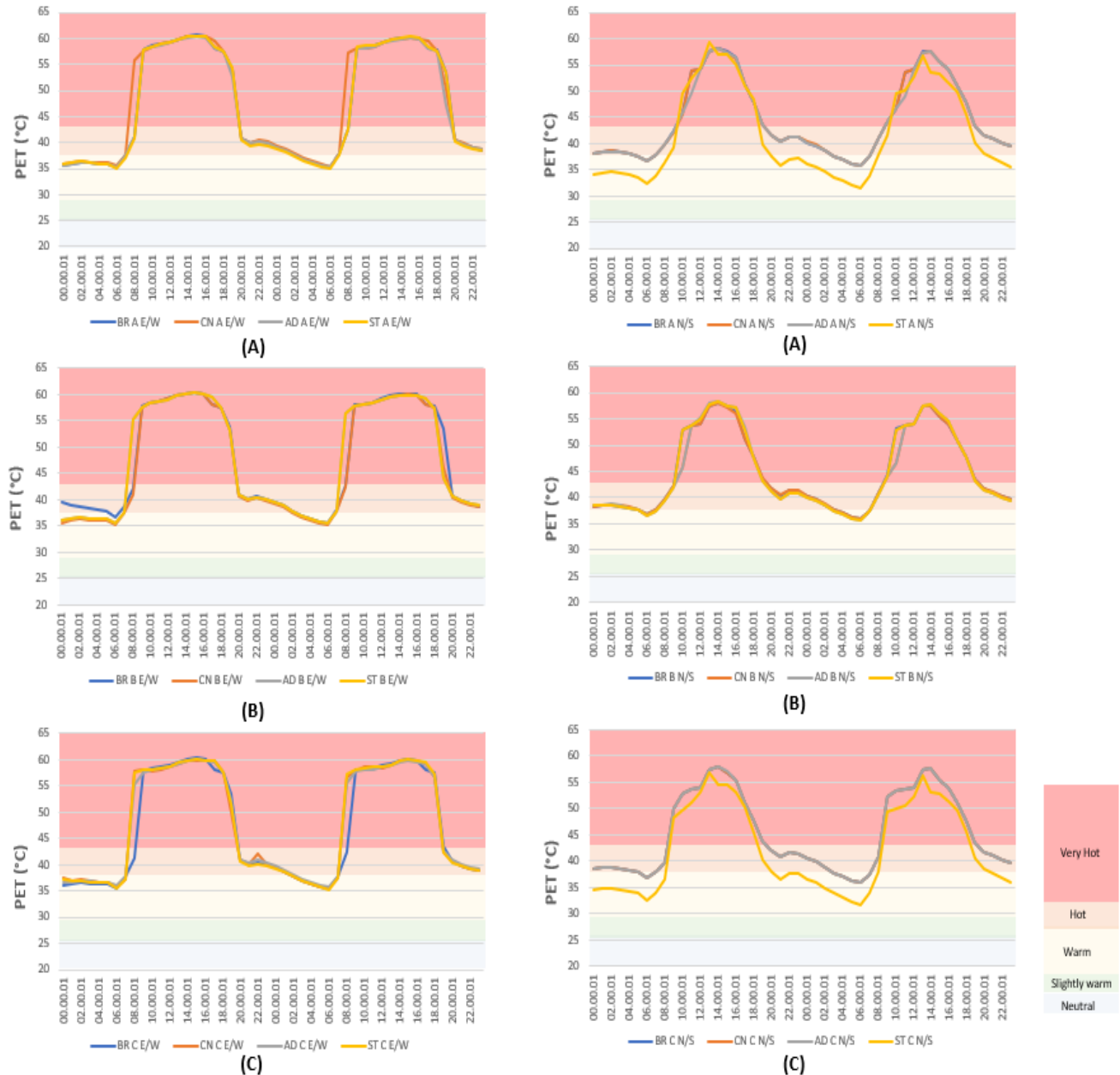


Figure 7.6. Hourly PET values for the 24 scenarios, E-W (left) for the (A, B, C) ratio. N-S (right) for the (A, B, C) ratio.

Source: Author, 2023.

3.1. Evaluation of the thermal stress levels

As shown in the Figure 7, results demonstrate three primary thermal stress categories: warm, hot, and very hot, with their distribution varying significantly between different street orientations, aspect ratios, and building materials. The East-West (E-W) oriented streets consistently show higher thermal stress levels, with 49.1% of the day experiencing very hot conditions, 30.6% hot

conditions, and 20.3% warm conditions. Notable variations exist between scenarios, such as the E-W orientation with H/W ratio of 1.25 (configuration B) using brick (BR) showing only 8% warm stress periods, while concrete (CN) in configuration A ($H/W = 1$) exhibited 27.1% hot stress periods.

North-South (N-S) oriented streets demonstrate moderately improved thermal conditions, with limestone (ST) scenarios showing the most favorable thermal performance. In the N-S configurations, limestone walls achieved 37.5% and 41.7% warm thermal range periods in configurations A ($H/W = 1$) and C ($H/W = 0.62$) respectively, while simultaneously exhibiting the lowest rates of hot thermal stress (20.8% and 16.7%) and very hot stress (41.7%) in these configurations. The daily PET values in N-S orientations ranged from a maximum of 59.2°C at 13:00 to a minimum of 32.2°C at 06:00, with an average of 44.6°C across all scenarios.

This part of results indicates that street orientation has a more significant impact on thermal stress mitigation than canyon geometry or building materials. N-S orientations consistently demonstrated more favorable thermal conditions compared to E-W orientations, primarily due to improved solar exposure management and shading effects. However, the anticipated cooling effect from varying canyon depths (H/W ratios) was less pronounced than expected, particularly in E-W orientations where even deep canyons ($H/W = 1.25$) showed limited thermal stress reduction. Limestone emerged as the most effective material for thermal stress mitigation, particularly in N-S orientations, though the magnitude of improvement remained modest. The material's performance suggests that while material selection can contribute to thermal comfort optimization, its impact is secondary to street orientation. The absence of significant cooling effects, even in deep canyons, highlights the critical need for additional shading strategies, particularly in E-W oriented streets where solar exposure remains a dominant factor in thermal stress conditions.

These findings have significant implications for urban design in hot dry climate, suggesting that prioritizing N-S street orientations and implementing complementary shading strategies may be more effective for thermal stress mitigation than relying solely on canyon geometry or building material selection. The data underscores the complexity of urban thermal comfort and the need for comprehensive approaches that consider multiple design factors simultaneously.

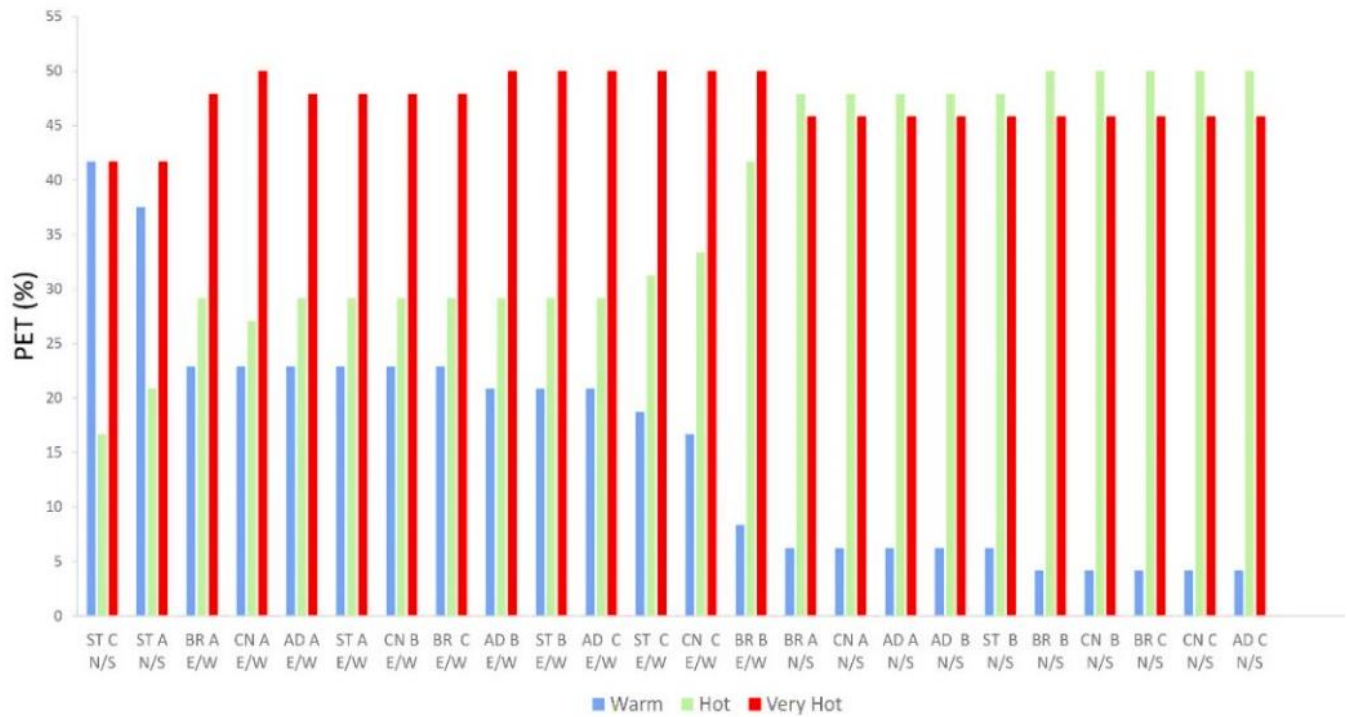


Figure 7.7. Variation of human thermal stress levels within the 24 scenarios.

Source: Author, 2023.

4. Categorization of the thermal behavior of the external building envelopes:

The analysis of outdoor thermal comfort within urban canyons reveals distinct thermal performance patterns across different building materials, street orientations, and aspect ratios. Results demonstrate a clear differentiation in material thermal response, which can be systematically categorized based on cooling efficiency and heat retention characteristics. In North-South (N-S) orientations, notably within configurations with height-to-width ratios of 1.25 (A) and 0.62 (C), as well as in East-West (E-W) orientations with $H/W = 1$ (B), limestone (ST) exhibits high cooling efficiency, consistently achieving above 60% cooling effectiveness. This high cooling category represents optimal thermal performance for pedestrian comfort. A medium cooling category, characterized by 40% - 60% cooling efficiency, is observed across both orientations in deeper canyons (configurations A and B), primarily with limestone and adobe materials. Conversely, results indicate a low cooling category (below 40% efficiency) predominantly in E-W orientations within shallow canyons, where brick (BR) and concrete (CN) materials demonstrate limited thermal regulation capabilities. The heat retention analysis reveals extreme

heating characteristics (60% - 100%) primarily in N-S orientations across all canyon geometries, with brick and concrete showing the highest heat accumulation, and adobe displaying slightly moderated effects. A distinct medium heating category (40 % - 60%) is uniquely observed with concrete walls in N-S orientations within configuration B, while low heating characteristics (below 40%) vary across both orientations and multiple canyon configurations.

Accordingly, this gradation of scenarios thermal behavior characterized six different categories as follows:

- a) **High cooling category:** [above 60% - 100%] of cooling efficiency, obtained predominantly within N-S orientation in A ($H/W = 1.25$) and C ($H/W = 0.62$) canyon groups, and E-W orientation in B ($H/W = 1$) canyon. Limestone (ST) was a prominent material in this category.
- b) **Medium cooling category:** [40% - 60%] of cooling efficiency, observed in both orientations within the deep canyons A and B, for limestone (ST) and adobe (AD) walls.
- c) **Low cooling category:** [below 40%] of cooling efficiency, notably observed in E-W orientation in the shallow canyon, with brick (BR) and concrete (CN) being the most affected materials.
- d) **Extreme Heating category:** [above 60% - 100%] of heat retention predominantly occurred in the N-S orientation within all canyons' forms. The most affected materials were brick (BR), concrete (CN) and slightly adobe (AD).
- e) **Medium heating category:** [40% - 60%] of heat retention, obtained solely with concrete (CN) wall inside the N-S orientation in B canyon.
- f) **Low heating category:** [below 40%] of heat retention, varied between E-W and N-S orientations across different canyon forms and walls.

This comprehensive categorization of thermal behavior highlights the complex interplay between material properties, street orientation, and canyon geometry in determining outdoor thermal comfort conditions (Figure 7.8). Results suggest that material selection should be carefully considered in conjunction with urban geometry to optimize thermal comfort in pedestrian spaces, with limestone emerging as the most effective material for heat mitigation, particularly in appropriately oriented and proportioned urban canyons.

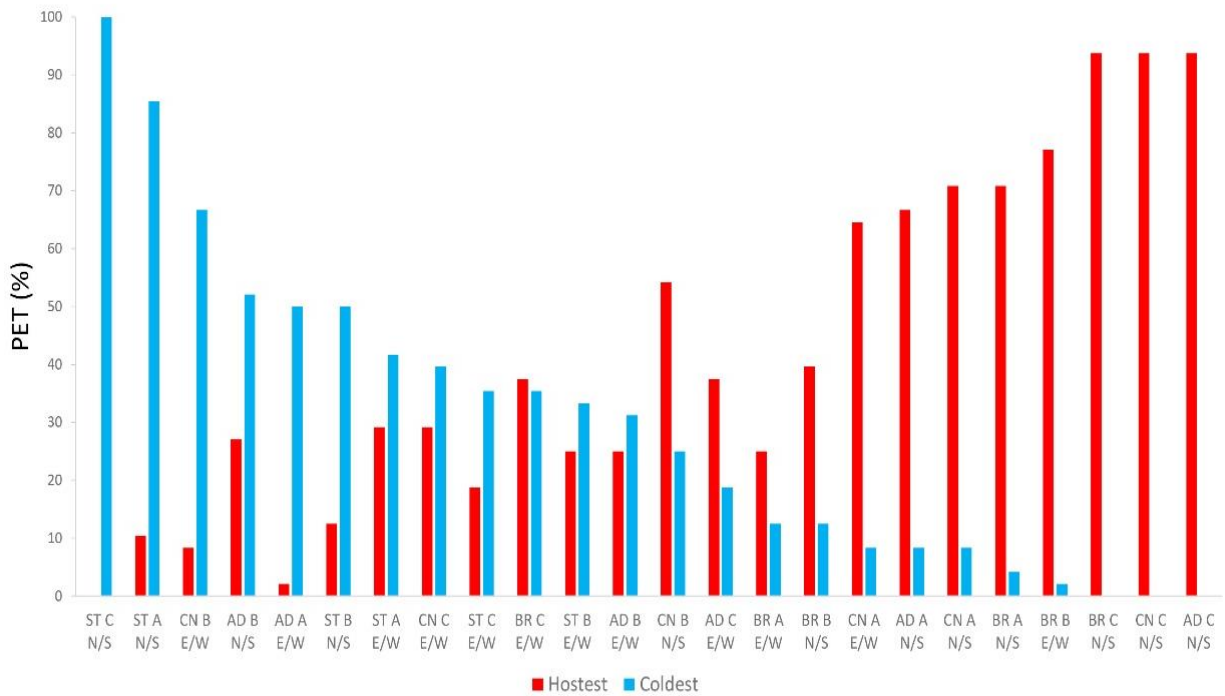


Figure 7.8. Thermal behavior of the externally modelled walls.

Source: Author, 2023.

5. Thermal efficiency of external building envelopes across street H/W and orientation:

The research framework demonstrates considerable strengths in its approach, particularly in the comprehensive examination of multiple variables including three distinct height-to-width (H/W) ratios (1.25, 1, and 0.62), two street orientations (N-S and E-W), and various building materials. This multi-faceted approach allows for a nuanced understanding of the complex interactions between urban geometry and thermal comfort. A key strength of the study lies in its quantitative rigor, providing specific efficiency ranges for different materials and configurations. The finding that limestone can achieve cooling efficiency between 85% and 100% in N-S oriented canyons, while brick walls may cause heat retention ranging from 70% to 93% in the same conditions, offers valuable practical insights for urban planning. The clear categorization of thermal comfort stress levels, coupled with corresponding Physiological Equivalent Temperature (PET) ranges, provides a useful framework for assessing thermal comfort in urban environments.

Examining the cooling efficiency data (Table 7.1) reveals noteworthy patterns across canyon geometries. In E-W oriented canyons, cooling efficiency exhibits significant variability, ranging from minimal cooling ($\nabla 2.1\%$ in canyon B with BR material) to substantial cooling effects ($\nabla 66.7\%$ in canyon B with CN material). This wide range suggests that material choice plays a crucial role in thermal performance within E-W orientations. Notably, the deepest canyon ($H/W = 1.25$) shows more consistent cooling efficiencies across materials, typically ranging between $\nabla 8.3\%$ and $\nabla 50.0\%$, indicating that canyon depth may help stabilize thermal performance regardless of material choice.

The N-S orientation presents a markedly different pattern. Most striking is the observation that canyon C ($H/W = 0.62$) shows zero cooling efficiency for BR, CN, and AD materials, but achieves 100% cooling efficiency with ST material. This extreme contrast highlights the critical interaction between canyon geometry and material properties in N-S orientations. The deeper canyons (A and B) exhibit more moderate cooling efficiencies, suggesting that increased canyon depth may provide more balanced thermal performance in N-S orientations.

Heat retention characteristics present equally compelling patterns. In E-W orientations, heat retention varies dramatically across materials and canyon geometries, from minimal retention ($\Delta 2.1\%$ in canyon A with AD material) to significant retention ($\Delta 77.1\%$ in canyon B with BR material). This variability underscores the importance of careful material selection in E-W canyons. The N-S orientation shows even more pronounced effects, with canyon C exhibiting uniform heat retention of $\Delta 93.8\%$ for BR, CN, and AD materials, while showing zero heat retention for ST material. This stark contrast emphasizes the critical role of material choice in shallow N-S canyons.

The thermal perception data adds another layer of complexity to the analysis. In E-W orientations, the perception of 'warm' conditions remains relatively consistent across canyon geometries and materials, typically ranging from 16.7% to 22.9%. However, N-S orientations show much greater variability, particularly for ST material, which results in significantly higher 'warm' perceptions (37.5% in canyon A and 41.7% in Canyon C). This suggests that the subjective experience of thermal comfort may be more sensitive to material choice in N-S oriented canyons. The 'hot' thermal perception category reveals interesting trends across canyon depths. In E-W orientations, canyon B ($H/W = 1.0$) generally shows higher percentages of 'hot' perception

compared to canyons A and C, particularly with BR material (41.7%). This suggests that intermediate canyon depths may create less favorable thermal conditions in E-W orientations. N-S orientations show more consistent ‘hot’ perceptions across materials and canyon geometries, except for ST material, which results in notably lower percentages (16.7% to 20.8%).

Extreme heat perception data presents the most uniform pattern across the entire dataset, with most configurations resulting in perceptions between 45.8% and 50%. This consistency suggests that once conditions reach the extreme heat threshold, canyon geometry and material choice have limited impact on thermal perception. The marginally lower percentages in N-S orientations with ST material (41.7%) indicate a slight advantage in mitigating extreme heat perception.

The inclusion of Physiological Equivalent Temperature (PET) ranges and corresponding thermal comfort stress levels provides valuable context for interpreting the percentage data. The progression from neutral (17°C - 26°C) to very hot (> 42°C) allows for a nuanced understanding of the thermal comfort implications of different canyon configurations. This calibration of perceived temperature ranges with physiological stress levels enhances the practical applicability of the findings. Looking at overall patterns, several key insights emerge. First, the interaction between canyon geometry and orientation appears to be more significant than material choice alone in determining thermal performance. Second, shallow canyons (H/W = 0.62) show the most extreme variations in both cooling efficiency and heat retention, suggesting that they are most sensitive to material selection. Third, intermediate canyon depths (H/W = 1.0) may not always provide optimal thermal conditions, particularly in E-W orientations.

Table 7.1. Building materials’ external thermal efficiency related to H/W ratio and street orientation.

Source: Author, 2023.

Categories		Canyon A (H/W = 1.25)				Canyon B (H/W = 1)				Canyon C (H/W = 0.62)			
		BR	CN	AD	ST	BR	CN	AD	ST	BR	CN	AD	ST
Cooling efficiency	E-	▽12.5%	▽8.3%	▽50.0%	▽41.7%	▽2.1%	▽66.7%	▽31.3%	▽33.3%	▽35.4%	▽39.6%	▽18.8%	▽35.4%
Heat retention	W	△25.5%	△64.6%	△2.1%	△29.2%	△77.1%	△8.3%	△25.0%	△25.0%	△37.5%	△29.2%	△37.5%	△18.8%
Cooling efficiency	N-	▽4.2%	▽8.3%	▽8.3%	▽85.4%	▽12.5%	▽25.0%	▽50.0%	▽50.0%	▽0.0%	▽0.0%	▽0.0%	▽100.0%
Heat retention	S	△70.8%	△70.8%	△66.7%	△10.4%	△39.6%	△54.2%	△27.1%	△12.5%	△93.8%	△93.8%	△93.8%	△0.0%
Thermal perception													

Chapter VII: Results and Analysis: Presentation and Interpretation of Field Measurements and Simulation Results

Warm	E-W	22.9%	22.9%	22.9%	22.9%	8.3%	22.9%	20.8%	20.8%	22.9%	16.7%	20.8%	18.8%
	N-S	6.3%	6.3%	6.3%	37.5%	4.2%	4.2%	6.3%	6.3%	4.2%	4.2%	4.2%	41.7%
Hot	E-W	29.2%	27.1%	29.2%	29.2%	41.7%	29.2%	29.2%	29.2%	29.2%	33.3%	50.0%	31.3%
	N-S	47.9%	47.9%	47.9%	20.8%	50.0%	50.0%	47.9%	47.9%	50.0%	50.0%	50.0%	16.7%
Extreme heat	E-W	47.9%	50%	47.9%	47.9%	50%	47.9%	50%	50%	47.9%	50%	50%	50%
	N-S	45.8%	45.8%	45.8%	41.7%	45.8%	45.8%	45.8%	45.8%	45.8%	45.8%	45.8%	41.7%
PET(°C)				17–26		26–28		28–37		37–42		>42	
Thermal comfort stress level				Neutral		Slightly warm		Warm		Hot		Very Hot	
				No thermal stress		Slight heat stress		Moderate heat stress		Strong heat stress		Extreme heat stress	

The study's examination of albedo and absorption as crucial parameters influencing surface temperatures represents an important contribution to the field. The observation that high albedo values combined with low absorption can reduce outdoor human thermal discomfort by 50% in extreme weather conditions is particularly noteworthy. However, this finding could be further strengthened by providing more detailed information about methodology, including instrumentation specifications, measurement protocols, and error margins. Such additions would enhance the reproducibility of the study and validate its accuracy. The study's finding that the effectiveness of building materials cannot be solely attributed to specific light or cool materials, but rather depends on canyon geometry and orientation, is particularly valuable. However, this could be further developed by incorporating additional factors such as sky view factor, surface roughness, and urban density metrics. The observation that N-S orientation with east and west-facing façades is most susceptible to overheating due to the solar radiation daily cycle could be enriched by computational fluid dynamics (CFD) modeling to analyze airflow patterns within urban canyons.

The integration of advanced materials with adaptive thermal properties could revolutionize urban thermal management. Additionally, modeling thermal behavior under various climate

change scenarios would enhance the long-term applicability of the findings. The development of more human-centric approaches, incorporating physiological and psychological factors in thermal comfort assessment, would also represent a valuable extension of the current work. To implement these improvements, a structured timeline could be beneficial. Short-term enhancements (0 - 6 months) could focus on improving data visualization and conducting additional statistical analyses. Medium-term developments (6 - 18 months) might include implementing CFD modeling and conducting longitudinal studies across seasons. Long-term research could involve integrating artificial intelligence and machine learning for predictive modeling and developing comprehensive urban design guidelines based on the findings.

The study's conclusion that the most effective bioclimatic passive strategy involves E-W orientation with $H/W < 1$ and high albedo building materials provides a valuable guideline for urban planners. However, this could be further validated through real implementation and monitoring. The development of decision support tools based on these findings would facilitate the practical application of the research in urban planning and design.

Conclusion

As conclusion of the study outcomes, we developed a virtual model presented (Figure 7.9) that effectively synthesizes the research findings, illustrating the thermal performance of building materials within urban fabrics. The visualization demonstrates that orientation and geometry significantly impact thermal behavior, with North-South oriented streets generally performing better than East-West orientations. The model particularly emphasizes how limestone emerged as the most effective material for heat mitigation, especially when combined with appropriate street orientations and proportions. This visualization serves as a valuable tool for urban planners and architects, providing a clear representation of how different materials and urban configurations interact to influence thermal comfort in arid climates. The model effectively translates complex technical findings into a practical visual guide that can inform future urban design decisions aimed at optimizing thermal comfort in hot urban environments.

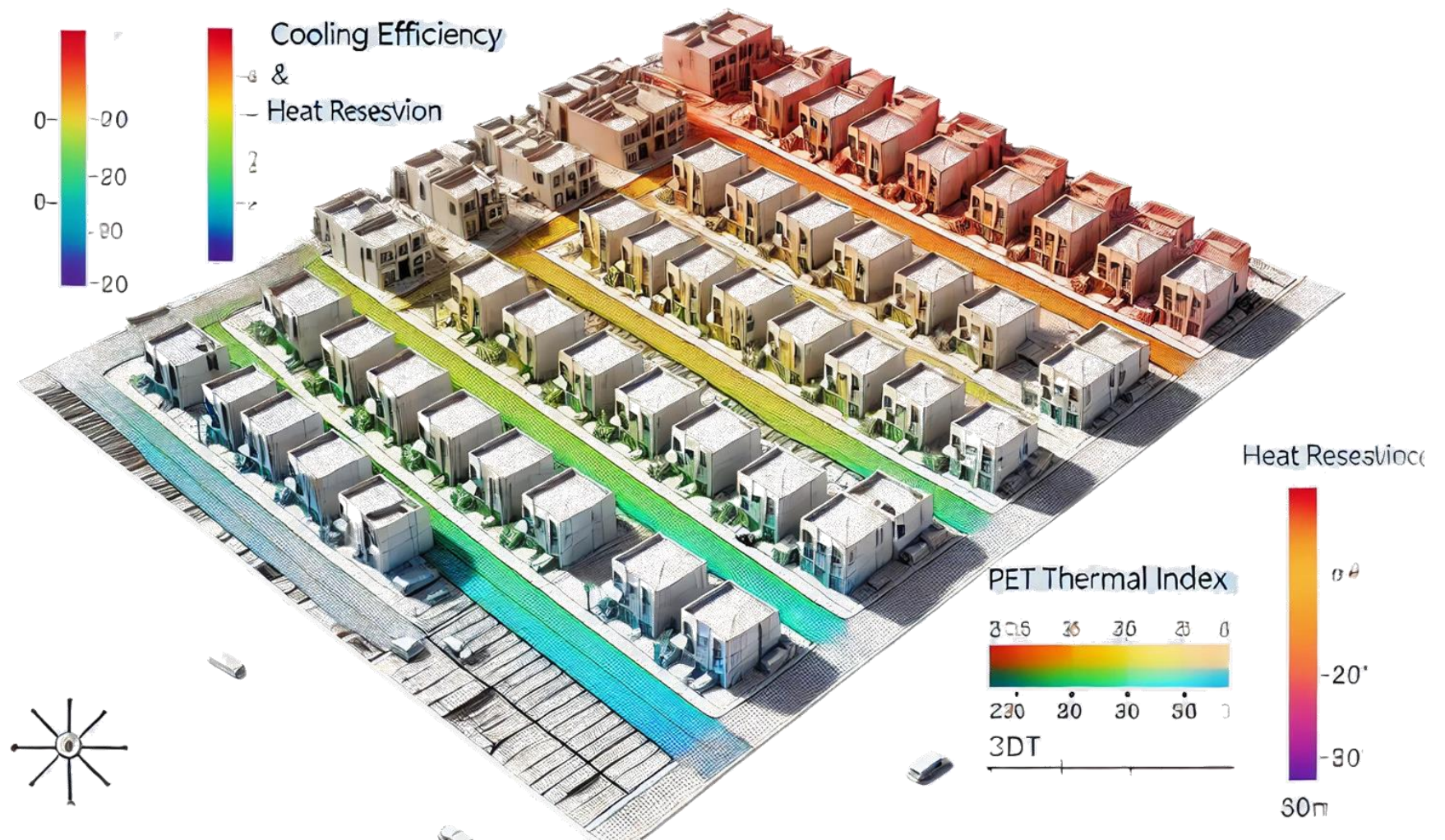


Figure 7.9. Virtual model of the thermal behavior of building materials within urban fabrics based on the research findings.

Source: Author, 2024.

CONCLUSION: CONCLUSION AND RECOMMENDATIONS

Conclusion and recommendations

The research has rigorously addressed the main targeted objectives by investigating the relationship between urban building materials, street geometries, and their combined impact on outdoor thermal comfort within the context of hot dry climate. By quantifying the thermal performance of various building materials such as limestone, adobe, brick, and concrete across different urban geometries, the research provides a nuanced understanding of how material properties and urban configurations influence microclimatic conditions, particularly surface temperatures (T_s), mean radiant temperatures (T_{mrt}), and Physiological Equivalent Temperature (PET). The study also delivers evidence-based guidelines for optimizing building material selection and urban geometry to mitigate urban heat stress, thereby contributing to the design of thermally comfortable and sustainable cities in hot dry regions. This research bridges significant knowledge gaps in urban climatology, focusing on pedestrian-level thermal comfort during extreme summer conditions, and aligns with the initial objectives of understanding the interactions between building material properties, urban morphology, and climatic conditions.

1. Main Findings:

1.1. Thermal behavior of building materials:

The choice of building materials significantly affects the microclimatic conditions of urban canyons, influencing surface temperatures (T_s), mean radiant temperatures (T_{mrt}), and ultimately physiological equivalent temperatures (PET), which are key metrics of outdoor thermal comfort.

1.1.1. Limestone emerged as the most effective material for mitigating heat stress:

It consistently displayed lower thermal storage and higher cooling efficiency, particularly in North-South (N-S) oriented streets. Limestone's light color and higher albedo contributed to reduced absorption of solar radiation, thereby lowering T_{mrt} by 0.5°C to 2.0°C during peak hours compared to other materials. In deeper urban canyons ($H/W = 1.25$), limestone walls reduced PET values by up to 5°C during peak hours, significantly enhancing pedestrian thermal comfort.

Therefore, the first hypothesis, that the thermal properties of building envelope materials significantly influence outdoor thermal comfort through their impact on surface temperatures and

radiation heat exchange, is validated. This finding demonstrates that materials with higher albedo, such as limestone, effectively reduce (T_s) and (T_{mrt}) values by reflecting solar radiation and minimizing heat retention.

1.1.2. Brick and Concrete showed pronounced thermal retention:

These materials exhibited higher thermal inertia, leading to prolonged heat storage and slower cooling rates. Surface temperatures (T_s) on brick and concrete façades were 3°C to 5°C higher than those of limestone, exacerbating heat stress, particularly in East-West (E-W) oriented streets exposed to prolonged solar radiation. Their high heat retention caused nighttime temperatures to remain elevated, reducing diurnal cooling cycles critical for thermal recovery in urban areas.

1.1.3. Adobe displayed intermediate performance:

Adobe's thermal behavior varied with orientation and canyon geometry. It provided moderate cooling benefits in shaded N-S orientations but performed poorly in shallow E-W canyons due to its relatively high thermal mass and darker hue, which amplified heat retention under direct solar exposure.

1.2. Integration of building materials with urban canyon (street):

The interaction between building materials and street geometry amplified their combined impact on outdoor thermal comfort:

1.2.1. Height-to-Width ratio (H/W):

Deep urban canyons (higher H/W ratios) are generally associated with lower T_{mrt} and improved shading, especially in N-S orientations. However, their cooling effects are less pronounced in E-W streets due to persistent solar radiation exposure.

1.2.1.1. Deep Urban Canyons (H/W = 1.25):

Materials like limestone showed maximum cooling potential in these configurations due to increased shading and reduced solar exposure. In N-S orientations, this combination resulted in up to 40% of the day being classified as “warm” rather than “hot” or “very hot” stress categories.

1.2.1.2. Shallow Urban Canyons ($H/W = 0.62$):

In the E-W streets, even highly reflective materials like limestone could not entirely offset the high T_{mrt} values caused by direct solar exposure throughout the daytime hours. Brick and concrete amplified this effect, creating extreme heat stress conditions during peak hours.

1.2.2. Impact of the street orientation:

- **East-West (E-W) Streets:** these orientations exhibit higher thermal stress due to extended exposure to direct solar radiation, with greater diurnal temperature fluctuations. Peak PET values in E-W streets often exceed those in North-South (N-S) streets by 5°C - 10°C .
- **North-South (N-S) streets:** N-S orientations demonstrate more moderated thermal stress, benefiting from increased shading and more balanced solar exposure. Maximum PET values are lower, making these configurations thermally preferable.

1.3. Surface Temperature (T_s) Dynamics:

The study's simulations demonstrated distinct surface temperature profiles across different materials and street configurations: Median T_s values ranged from 40°C to 42°C , with variations driven more by material properties than by canyon geometry. Maximum surface temperatures were recorded on brick and concrete façades in E-W orientations, reaching up to 63°C in shallow configurations ($H/W = 0.62$). Such extreme temperatures contributed to increased T_{mrt} and PET, elevating thermal stress levels. Limestone's reflective properties maintained lower T_s values, particularly in shaded configurations, reducing radiative heat transfer to pedestrians and surrounding spaces.

1.4. Mean Radiant Temperature (T_{mrt}) and radiative heat exchange:

T_{mrt} , as a key determinant of outdoor thermal comfort, was highly sensitive to the thermal properties of building materials:

- N-S oriented streets with limestone façades consistently achieved lower T_{mrt} values (0.2°C to 0.5°C below the average of other materials), emphasizing the material's role in enhancing shaded environments.

- Adobe and limestone walls provided more stable thermal conditions during transition periods (morning and evening), while concrete and brick exhibited steeper radiative heat flux variations, leading to discomfort during peak solar hours.

1.5. Physiological Equivalent Temperature (PET):

PET values, reflecting human thermal perception, varied significantly across materials and configurations:

- In N-S orientations, streets with limestone façades recorded PET values that were 5°C to 10°C lower than those with concrete or brick, particularly during peak afternoon hours.
- E-W orientations consistently experienced higher PET values, with extreme thermal stress dominating over 49% of the day. Materials with low albedo, such as brick and concrete, further exacerbated these conditions, demonstrating the need for reflective or adaptive materials in such configurations.
- Adobe walls in deeper canyons ($H/W = 1.25$) moderately reduced PET values but lacked the cooling efficiency of limestone in mitigating extreme thermal stress.

1.6. Temporal patterns and diurnal cooling cycles:

The diurnal thermal performance of materials was another critical finding:

- Materials with high thermal mass (e.g., brick and concrete) delayed nocturnal cooling, maintaining elevated temperatures late into the night. This phenomenon compounded urban heat island (UHI) effects, making them less suitable for arid climates where nighttime cooling is crucial.
- Limestone and adobe, with their lower heat retention properties, facilitated faster cooling, allowing for improved thermal comfort during evening and early morning hours.

Overall, our second hypothesis, proposing that optimizing specific building material parameters (e.g., albedo, emissivity, and thermal mass) in specific spatial configurations can lead to significant improvements in outdoor thermal comfort, is also confirmed. The research highlights that high-albedo materials like limestone and reflective coatings, when applied in deep urban canyons ($H/W = 1.25$), maximize shading and cooling effects, leading to a significant decrease in PET values and a more comfortable thermal environment. Conversely, materials with high thermal mass, such as

concrete and brick, were shown to exacerbate thermal stress, particularly in East-West (E-W) street orientations, where prolonged solar exposure intensified heat retention and delayed nocturnal cooling cycles.

2. Strengths of the research:

The study's strengths are rooted in its robust methodological approach, comprehensive analysis, and practical contributions to urban climate and thermal comfort research. Below are detailed strengths that highlight its academic rigor and relevance.

2.1. Innovative research focus:

The study addresses a critical gap in the intersection of building materials, and outdoor thermal comfort, particularly in hot dry climates. By focusing on the microclimatic performance of building materials in diverse urban canyon configurations, it provides novel insights into the nuanced relationships that shape thermal comfort in extreme climates.

2.1.1. Comprehensive and systematic scenario design:

The research employs a detailed and systematic scenario-based approach, analyzing:

- **Three H/W ratios:** (1, 1.25, and 0.62), covering a spectrum from shallow to deep urban canyons.
- **Two street orientations:** (East-West and North-South), capturing variations in solar exposure and shading.
- **Four building materials:** (brick, concrete, adobe, and limestone), representing a wide range of thermal properties and practical applications.

This multidimensional analysis allows the study to explore interactions between urban form and material properties across **24 distinct scenarios**, providing results that are both specific and generalizable.

2.1.2. Advanced methodological numerical tools:

The study integrates cutting-edge simulation software and tools:

- ***ENVI-met***: used for three-dimensional microclimatic modeling, offering high-resolution insights into the effects of urban geometry and material properties on outdoor thermal conditions.
- ***BIO-met***: Ensures accurate thermal comfort assessment by utilizing globally recognized indices (e.g., PET and UTCI) and conforming to ISO 7730 standards.
- ***Field measurements***: Accuracy of simulation results enhances the reliability and validity of findings by comparing modeled data with real observations.

This combination of advanced numerical modeling and empirical validation ensures that the results are both accurate and practically applicable.

2.2. Localized relevance with broader implications:

The study focuses on Biskra region, a hot dry climate with significant urban heat challenges, ensuring its findings are deeply relevant to the local context. Simultaneously, the methods and conclusions have broader robustness, offering transferable insights for other arid and semi-arid regions facing similar climatic and urbanization challenges.

2.3. Granular analysis of building materials:

The detailed categorization of building materials based on their cooling efficiency and heat retention offers a refined understanding of their thermal behavior:

- ***Quantified efficiency ranges***: limestone achieves 60% - 85% cooling efficiency in N-S orientations, while brick retains 70% - 93% of heat in similar configurations.
- ***Thermal profiles***: the study dissects surface temperature (T_s), mean radiant temperature (T_{mrt}), and PET metrics for each material, providing a clear picture of their impact on pedestrian thermal comfort.

These findings offer applicable standards for architects and urban planners to optimize material selection in urban design projects.

2.4. Interdisciplinary approach:

The research bridges multiple disciplines, including:

- ***Urban design and architecture:*** analyzing the spatial and geometric characteristics of urban canyons.
- ***Material science:*** evaluating the thermal properties of building materials under diverse conditions.
- ***Environmental science and climatology:*** investigating the impacts of solar radiation, shading, and urban microclimates on thermal comfort.

This holistic approach enables the study to address the multifaceted nature of urban thermal comfort comprehensively.

2.5. Practical urban design applications:

The study provides:

- ***Applicable guidelines:*** recommendations for street orientation and material selection are tailored to maximize thermal comfort in hot dry environments.
- ***Categorization of thermal stress levels:*** the clear delineation of ‘warm,’ ‘hot,’ and ‘very hot’ stress categories for each configuration aids in identifying priority areas for intervention.
- ***Scalable solutions:*** insights are applicable to urban areas of varying scales, from individual streets to entire neighborhoods.

2.6. Climate-Responsive and sustainable focus:

By emphasizing materials like limestone, which mitigate heat stress and have low thermal inertia, the study aligns with sustainability goals, promoting urban designs that reduce energy consumption and enhance livability in hot climates.

3. Limitations of the research:

While the study is robust and comprehensive, certain limitations should be acknowledged to provide a balanced evaluation of its scope and findings. These limitations primarily pertain to the methodological constraints, scope of the analysis, and generalizability of results.

3.1. Limited temporal scope:

- Seasonal variability: the research primarily focuses on typical summer days, which may not capture thermal comfort variations during other seasons. For instance: winter or other seasons (spring and autumn) might exhibit different patterns in solar exposure, shading, and material thermal behavior.
- Thermal comfort indices such as PET may vary significantly across seasons due to differences in ambient temperature and relative humidity.
- Short simulation periods: simulations are constrained to a limited number of days and do not account for long-term variations or extreme weather events, such as heat waves or cold days, which could influence urban thermal dynamics.

3.2. Assumptions in simulation models:

- Boundary conditions: the ENVI-met model assumes fixed meteorological inputs, which might not fully represent real cases variability in wind speed, humidity, or cloud cover.
- Uniform material properties and surface albedos are applied across scenarios, potentially oversimplifying the diverse thermal behaviors of real building materials.
- Simplified human parameters: thermal comfort calculations are based on standardized human parameters (e.g., a 35-year-old male), which may not represent the diverse thermal perceptions and physiological responses of different population groups (e.g., children, elderly individuals, or those with medical conditions).

3.3. Limited exploration of energy implications:

The study focuses on outdoor thermal comfort but does not address the implications of material properties on building energy performance (e.g., cooling loads or insulation benefits). The potential trade-offs between pedestrian thermal comfort and building energy efficiency are not analyzed, which could offer more integrated urban design recommendations.

3.4. Social and Behavioral Dimensions:

The study does not incorporate human behavioral patterns (qualitative approach) or adaptive strategies (e.g., use of shaded areas, timing of outdoor activities) that could influence thermal comfort perceptions. It assumes thermal indices as objective measures of comfort without integrating subjective thermal experiences or cultural variations in thermal acceptance.

4. Recommendations for further research:

Building on the findings and limitations of this study, several avenues for future research can be proposed to advance the understanding of outdoor thermal comfort and the role of urban design in mitigating heat stress. These perspectives aim to refine methodologies, broaden applicability, and deepen insights into the complex interplay between urban geometry, building materials, and climate.

4.1. Seasonal and longitudinal analysis:

Future studies should extend beyond the summer season to include all seasons (winter, spring, autumn) to provide more comprehensive understanding of year-round thermal comfort dynamics:

- Seasonal variations: investigate how material properties and urban configurations interact with solar radiation, ambient temperatures, and wind patterns across different seasons.
- Long-term monitoring: incorporate longitudinal studies that evaluate microclimatic and material performance changes during time, including extreme events such as heat waves or cold spells.

4.2. Dynamic vegetation modeling:

The role of vegetation as a thermal mitigation strategy needs more exploration:

- Species-specific analysis: study the thermal impacts of various plant species, focusing on factors such as canopy density, leaf albedo, evapotranspiration rates, and seasonal foliage changes.
- Dynamic growth patterns: integrate models that account for the growth, maintenance, and water needs of vegetation to simulate real conditions.
- Green-blue infrastructure synergies: investigate the combined effects of vegetation and water bodies (e.g., fountains, ponds) on urban thermal comfort.

4.3. Innovative and emerging building materials:

Future research should explore the potential of new materials and technologies in urban thermal regulation:

- Adaptive materials: assess the performance of phase-change materials, thermochromic coatings, and other innovative materials that dynamically respond to temperature fluctuations.
- Reflective and high-albedo surfaces: examine materials with enhanced reflective properties to mitigate heat retention in urban environments.
- Durability and aging: evaluate how materials' thermal performance evolves over time due to weathering, pollution, and wear.

4.4. Human-centric approaches:

Incorporating human behavioral, physiological, and psychological factors can provide more nuanced insights into thermal comfort:

- Subjective thermal perception: conduct surveys and experiments to understand how different demographic groups (e.g., age, gender, cultural background) perceive thermal comfort.
- Behavioral adaptation: study how people adjust their activities and use urban spaces in response to thermal stress, including the role of shading, clothing, and hydration.
- Inclusive design: explore how urban designs can cater to vulnerable populations, such as the elderly, children, and individuals with health conditions.

REFERENCES

- Ackerman, W. C. (1987). Weather and climate: An introduction to atmospheric science. Macmillan.
- Addis, B. (2007). Building materials through the ages: From prehistoric times to the present. *Construction History*, 19(1), 15-30.
- Akbari, H., Pomerantz, M., & Taha, H. (2005). "Cool surfaces and shade trees to reduce energy use and improve air quality in urban areas." *Solar Energy*, 70(3), 295–310.
- Al-Sanea, S. A., & Zedan, M. F. (2001). Effect of insulation location on thermal performance of building walls.
- Al-Sanea, S. A., & Zedan, M. F. (2001). Thermal properties and their influence on heat transfer in hot climates. *Energy and Buildings*, 33(7), 667-676.
- Al-Sanea, S., & Zedan, M. (2001). The thermal performance of building materials in hot climates: Influence of thermal conductivity and emissivity. *Energy and Buildings*, 33(8), 921-927.
- Algeria's Thermal Regulations of Residential Buildings. (1997). DTR C 3-2 : Réglementation Thermique des Bâtiments d'Habitation. Ministère de l'Habitat et de l'Urbanisme.
- Algerian National Statistics Office (ONS). (2018). National Statistical Report. Office National des Statistiques, Algeria.
- Ali-Toudert, F. (2021). Exploration of the thermal behaviour and energy balance of urban canyons in relation to their geometrical and constructive properties. *Building and Environment*, 188, 107466.
- Ali-Toudert, F., & Mayer, H. (2006). Numerical study on the effects of aspect ratio and orientation of an urban street canyon on outdoor thermal comfort in hot and dry climate. *Building and environment*, 41(2), 94-108.
- American Meteorological Society. (2019). Glossary of meteorology.
- American Society of Heating, Refrigerating and Air-Conditioning Engineers (ASHRAE). (2004). *ASHRAE Handbook - Fundamentals*. American Society of Heating, Refrigerating and Air-Conditioning Engineers.
- Arnfield, A. J. (2003). Two decades of urban climate research: a review of turbulence, exchanges of energy and water, and the urban heat island. *International Journal of Climatology: a Journal of the Royal Meteorological Society*, 23(1), 1-26.

- Ashby, M. F., & Jones, D. R. H. (2012). *Engineering Materials 1: An Introduction to Properties, Applications, and Design*.
- Ashby, M. F., & Jones, D. R. H. (2012). *Engineering materials 1: An introduction to properties, applications, and design*. Elsevier.
- Ashby, M. F., & Jones, D. R. H. (2023). *Materials and design: Introduction to materials selection and design* (2nd ed.). Butterworth-Heinemann.
- Ashby, M. F., Shercliff, H., & Cebon, D. (2018). *Materials: engineering, science, processing and design*. Butterworth-Heinemann.
- ASHRAE. (2004). *ASHRAE Handbook—Fundamentals* (SI Edition). American Society of Heating, Refrigerating, and Air-Conditioning Engineers.
- ASHRAE. (2017). *ASHRAE Standard 55-2017: Thermal Environmental Conditions for Human Occupancy*. American Society of Heating, Refrigerating, and Air-Conditioning Engineers.
- ASHRAE. (2019). *ANSI/ASHRAE/IES Standard 90.1-2019: Energy Standard for Buildings Except Low-Rise Residential Buildings*. American Society of Heating, Refrigerating and Air-Conditioning Engineers.
- ASHRAE. (2020). *ANSI/ASHRAE Standard 55-2020: Thermal Environmental Conditions for Human Occupancy*. American Society of Heating, Refrigerating, and Air-Conditioning Engineers.
- ASHRAE. (2021). *ASHRAE Handbook—Fundamentals*. American Society of Heating, Refrigerating and Air-Conditioning Engineers.
- BADACHE, H. (2021). *L’impact de la végétation sur le microclimat et le confort extérieur des usagers dans les espaces publics: Cas de la ville de Biskra* (Doctoral dissertation, Université Mohamed Khider–Biskra).
- Balaji, N., Suribabu, C. R., & Mani, A. (2013). Thermal performance analysis of building materials using time lag and decrement factor. *Energy Procedia*, 54, 399-411.
- Barlow (2014): Barlow, J. F. (2014). Urban heat islands and urban weather forecasting: The importance of climate modeling for cities. *Environmental Science & Technology*, 48(19), 11222–11230.
- Beckman, W. A., Broman, L., Fiksel, A., Klein, S. A., Lindberg, E., Schuler, M., & Thornton, J. (1994). TRNSYS The most complete solar energy system modeling and simulation software. *Renewable energy*, 5(1-4), 486-488.

- Binarti, F., Koerniawan, M. D., Triyadi, S., Utami, S. S., & Matzarakis, A. (2020). A review of outdoor thermal comfort indices and neutral ranges for hot-humid regions. *Urban Climate*, 31, 100531.
- Blazejczyk, K., Epstein, Y., Jendritzky, G., Staiger, H., & Tinz, B. (2012). Comparison of UTCI to selected thermal indices. *International journal of biometeorology*, 56, 515-535.
- Bourbia, F., & Awbi, H. B. (2004). Building cluster and shading in urban canyon for hot dry climate: Part 1: Air and surface temperature measurements. *Renewable energy*, 29(2), 249-262.
- Bourbia, F., & Boucheriba, F. (2010). Impact of street design on urban microclimate for semi arid climate (Constantine). *Renewable energy*, 35(2), 343-347.
- Britter, R. E., Hanna, S. R., Briggs, G. A., & Robins, A. (2003). Short-range vertical dispersion from a ground level source in a turbulent boundary layer. *Atmospheric Environment*, 37(27), 3885-3894.
- Bruse, M. (2004). ENVI-met 3.0: updated model overview. University of Bochum. Retrieved from: www.envi-met.com, 3.
- Building Science Corporation. (2022).
- CBE Clima Tool, Berkeley University, USA. (2023). Center for the Built Environment. [Online] Available at: <https://cbe.berkeley.edu/clima-tool/>
- Center for the Built Environment (CBE). (2021). Climate Data Analysis of Biskra Region: 1958–2021. Center for the Built Environment (CBE).
- Charalampopoulos, I., Tsiros, I., Chronopoulou-Sereli, A., & Matzarakis, A. (2013). Analysis of thermal bioclimate in various urban configurations in Athens, Greece. *Urban Ecosystems*, 16, 217-233.
- Clarke, J. A., & Yaneske, P. (2022). Building energy performance: Evaluation and optimization of energy consumption. Routledge.
- Coccolo, S., Kämpf, J., Scartezzini, J. L., & Pearlmutter, D. (2016). Outdoor human comfort and thermal stress: A comprehensive review on models and standards. *Urban Climate*, 18, 33-57.
- Collins, J. (2004). Reinforced concrete and advanced glass in the 20th century construction. *Architectural Technology Review*, 30(1), 55-68.

- Comet, S. (2016). Understanding relative humidity and air temperature relationships. *Journal of Applied Meteorology and Climatology*, 55(6), 1415–1428.
- Compagnon, R. (1997). RADIANCE: a simulation tool for daylighting systems. The Martin Centre for Architectural and Urban Studies University of Cambridge Department of Architecture.
- Correa, E., Ruiz, M. A., Canton, A., & Lesino, G. (2012). Thermal comfort in forested urban canyons of low building density. An assessment for the city of Mendoza, Argentina. *Building and environment*, 58, 219-230.
- Coseo, P., & Larsen, L. (2014). How factors of land use/land cover, building configuration, and adjacent heat sources and sinks explain urban heat islands in Chicago. *Landscape and Urban Planning*, 125, 117–129.
- Darbani, E. S., Rafieian, M., Parapari, D. M., & Guldmann, J. M. (2023). Urban design strategies for summer and winter outdoor thermal comfort in arid regions: The case of historical, contemporary and modern urban areas in Mashhad, Iran. *Sustainable Cities and Society*, 89, 104339.
- Darbani, E. S., Rafieian, M., Parapari, D. M., & Guldmann, J. M. (2023). Urban design strategies for summer and winter outdoor thermal comfort in arid regions: The case of historical, contemporary and modern urban areas in Mashhad, Iran. *Sustainable Cities and Society*, 89, 104339.
- Deng, J. Y., & Wong, N. H. (2020). Impact of urban canyon geometries on outdoor thermal comfort in central business districts. *Sustainable Cities and Society*, 53, 101966.
- Desjarlais, A., & Zarr, M. (2023). *Energy-efficient buildings: Thermal performance and sustainability*. Springer.
- Di Napoli, C., Messeri, A., Novák, M., Rio, J., Wieczorek, J., Morabito, M., ... & Pappenberger, F. (2021). The universal thermal climate index as an operational forecasting tool of human biometeorological conditions in Europe. *Applications of the Universal Thermal Climate Index UTCI in Biometeorology: Latest Developments and Case Studies*, 193-208.
- Domone, P. L. J., & Illston, J. M. (2010). *Construction materials: Their nature and behaviour* (4th ed.). Spon Press.
- Domone, P. L. J., & Illston, J. M. (2022). *Construction materials: Their nature and behaviour* (5th ed.). Spon Press.

- Dorer, V., Allegrini, J., Orehounig, K., Kämpf, J., Wilke, U., & Robinson, D. (2013). Modelling the urban microclimate and its impact on building energy performance. *Journal of Building Performance Simulation*, 6(2), 84–102.
- Duggal, S. (2008). *Building materials: Nature and man-made products in construction*. New York: McGraw-Hill.
- El Mghouchi, Y. (2022). On the prediction of daily global solar radiation using temperature as input. An application of hybrid machine learners to the six climatic Moroccan zones. *Energy Conversion and Management: X*, 13, 100157.
- Elnahas, M. M. (2003). The effects of urban configuration on urban air temperatures. *Architectural Science Review*, 46(2), 135-138.
- Erell, E. (2017). Urban greening and microclimate modification. *Greening Cities: Forms and Functions*, 73-93.
- Erell, E., Pearlmutter, D., Boneh, D., & Kutiel, P. B. (2014). Effect of high-albedo materials on pedestrian heat stress in urban street canyons. *Urban climate*, 10, 367-386.
- Fanger, P. O. (1970). *Thermal Comfort: Analysis and Applications in Environmental Engineering*. Danish Technical Press.
- Fanger, P. O. (1970). *Thermal comfort: Analysis and applications in environmental engineering*. Danish Technical Press.
- Fiala, D., Lizard, S. H., & Parsons, K. C. (2012). A simulation model of human thermal physiology and comfort. *Building and Environment*, 47, 75–85.
- Fiorillo, E., Brilli, L., Carotenuto, F., Cremonini, L., Gioli, B., Giordano, T., & Nardino, M. (2023). Diurnal outdoor thermal comfort mapping through envi-met simulations, remotely sensed and in situ measurements. *Atmosphere*, 14(4), 641.
- Fitchen, J. (1961). Stone masonry and timber framing in medieval construction. *Journal of Building Engineering*, 12(4), 78-92.
- Friedman, R. (2010). Building materials in the Industrial Revolution: Concrete and steel's impact on construction. *Historical Review of Industrial Architecture*, 15(4), 133-142.
- Friedman, R. (2010). Building materials in the Industrial Revolution: Concrete and steel's impact on construction. *Historical Review of Industrial Architecture*, 15(4), 133-142.
- Gachkar, D., Taghvaei, S. H., & Norouzian-Maleki, S. (2021). Outdoor thermal comfort enhancement using various vegetation species and materials (case study: Delgosha Garden, Iran). *Sustainable Cities and Society*, 75, 103309.

- Gagge, A. P., Stolwijk, J. A. J., & Nishi, Y. (1986). An effective temperature scale based on a simple model of human heat exchange. *ASHRAE Transactions*, 92(2), 109–122.
- Gerundo, R., Fasolino, I., & Grimaldi, M. (2016). ISUT Model. A composite index to measure the sustainability of the urban transformation. *Smart Energy in the Smart City: Urban Planning for a Sustainable Future*, 117-130.
- Giannopoulou, K., Santamouris, M., Livada, I., Georgakis, C., & Caouris, Y. (2010). The impact of canyon geometry on intra urban and urban: suburban night temperature differences under warm weather conditions. *Pure and applied geophysics*, 167, 1433-1449.
- Givoni, B. (1978). *L'homme, l'architecture et le climat*. (Trad. de l'angl.).
- Givoni, B. (1998). *Climate considerations in building and urban design*. John Wiley & Sons.
- Grimmond et al. (2010): Grimmond, C. S. B., Souch, C., & Oke, T. R. (2010). The urban climate: A review of urban microclimate studies. *Progress in Physical Geography: Earth and Environment*, 34(2), 239–258.
- Grimmond, C. S. B., & Oke, T. R. (1999). Heat storage in urban areas: Local-scale observations and evaluation of a simple model. *Journal of Applied Meteorology*, 38(7), 922–940.
- Grimmond, C. S. B., & Oke, T. R. (2002). Turbulent heat fluxes in urban areas: Observations and a local-scale urban meteorological parameterization scheme (LUMPS). *Journal of Applied Meteorology and Climatology*, 41(7), 792-810.
- Guha, S., & Chowdhuri, S. (1996). Heat Transfer and Surface Roughness: Implications for Material Design. *Journal of Heat Transfer Engineering*, 17(4), 45–55.
- Hall, M. A., & Allinson, D. (2009). The role of thermal mass in energy-efficient buildings. *Journal of Building Performance*, 5(3), 15-26.
- Hall, M. R., & Allinson, D. W. (2023). *Materials for Energy Efficiency and Thermal Comfort in Buildings*. Woodhead Publishing.
- Hamouda, M., & Outtas, D. (2011). "Sustainable Use of Palm Tree Trunks and Fronds in Traditional Algerian Architecture." *Sustainable Architecture Review*, 14(1), 45-53.
- Hang, J., Li, Y., & Sandberg, M. (2012). Experimental and numerical studies of flows through and within high-rise building arrays and their implications on pollutant dispersion. *Building and Environment*, 50, 167–181.

- Hanus, B., & Harris, K. (2013). Bio-based products in sustainable architecture. *Green Building Materials Review*, 7(2), 45-53.
- Hanus, B., & Harris, K. (2013). Bio-based products in sustainable architecture. *Green Building Materials Review*, 7(2), 45-53.
- Harman & Belcher (2006): Harman, I. N., & Belcher, S. E. (2006). The structure of the urban boundary layer in a wind tunnel. *Atmospheric Environment*, 40(23), 4171–4184.
- Harrison, R. (2014). "Measurement Techniques in Environmental Monitoring: Protocols and Equipment." *Environmental Monitoring Journal*, 22(3), 45-57
- Hewlett, P. (2003). Portland cement: The history and evolution of modern concrete. *Building Materials Journal*, 23(3), 34-46.
- Hinkle, K. (2016). Albedo and its implications for urban environments. *Environmental Research Letters*.
- Hornbostel, M. (1991). The role of building materials in urban performance. *Architectural Journal*, 45(3), 124-138.
- Hornbostel, M. (1991). The role of building materials in construction: Natural and man-made materials. *Architectural Journal*, 45(3), 124-138.
- Houda, S., Zemmouri, N., Athmani, R., & Belarbi, R. (2011). Effect of urban morphology on wind flow distribution in dense urban areas. *Journal of Renewable Energies*, 14(1), 85-94.
- Hu, X., Li, D., Sun, T., & Wang, Z.-H. (2021). Surface energy balance and its implications for urban heat islands: A review and perspective. *Atmospheric Research*, 249, 105363.
- Hudişteanu, S. V., Popovici, C. G., & Cherecheş, N. C. (2018). Wind tunnel study of natural ventilation of building integrated photovoltaics double skin façade. In *E3S Web of Conferences* (Vol. 32, p. 01020). EDP Sciences.
- Höppe, P. (1999). The physiological equivalent temperature—A universal index for the biometeorological assessment of the thermal environment. *International Journal of Biometeorology*, 43(2), 71–75.
- Intergovernmental Panel on Climate Change (IPCC). (2014). *Climate change 2014: Impacts, adaptation, and vulnerability. Part A: Global and sectoral aspects. Contribution of Working Group II to the Fifth Assessment Report of the Intergovernmental Panel on Climate Change*. Cambridge University Press. Retrieved from
- International Council for Research and Innovation in Building and Construction (CIB, 2022).

- International Organization for Standardization. (1989). ISO 7243: Ergonomics of the thermal environment—Determination of the heat stress using a hot/warm environment. International Organization for Standardization.
- International Organization for Standardization. (1998). ISO 7726: Ergonomics of the thermal environment—Instruments for measuring physical quantities.
- International Organization for Standardization. (2004). ISO 8996: Ergonomics of the thermal environment—Determination of metabolic rate.
- International Organization for Standardization. (2005). ISO 7730: Ergonomics of the thermal environment—Analytical determination and interpretation of thermal comfort using calculation of the PMV and PPD indices and local thermal comfort criteria.
- International Organization for Standardization. (2005). ISO 7730: Ergonomics of the thermal environment—Analytical determination and interpretation of thermal comfort using calculation of the PMV and PPD indices and local thermal comfort criteria. International Organization for Standardization.
- International Organization for Standardization. (2005). ISO 15927-4: Hygrothermal performance of buildings—Calculation and presentation of climatic data—Part 4: Hourly data for building energy calculations. International Organization for Standardization.
- International Organization for Standardization. (2007). ISO 9920: Ergonomics of the thermal environment—Estimation of the thermal insulation and water vapour resistance of a clothing ensemble. International Organization for Standardization.
- International Organization for Standardization. (2014). ISO 10456: Building materials and products Hygrothermal properties—Tabulated design values. International Organization for Standardization.
- International Organization for Standardization. (2014). ISO 9869-1: Thermal insulation—Building elements—In-situ measurement of thermal resistance and thermal transmittance—Part 1: Heat flow meter method. International Organization for Standardization.
- International Organization for Standardization. (2017). ISO 13786: Thermal performance of building components—Dynamic thermal characteristics—Calculation methods. International Organization for Standardization.

- International Organization for Standardization. (2017). ISO 6946: Building components and building elements—Thermal resistance and thermal transmittance—Calculation methods. International Organization for Standardization.
- ISO 10456. (2007). Building materials and products – Hygrothermal properties – Tabulated design values. International Organization for Standardization.
- Izemouren, A., & Guettala, S. (2014). "Traditional Building Materials in Algeria: An Overview." *Journal of Construction and Building Materials*, 56, 22-32.
- Jadhav, S. (2018). Various thermal comfort indices and the role of CFD in evaluating thermal comfort in occupied spaces. *Linekin*.
- Jamei, E., Rajagopalan, P., Seyedmahmoudian, M., & Jamei, Y. (2016). Review on the impact of urban geometry and pedestrian level greening on outdoor thermal comfort. *Renewable and Sustainable Energy Reviews*, 54, 1002-1017.
- Johansson, E. (2006). Influence of urban geometry on outdoor thermal comfort in a hot dry climate: A study in Fez, Morocco. *Building and environment*, 41(10), 1326-1338.
- Johansson, E., Spangenberg, J., Gouvêa, M. L., & Freitas, E. D. (2013). Scale-integrated atmospheric simulations to assess thermal comfort in different urban tissues in the warm humid summer of São Paulo, Brazil. *Urban Climate*, 6, 24-43.
- Johansson, E., Thorsson, S., Emmanuel, R., & Krüger, E. (2014). Instruments and methods in outdoor thermal comfort studies—The need for standardization. *Urban Climate*, 10(Part 2), 346–366.
- Kalogeropoulos, G., Dimoudi, A., Touboulidis, P., & Zoras, S. (2022). Urban heat island and thermal comfort assessment in a medium-sized Mediterranean City. *Atmosphere*, 13(7), 1102.
- Karimi, A., Bayat, A., Mohammadzadeh, N., Mohajerani, M., & Yeganeh, M. (2023). Microclimatic analysis of outdoor thermal comfort of high-rise buildings with different configurations in Tehran: Insights from field surveys and thermal comfort indices. *Building and Environment*, 240, 110445.
- Karlický, J., Huszár, P., Halenka, T., Belda, M., Žák, M., Pišoft, P., & Mikšovský, J. (2018). Multi-model comparison of urban heat island modelling approaches. *Atmospheric Chemistry and Physics*, 18(14), 10655-10674.

- Kim, S. W., & Brown, R. D. (2022). Pedestrians' behavior based on outdoor thermal comfort and micro-scale thermal environments, Austin, TX. *Science of the total environment*, 808, 152143.
- Kim, Y., Li, D., Xu, Y., Zhang, Y., Li, X., Muhlenforth, L., ... & Brown, R. (2023). Heat vulnerability and street-level outdoor thermal comfort in the city of Houston: Application of google street view image derived SVFs. *Urban Climate*, 51, 101617.
- Kleerekoper, L., Van Esch, M., & Salcedo, T. B. (2012). How to make a city climate-proof, addressing the urban heat island effect. *Resources, Conservation and Recycling*, 64, 30-38.
- Kottek, M., Grieser, J., Beck, C., Rudolf, B., & Rubel, F. (2006). World map of the Köppen-Geiger climate classification updated.
- Kumaran, M. K. (2021). Thermal Properties of Building Materials: An Engineering Perspective. *Journal of Building Physics*, 45(1), 85–101.
- Kuzmanović, D., Banko, J., & Skok, G. (2024). Improving the operational forecasts of outdoor Universal Thermal Climate Index with post-processing. *International journal of biometeorology*, 68(5), 965-977.
- Kántor, N., & Unger, J. (2011). The most problematic variable in the course of human biometeorological comfort assessment—The mean radiant temperature. *Open Geosciences*, 3(1), 90–100.
- Lam, C. K. C., Lee, H., Yang, S. R., & Park, S. (2021). A review on the significance and perspective of the numerical simulations of outdoor thermal environment. *Sustainable Cities and Society*, 71, 102971.
- Lancaster, T. (2005). The evolution of building materials in human civilization. *Journal of Architectural History*, 29(2), 101-118.
- Lancaster, T. (2005). The evolution of building materials in human civilization. *Journal of Architectural History*, 29(2), 101-118.
- Landsberg, P. T. (1981). Einstein and statistical thermodynamics. III. The diffusion-mobility relation in semiconductors. *European Journal of Physics*, 2(4), 213.
- Laouadi, A. (2022). A new general formulation for the PMV thermal comfort index. *Buildings*, 12(10), 1572.
- Li, X. (2011). *Construction materials: Their properties and uses*. Science Press.

- Lindberg, F., & Grimmond, C. S. B. (2011). The influence of vegetation and building morphology on shadow patterns and mean radiant temperatures in urban areas: model development and evaluation. *Theoretical and applied climatology*, 105, 311-323.
- Lindberg, F., Holmer, B., & Thorsson, S. (2008). SOLWEIG 1.0—Modelling spatial variations of 3D radiant fluxes and mean radiant temperature in complex urban settings. *International journal of biometeorology*, 52, 697-713.
- Liu, J., Zheng, B., & Yang, F. (2023). A Simulation Study of the Impact of Urban Street Greening on the Thermal Comfort in Street Canyons on Hot and Cold Days. *Forests*, 14(11), 2256.
- Magli, S., Lodi, C., Lombroso, L., Muscio, A., & Teggi, S. (2015). Analysis of the urban heat island effects on building energy consumption. *International Journal of Energy and Environmental Engineering*, 6, 91-99.
- Mahdavinejad, M., Shaeri, J., Nezami, A., & Goharian, A. (2024). Comparing universal thermal climate index (UTCI) with selected thermal indices to evaluate outdoor thermal comfort in traditional courtyards with BWh climate. *Urban Climate*, 54, 101839.
- Mamlouk, M. S., & Zaniewski, J. P. (2011). *Materials for civil and construction engineers* (2nd ed.). Pearson.
- Mamlouk, M. S., & Zaniewski, J. P. (2011). *Materials for civil and construction engineers*, by Pearson Education. Inc., Upper Saddle River, New Jersey, 7458
- Matsson, J. E. (2023). *An introduction to ansys fluent 2023*. Sdc Publications.
- Matzarakis, A., & Rutz, F. (2007). RayMan: a tool for tourism and applied climatology. *Development in Tourism Climatology*, 129-138.
- Matzarakis, A., Fröhlich, D., & Zorita, E. (2015). Modelling radiation fluxes in simple and complex environments—Application of the RayMan model. *International Journal of Biometeorology*, 59(4), 591–601.
- Matzarakis, A., Mayer, H., & Iziomon, M. G. (1999). Applications of a universal thermal index: physiological equivalent temperature. *International journal of biometeorology*, 43, 76-84.
- Matzarakis, A., Rutz, F., & Mayer, H. (2010). Modelling radiation fluxes in simple and complex environments: basics of the RayMan model. *International journal of biometeorology*, 54, 131-139.
- Mehta, P. K., & Monteiro, P. J. M. (2014). *Concrete: Microstructure, Properties, and Materials*.

- Mehta, P. K., & Monteiro, P. J. M. (2021). *Concrete: Microstructure, properties, and materials* (4th ed.). McGraw-Hill.
- Millstein, D., & Menon, S. (2011). Regional climate consequences of large-scale cool roof and photovoltaic array deployment. *Environmental Research Letters*, 6(3), 034001.
- Mohajerani, A., Bakaric, J., & Jeffrey-Bailey, T. (2017). "The urban heat island effect, its causes, and mitigation, with reference to the thermal properties of asphalt concrete." *Journal of Environmental Management*, 197, 522–538.
- Morris, C. J. G., & Simmonds, I. (2000). Associations between varying magnitudes of the urban heat island and the synoptic climate in Melbourne, Australia. *International Journal of Climatology*, 20(15), 1931–1954.
- Muniz-Gaal, L. P., Pezzuto, C. C., de Carvalho, M. F. H., & Mota, L. T. M. (2020). Urban geometry and the microclimate of street canyons in tropical climate. *Building and Environment*, 169, 106547.
- Naboni, E., Carrión, D., & Castello, J. (2019). Relevant radiation fluxes and urban entities on the determination of outdoor mean radiant temperature (MRT). *Building and Environment*, 158, 191–200.
- Naidja, M., Bouguerra, A., & Hamouda, M. (2022). "The Role of Local Stones in Traditional Algerian Architecture." *Building Materials Journal*, 36(3), 158-167.
- National Oceanic and Atmospheric Administration (NOAA), National Weather Service. (n.d.). Heat index. Retrieved from <https://www.weather.gov/heatindex>.
- Ng, E., Chen, L., Wang, Y., & Yuan, C. (2011). A study on the cooling effects of greening in a high-density city: An experience from Hong Kong. *Building and Environment*, 46(5), 1032-1044.
- Ng, E., Chen, L., Wang, Y., & Yuan, C. (2012). A study on the cooling effects of greening in a high-density city: An experience from Hong Kong. *Building and Environment*, 47, 256–271.
- Nikolopoulou, M., & Steemers, K. (2003). Thermal comfort and psychological adaptation as a guide for designing urban spaces. *Energy and Buildings*, 35(1), 95–101.
- Nunez, M., & Oke, T. R. (1977). The energy balance of an urban canyon. *Journal of Applied Meteorology and Climatology*, 16(1), 11-19.

- Oke, T. R. (1976). The distinction between canopy and boundary-layer urban heat islands. *Atmosphere*, 14(4), 268-277.
- Oke, T. R. (1982). The energetic basis of the urban heat island. *Quarterly journal of the royal meteorological society*, 108(455), 1-24.
- Oke, T. R. (1988). The urban energy balance. *Progress in Physical geography*, 12(4), 471-508.
- Oke, T. R., & Cleugh, H. A. (1987). Urban heat storage derived as energy balance residuals. *Boundary-Layer Meteorology*, 39, 233-245.
- Oke, T. R., Mills, G., Christen, A., & Voogt, J. A. (2017). *Urban climates*. Cambridge university press.
- Oke, T. R., Mills, G., Christen, A., & Voogt, J. A. (2017). *Urban climates*. Cambridge university press.
- Oliver, J. E. (Ed.). (2008). *Encyclopedia of world climatology*. Springer Science & Business Media.
- Pacheco, F., & Jalali, S. (2011). Sustainable building materials: The future of construction in hot climates. *Environmental Design Journal*, 20(3), 210-219.
- Pacheco, F., & Jalali, S. (2011). Sustainable building materials: The future of construction in hot climates. *Environmental Design Journal*, 20(3), 210-219.
- Pacheco-Torgal, F., et al. (2023). *Sustainability of construction materials* (2nd ed.). Woodhead Publishing.
- Pantavou, K., Lykoudis, S., Michael, N., Stylianou, E., Christou, R., Giallourous, G., ... & Nikolopoulos, G. K. (2020). Thermal sensation and indices in the urban outdoor hot Mediterranean environment of Cyprus. *Theoretical and Applied Climatology*, 140, 1315-1329.
- Potchter, O., Cohen, P., Lin, T. P., & Matzarakis, A. (2018). Outdoor human thermal perception in various climates: A comprehensive review of approaches, methods and quantification. *Science of the Total Environment*, 631, 390-406.
- Pérez-Lombard, L., Ortiz, J., & Pout, C. (2008). A review on buildings energy consumption information. *Energy and buildings*, 40(3), 394-398.
- Rahmani, S., Benassi, M., & Cheikh, R. (2022). "The Role of Concrete Blocks in Modern Algerian Architecture: Applications in Hot and Dry Climates." *Journal of Construction and Building Materials*, 45(2), 110-119.

- Roberts, A., & Marsh, A. (2001, August). ECOTECT: environmental prediction in architectural education. In Cardiff University, Wales, Proceedings of ECAADE Conference.
- Rockel, B., Will, A., & Hense, A. (2008). The regional climate model COSMO-CLM (CCLM). *Meteorologische zeitschrift*, 17(4), 347.
- Rosenfeld, A. H., Akbari, H., Romm, J. J., & Pomerantz, M. (1998). Cool communities: strategies for heat island mitigation and smog reduction. *Energy and buildings*, 28(1), 51-62.
- Rosso, F., Golasi, I., Castaldo, V. L., Piselli, C., Pisello, A. L., Salata, F., ... & de Lieto Vollaro, A. (2018). On the impact of innovative materials on outdoor thermal comfort of pedestrians in historical urban canyons. *Renewable Energy*, 118, 825-839.
- Rotach, M. W. (1993). Turbulence close to a rough urban surface part I: Reynolds stress. *Boundary-Layer Meteorology*, 65(1), 1-28.
- Roth, M., & Chow, W. T. (2012). A historical review and assessment of urban heat island research in S singapore. *Singapore Journal of Tropical Geography*, 33(3), 381-397.
- Rydin, Y. (2012). *Governing for sustainable urban development*. Routledge.
- Rydin, Y., Bleahu, A., Davies, M., Dávila, J. D., Friel, S., De Grandis, G., ... & Wilson, J. (2012). Shaping cities for health: complexity and the planning of urban environments in the 21st century. *The lancet*, 379(9831), 2079-2108.
- Sadeghipour Roudsari, M., Pak, M., & Viola, A. (2013, August). Ladybug: a parametric environmental plugin for grasshopper to help designers create an environmentally-conscious design. In *Building Simulation 2013* (Vol. 13, pp. 3128-3135). IBPSA.
- Sadineni, S. B., & al., et al. (2011). Role of thermal mass in sustainable energy-efficient buildings. *Renewable and Sustainable Energy Reviews*, 15(9), 4874-4891.
- Santamouris, M. (2013). Using cool pavements as a mitigation strategy to fight urban heat island—A review of the actual developments. *Renewable and Sustainable Energy Reviews*, 26, 224-240.
- Santamouris, M. (2014). Cooling the cities: A review of reflective and green roof mitigation technologies to fight heat island and improve comfort in urban environments. *Solar Energy*, 103, 682–703.

- Santamouris, M. (2015). Analyzing the effect of urban heat islands on urban comfort and energy demand. *Energy and Buildings*, 98, 119–124.
- Santamouris, M. (2020). Recent progress on urban overheating and heat island research. Integrated assessment of the energy, environmental, vulnerability and health impact. Synergies with the global climate change. *Energy and Buildings*, 207, 109482.
- Santamouris, M., & Kolokotsa, D. (2013). *Urban climate mitigation techniques*. Routledge.
- Santamouris, M., Cartalis, C., Synnefa, A., & Kolokotsa, D. (2015). On the impact of urban heat island and global warming on the power demand and electricity consumption of buildings—A review. *Energy and buildings*, 98, 119-124.
- Santamouris, M., Feng, J., & Kolokotsa, D. (2015). Urban heat island and cooling technologies—An overview of current strategies to reduce heat island intensity. *Journal of Environmental Management*, 146, 443–458.
- Santamouris, M., Haddad, S., Saliari, M., Vasilakopoulou, K., Synnefa, A., Paolini, R., & Fiorito, F. (2018). On the energy impact of urban heat island in Sydney: Climate and energy potential of mitigation technologies. *Energy and Buildings*, 166, 154-164.
- Santamouris, M., Papanikolaou, N., Koronakis, I., Livada, I., & Asimakopoulos, D. (1999). Thermal and air flow characteristics in a deep pedestrian canyon under hot weather conditions. *Atmospheric Environment*, 33(27), 4503-4521.
- Santamouris, M., Papanikolaou, N., Livada, I., Koronakis, I., Georgakis, C., Argiriou, A., & Assimakopoulos, D. N. (2001). On the impact of urban climate on the energy consumption of buildings. *Solar Energy*, 70(3), 201–216.
- Santamouris, M., Synnefa, A., & Karlessi, T. (2011). Using advanced cool materials in the urban built environment to mitigate heat islands and improve thermal comfort conditions. *Solar energy*, 85(12), 3085-3102.
- Scott, L. M., & Janikas, M. V. (2009). Spatial statistics in ArcGIS. In *Handbook of applied spatial analysis: Software tools, methods and applications* (pp. 27-41). Berlin, Heidelberg: Springer Berlin Heidelberg.
- Sharma, R., Pradhan, L., Kumari, M., & Bhattacharya, P. (2021). Assessing urban heat islands and thermal comfort in Noida City using geospatial technology. *Urban Climate*, 35, 100751.

- Sharmin, T., Steemers, K., & Matzarakis, A. (2017). Microclimatic modelling in assessing the impact of urban geometry on urban thermal environment. *Sustainable cities and society*, 34, 293-308.
- Shenwei, W., Yang, L., & Zhang, L. (2022). Thermal mass and its impact on building energy performance and thermal comfort: A review. *Renewable and Sustainable Energy Reviews*, 157, 112052.
- Steemers, K., Baker, N., Crowther, D., Dubiel, J., Nikolopoulou, M. H., & Ratti, C. (1997). City texture and microclimate. *Urban Design Studies*, 3(1997), 25-50.
- Stocks, L. (2003). The material innovations of ancient Egypt. *Journal of Ancient Architecture*, 8(2), 102-113.
- Sun, C., Lian, W., Liu, L., Dong, Q., & Han, Y. (2022). The impact of street geometry on outdoor thermal comfort within three different urban forms in severe cold region of China. *Building and Environment*, 222, 109342.
- Taha, H. (2008). Episodic performance and sensitivity of the urbanized MM5 (uMM5) to perturbations in surface properties in Houston Texas. *Boundary-Layer Meteorology*, 127(2), 193-218.
- Taleb, D., & Abu-Hijleh, B. (2013). Urban heat islands: Potential effect of organic and structured urban configurations on temperature variations in Dubai, UAE. *Renewable energy*, 50, 747-762.
- Taleb, H., & Taleb, D. (2014). Enhancing the thermal comfort on urban level in a desert area: Case study of Dubai, United Arab Emirates. *Urban forestry & urban greening*, 13(2), 253-260.
- Taleghani, M. (2018). Outdoor thermal comfort by different heat mitigation strategies-A review. *Renewable and Sustainable Energy Reviews*, 81, 2011-2018.
- Taleghani, M., Kleerekoper, L., Tenpierik, M., & van den Dobbelsteen, A. (2015). Outdoor thermal comfort within five different urban forms in the Netherlands. *Building and Environment*, 83, 65–78.
- Taleghani, M., Tenpierik, M., van den Dobbelsteen, A., & Sailor, D. J. (2014). Heat in courtyards: A validated and calibrated parametric study of heat mitigation strategies for urban courtyards in the Netherlands. *Solar Energy*, 103, 108-124.

- Thorsson, S., Lindqvist, M., & Lindqvist, S. (2007). Thermal bioclimatic conditions and patterns in a hot urban area: The implications of measured T_{mrt} and physiological equivalent temperature (PET). *International Journal of Biometeorology*, 52(2), 143–156.
- Tiwari, G. N., & Ghosal, M. K. (2011). *Renewable energy resources: Basic principles and applications*. Alpha Science International.
- United Nations, Department of Economic and Social Affairs (UN DESA). (2018). *World urbanization prospects: The 2018 revision*. Retrieved from
- Voogt, J. A. (2003). Urban heat islands: Hotter cities. *Weather*, 58(11), 366–371.
- Wang, H., & Salmon, J. (2014). Building materials and their impact on thermal performance in hot climates. *Construction Science and Technology*, 22(1), 55-64.
- Wang, H., & Salmon, J. (2014). Building materials and their impact on thermal performance in hot climates. *Construction Science and Technology*, 22(1), 55-64.
- Ward, G. J. (1994, July). The RADIANCE lighting simulation and rendering system. In *Proceedings of the 21st annual conference on Computer graphics and interactive techniques* (pp. 459-472).
- Weather Briefing, L.C. <https://www.weatherbriefing.com/>.
- Wonorahardjo, S., Sutjahja, I. M., Mardiyati, Y., Andoni, H., Thomas, D., Achsani, R. A., & Steven, S. (2020). Characterising thermal behaviour of buildings and its effect on urban heat island in tropical areas. *International Journal of Energy and Environmental Engineering*, 11, 129-142.
- World Meteorological Organization. (2017). *Climate services for supporting climate change adaptation*.
- Xiong, K., Yang, Z., & He, B. J. (2022). Spatiotemporal heterogeneity of street thermal environments and development of an optimised method to improve field measurement accuracy. *Urban Climate*, 42, 101121.
- Yan, H., Fan, S., Guo, C., Wu, F., Zhang, N., & Dong, L. (2014). Assessing the effects of landscape design parameters on intra-urban air temperature variability: The case of Beijing, China. *Building and environment*, 76, 44-53.
- Yilmaz, Z. (2007). Thermal mass and thermal resistance in urban materials: Implications for outdoor comfort. *Journal of Thermal Environment and Building Science*, 10(1), 68-77.

- Yin, Z., Liu, Z., Liu, X., Zheng, W., & Yin, L. (2023). Urban heat islands and their effects on thermal comfort in the US: New York and New Jersey. *Ecological Indicators*, 154, 110765.
- Yuan, J., Masuko, S., Shimazaki, Y., Yamanaka, T., & Kobayashi, T. (2022). Evaluation of outdoor thermal comfort under different building external-wall-surface with different reflective directional properties using CFD analysis and model experiment. *Building and Environment*, 207, 108478.
- Zeng, D., Wu, J., Mu, Y., Deng, M., Wei, Y., & Sun, W. (2020). Spatial-temporal pattern changes of UTCI in the China-Pakistan economic corridor in recent 40 years. *Atmosphere*, 11(8), 858.
- Zheng, Y., Han, Q., & Keeffe, G. (2024). An evaluation of different landscape design scenarios to improve outdoor thermal comfort in Shenzhen. *Land*, 13(1), 65.
- Zhou, Y., & Shepherd, J. M. (2010). Atlanta's urban heat island under extreme heat conditions and potential mitigation strategies. *Natural hazards*, 52, 639-668.
- Çengel, Y. A., & Boles, M. A. (2008). *Thermodynamics: An Engineering Approach* (6th ed.). McGraw Hill.